MODELING AN INDUSTRIAL DEA UNIT WITH THE CPA EOS: A PARAMETER ESTIMATION STUDY AND DATA ANALYTICS

Victor Virgens de França

Rio de Janeiro

2019

MODELING AN INDUSTRIAL DEA UNIT WITH THE CPA EOS: A PARAMETER ESTIMATION STUDY AND DATA ANALYTICS

Victor Virgens de França

Dissertação de Mestrado apresentada ao Programa de Pós-graduação em Engenharia Química, COPPE, da Universidade Federal do Rio de Janeiro, como parte dos requisitos necessários à obtenção do título de Mestre em Engenharia Química.

Orientadores: Frederico Wanderley Tavares
Letícia Cotia dos Santos

Rio de Janeiro
Fevereiro de 2019

MODELING AN INDUSTRIAL DEA UNIT WITH THE CPA EOS: A PARAMETER ESTIMATION STUDY AND DATA ANALYTICS

Victor Virgens de França

DISSERTAÇÃO SUBMETIDA AO CORPO DOCENTE DO INSTITUTO ALBERTO LUIZ COIMBRA DE PÓS-GRADUAÇÃO E PESQUISA DE ENGENHARIA (COPPE) DA UNIVERSIDADE FEDERAL DO RIO DE JANEIRO COMO PARTE DOS REQUISITOS NECESSÁRIOS PARA A OBTENÇÃO DO GRAU DE MESTRE EM CIÊNCIAS EM ENGENHARIA QUÍMICA.

Examinada por:

_____
Prof. Frederico Wanderley Tavares, D. Sc.

_____
Eng. Letícia Cotia dos Santos, D. Sc.

_____
Prof. Frederico de Araújo Kronemberger, D. Sc

_____
Prof. Lizandro de Sousa Santos, D. Sc.

RIO DE JANEIRO, RJ – BRASIL
FEVEREIRO DE 2019

França, Victor Virgens de

Modeling an Industrial Dea Unit with the CPA EoS: a Parameter Estimation Study and Data Analytics/ Victor Virgens de França. – Rio de Janeiro: UFRJ/COPPE, 2019

XXVIII, 160p.: il.; 29,7 cm.

Orientadores: Frederico Wanderley Tavares

Letícia Cotia dos Santos

Dissertação (mestrado)– UFRJ/COPPE/Programa de Engenharia Química, 2019.

Referências Bibliográficas: p. 106-112

1. Equations of State. 2. Parameter Estimation. 3. Acid Gas Absorption. I. Tavares, Frederico Wanderley *et al*. II. Universidade Federal do Rio de Janeiro, COPPE, Programa de Engenharia Química. III. Título.

Acknowledgements

During those long, tiring and painful years in which I was pursuing my master's degree, I wondered what the main role of a professional in Thermodynamics was. And today it is very clear to me that our main goal is to attract new professionals to the area. And the best way to do this is by setting an example and inspiring people. And my advisors Frederico Tavares and Leticia Cotia did this brilliantly. And that is why I thank them immensely. Thank you for inspiring me as my examples.

I thank my family and friends for their unconditional love and understanding. I am sure that this master's degree is an achievement for all of us. Thank you for understanding my “I will not”, "I can not" and "I don’t have time" and for encouraging me to continue on my path.

In particular I would like to thank the friends and colleagues I met at PEQ: Omayra, Bernardo, Agnaldo, Maria, Eduardo, Elisa, Ângela, Carlos and Christian. I have no doubt that the greatest wealth we can derive from experiences is to be able to get to know people better. And this is the part that most interests me in my daily life, the process of knowing, understanding, respecting and valuing each other.

Thank you to my workmates who supported me in choosing to continue my postgraduate education, especially Sabrina and Rafael (today my dear friends), for whom I have a great affection. I also thank my colleague Samir for always being available to help me during the mathematical difficulties of the dissertation and for allowing me to use his parameter estimation program, ThermOptimizer.

I thank my family from Rio de Janeiro, Thais, Bira, David, Tayná, Dani, Renata, Naty, Gesner, Giga, Paul, Carol, Camila, Pitty, Mone and Rick. It was with you that whenever I had a free time, I was able to go to the movies, play board games, gossip a lot and have a few drinks. Thanks for being my chosen family and for letting everything seem lighter, easier and more uncomplicated.

Thank you to my longtime partner, Arley, for always being there and supporting me in any decision. Sharing my life with you is synonymous with multiplying joy, laughing a lot and sharing any kind of problem. Thanks for always being there when I needed to.

I thank my family from Salvador, who from the time I was very young pushed me to be who I wanted to be.

I thank my grandmother Antonia for being my example of sensitivity and humanity.

I thank my parents, Cristina and Cicero, for the happy childhood that was given to me and for being my example of strength and determination.

Resumo da Dissertação apresentada à COPPE/UFRJ como parte dos requisitos necessários para a obtenção do grau de Mestre em Ciências (M.Sc.)

MODELAGEM DE UMA PLANTA INDUSTRIAL DE DEA UTILIZANDO-SE A EQUAÇÃO DE ESTADO CPA: ESTUDO SOBRE A ESTIMAÇÃO DE PARÂMETROS E ANÁLISE DE DADOS

Victor Virgens de França

Fevereiro/2019

Orientadores: Frederico Wanderley Tavares
Letícia Cotia dos Santos

Programa: Engenharia Química

Neste trabalho foram estudadas duas alcanolaminas, DEA e MEA, para, respectivamente, modelar um sistema de tratamento de gases ácidos para especificação do teor de H_2S e selecionar a melhor Equação de Estado (EdE) a ser utilizada na modelagem deste sistema. Comparou-se as EdEs SRK, PR e CPA através da estimação de parâmetros da MEA a partir de dados da substância pura. A EdE CPA apresentou melhores resultados que as outras duas, com desvio absoluto médio em relação à pressão de vapor em 1,694% e, portanto, foi escolhida como principal modelo termodinâmico para a modelagem de processos. A CPA foi então aplicada na estimação dos parâmetros de DEA Pura, gerando valores de desvio absoluto médio em relação à pressão de vapor de 0,3%, o que indica proximidade dos valores calculados pelo modelo com os dados experimentais. Prosseguiu-se com a estimação de parâmetros dos principais sistemas binários presentes na unidade de tratamento de gases ácidos e estes então foram inseridos no simulador Petrox. Para a estimação de parâmetros utilizou-se o software ThermOptimizer, aplicando-se os métodos de Otimização PSO e Simplex. Os resultados das simulações foram avaliados através da comparação com dados operacionais e resultados de análises laboratoriais disponíveis.

Abstract of Dissertation presented to COPPE/UFRJ as a partial fulfillment of the requirements for the degree of Master of Science (M.Sc.)

MODELING AN INDUSTRIAL DEA UNIT WITH THE CPA EOS: A PARAMETER ESTIMATION STUDY AND DATA ANALYTICS

Victor Virgens de França

February/2019

Advisors: Frederico Wanderley Tavares
Letícia Cotia dos Santos

Department: Chemical Engineering

In this work, two alkanolamines, DEA and MEA, were studied, respectively, to model an acid gas treatment system to reduce H_2S content and to select the most suitable Equation of State (EoS) to be used in this system modeling. The EoS SRK, PR and CPA were applied for pure MEA parameter estimation using pure substance data. The EoS CPA presented better results than the other two, with a mean absolute deviation from the vapor pressure of 1.694% and, therefore, was chosen as the main thermodynamic model for the process modeling. The CPA was then applied for pure DEA parameter estimation, generating mean absolute deviation values in relation to vapor pressure of 0.3%, which indicates proximity of the values calculated by the model with the experimental data. It was proceeded to estimate the parameters of the main binary systems present in an acid gas treatment unit and these were then inserted in the Petrox simulator. For the parameters estimation the ThermOptimizer software was used, applying the optimization methods PSO and Simplex. The results of the simulations were evaluated via comparison with operational data and results of available laboratory analyzes.

Contents

List of Figures

List of Tables

List of Symbols and Abbreviations

Abbreviations

4C	Scheme of association
ABSV	Absorbing Column in Petrox Simulation
AMP	2-amino-2methyl-1-propanol
AGASA	Acid Gases Absorption System
CARG	Acid Gas Stream in Petrox Simulation
CERE	Center for Energy Resources Engineering
CR-1	Combining Rule 1
CPA	Cubic Plus Association
DIPPR	Design Institute for Physical Property
DEA	Diethanolamine
DEAP	Poor DEA Stream in Petrox Simulation
DEAR	Rich DEA Stream in Petrox Simulation
DGA	Diglycolamine
EoS	Equation of State
GAST	Treated Gas Stream in Petrox Simulation
LLE	Liquid-Liquid Equilibrium
MDEA	Methyldiethanolamine
MEA	Monoethanolamine
NRTL	Non-random two-liquid model
PSO	Particle Swarm Optimization
PR	Peng-Robinson
SRK	Soave Redlich-Kwong
SAFT	Statistical Associating Fluid Theory
SIMPLEX	Flexible Polyhedra Method

SRU	Sulphur Recovery Unit
TPT-1	Thermodynamic Pertubation Theory
TEA	Triethanolamine
VLE	Vapor-Liquid Equilibrium

Symbols

AAρ%	Average absolute deviation of liquid density
AAP%	Average absolute deviation of pressure
x_{glo}	Best position by the whole swarm
x_{ind}	Best position for each particle
k_{ij}	Binary Interaction Parameter
l_{ij}	Binary Interaction Parameter
b	Covolume
w_f	Final inertia factor in PSO Method
X_{Ai}	Fraction of sites A in molecule i not bonded at other sites
A	Helmholtz energy
$A_{association}$	Helmholtz energy for association interactions
A_{chain}	Helmholtz energy for chain interactions
$A_{dispersion}$	Helmholtz energy for dispersion interactions
$A_{hard\ sphere}$	Helmholtz energy for hard sphere interactions
$A_{ideal\ gas}$	Helmholtz energy for ideal gas interactions
R	Ideal Gás Universal Constante
w_0	Initial inertia factor in PSO Method
x_i	Mol fraction of component i
V_m	Molar Volume
σ	Molecular diameter
n	Mols
N	Number of components
N_{exp}	Number of Experiments

N_{inter}	Number of iterations in PSO Method
p_{id}^{t}	Particle best position in PSO Method
x_{id}^{t}	particle current position in PSO Method
v_{id}^{t}	Particle current velocity in PSO Method
p_{gd}^{t}	Particle flock best position in PSO Method
x_{id}^{t+1}	Particle next position in PSO Method
v_{id}^{t+1}	Particle next velocity in PSO Method
a_0	Physical energy parameter of CPA EoS (barL-2mol-2)
P	Pressure
P_A	Pressure of attraction
v	Pseudo-velocity
w	PSO search parameters
g	Radial distribution function
r_1	Random number between [0,1]
r_2	Random number between [0,1]
P_R	Repulsion pressure
T	Temperature

Greek symbols

$\varepsilon^{A_iB_j}$	Association energy between a type-A site in molecule i and a type-B site in molecule j (bar L mol-1).
$\Delta^{A_iB_j}$	Association strength between a type-A site in molecule i and a type-B site in molecule j (Lmol-1).
$\beta^{A_iB_j}$	Association volume parameter between a type-A site in molecule i and a type-B site in molecule j.
ξ	Fluid reduced density
ρ	Liquid density
γ_1	PSO search parameters
γ_2	PSO search parameters

Subscript and Superscript

calc	calculated
exp	experimental
gd	global
hc	hydrocarbon
id	individual
o	organic phase
p	polar phase
R	reduced
sat	saturated

Chapter 1

Introduction

1.1 Motivation

Increasingly stringent environmental restrictions orientate oil refineries to adapt to new legal requirements, which demand that gases emitted into the atmosphere have to be cleaner and safer (JUNGE, 1963). In addition, the specification of the fuel gas (or refinery gas) to be used in the internal processes of the refinery (as furnace fuel gas and in the generation of hydrogen) is also deeply restricted, mainly due to corrosive attacks by acidic compounds and generation of pollutants during the gas burning. In order to adapt the gaseous product to the legal restrictions, processes of absorption of acid gases using amines are widely used. The treatment of acidic streams minimizes the generation of solid waste and generates revenue for the company (BASTOS *et al.*, 2015). Removal of CO_2 and others acidic compounds can occur through various treatments such as membrane separation processes, separation through the formation of emulsions, adsorption towers and, most commonly, amine treatment. Several amines have been used over the years in the acid gas treatment. One of the most important factors to be considered in the amine field is the solubility of the solute relative to the absorber solution. The solubility is required to be high enough to remove the acid gases from the process feed however the interaction may not be strong enough to prevent the amine recovery (ZARE; MIRZAEI, 2009). Within the amine group, the alkanolamines, which are compounds with low volatility, high reactivity and good thermal stability, stand out. These are excellent characteristics for a solvent. About the alkanolamines, the one that presents the best compromise between affinity with the solute and regeneration capacity, considering an industrial environment, is diethanolamine (DEA).

In this work, the absorber tower of a DEA plant is modeled, whose objective is the removal of hydrogen sulphide from an acid gas stream.

In the literature there are several approaches for the equilibrium modeling involving amine compounds (AVLUND *et al.*, 2011; AVLUND; KONTOGEORGIS; MICHELSEN, 2008; BARREAU *et al.*, 2006; FARAMARZI *et al.*, 2009; MANDAL; BANDYOPADHYAY, 2006; OLIVEIRA *et al.*, 2011). A rigorous approach is the procedure through the mass transfer model, which takes into account the species diffusion coefficient in each phase. A less rigorous approach, which presents less complexity in terms of mathematical equation, is the method through thermodynamic models. In this approach it is considered that the system reaches the thermodynamic equilibrium and that there are no macro level transients. This is the most commonly utilized approach in the industrial environment where it is seeking for a better compromise between good predictions and simplicity. Among the different models available to characterize the thermodynamic equilibrium, it is highlighted the Cubic Equations of State (EoS), which has the advantage of simplicity and great application in several areas (ex: large amount of data available in the literature). The most utilized cubic EoS, Peng-Robinson (PR) and Soave Redlich-Kwong (SRK), do not take into account the association phenomena between species. The Cubic Plus Association (CPA) Equation takes this phenomenon into account without adding a high level of complexity to the equation (KONTOGEORGIS, GEORGIOS M, 2004). In the literature, there are several areas (FOLAS *et al.*, 2005) that the CPA has already presented better performance when compared with classical EoS.

Based on the study of the most suitable solvent for the gas absorption, a comparative analysis of the EoS mentioned is carried out. For this, the pure monoethanolamine (MEA) parameter estimation was performed, so that the EoS that presented the best results could be chosen as the standard thermodynamic model to be applied in the modeling and simulation of the absorber tower.

The strategy for parameter estimation chosen is based on the most recent study of the subject (SANTOS *et al.*, 2015). The tool adopted for parameter estimation was the ThermOptimizer software.

It was proceeded with the absorption process simulation, employing an operational plant data, with the usage of Petrox software, with the objective of comparing the simulation results with data from the industrial plant.

1.2 Objective

The objective of this dissertation is to apply a relatively higher complex EoS (CPA) in a known industrial system with the aim to verify if it presents better results than more widely used EoS (SRK and PR). It is seeking not only for better results, but also for no need for greater computational demand. In addition, a second objective is to verify if the CPA presents reasonable results on modeling the vapor-liquid equilibrium (VLE) of a system containing DEA, water, H_2S and light hydrocarbons.

As specific targets can be listed:

- To study MEA with a proposed methodology and compare with literature results using different EoS.
- Perform a parameter estimation for modelling pure DEA and binary mixtures – DEA-water, DEA-H_2S.
- Apply these data in a Process Simulator.
- Study an industrial DEA absorption unit, analyze plant data and perform comparisons with a process simulation result.

1.3 Text Organization

This work is divided into 5 main chapters. The first chapter is the Introduction, which brings to the reader a brief work presentation, with the main points to be developed and possible subjects to be clarified and proven. In addition, it will be indicated how the work is organized and its main goals will be clearly stated. The knowledge of the study objectives is important because it will guide the entire research throughout this work.

The second chapter is the Literature Review, which presents the relevant theoretical aspects in order to help the reader to understand the technical considerations and some of the author's conclusions. This chapter addresses the basics of gas absorption theory, including

the main alkanolamines used. A flowchart of a refinery alkanolamine treatment process is presented.

The third chapter indicates the mathematical tools and the parameter estimation strategy.

The fourth chapter presents the results and discussions while the fifth chapter deals with its conclusions and suggestions.

Chapter 2

Literature Review

2.1 Gas Absorption Theory

2.1.1 Introduction

The absorption is aimed at separating components from a gaseous mixture to obtain a purer product stream. This separation involves the transfer of a substance from the gaseous stream (process feed) to a liquid stream (solvent). The absorbed compound may undergo to physical (no chemical reaction) or chemical (with chemical reaction) absorption (KOHL; NIELSEN, 1997).

2.1.2 Acid Gas Treatment

At the refinery, the industrial units responsible for the treatment of sulfur streams are called the sulfur block, which is made up of the following industrial plants: sulfur recovery units, waste gas treatment, acid water treatment and gas treatment with amines.

Figure 1 represents an acid gas absorption process flow chart in a typical Petrobras plant (INDIO DO BRASIL; ARAÚJO; SOUSA, 2012).

The gas to be treated, containing H_2S, as observed in Figure 1, passes through a vessel to remove liquids and entrained solids. This separator is called a knock-out vessel. After this step, this condensate free gas enters the absorption column bottom. In this column an aqueous amine solution flows counter-current to absorb the acidic compounds from the gas stream. The treated gas (leaving the top of the absorption column) then passes through a new separator, which will retain a possible amount of the amine solution that has been drawn.

This current then leaves the treatment unit. The fuel gas main destination is to make up the refinery fuel gas header.

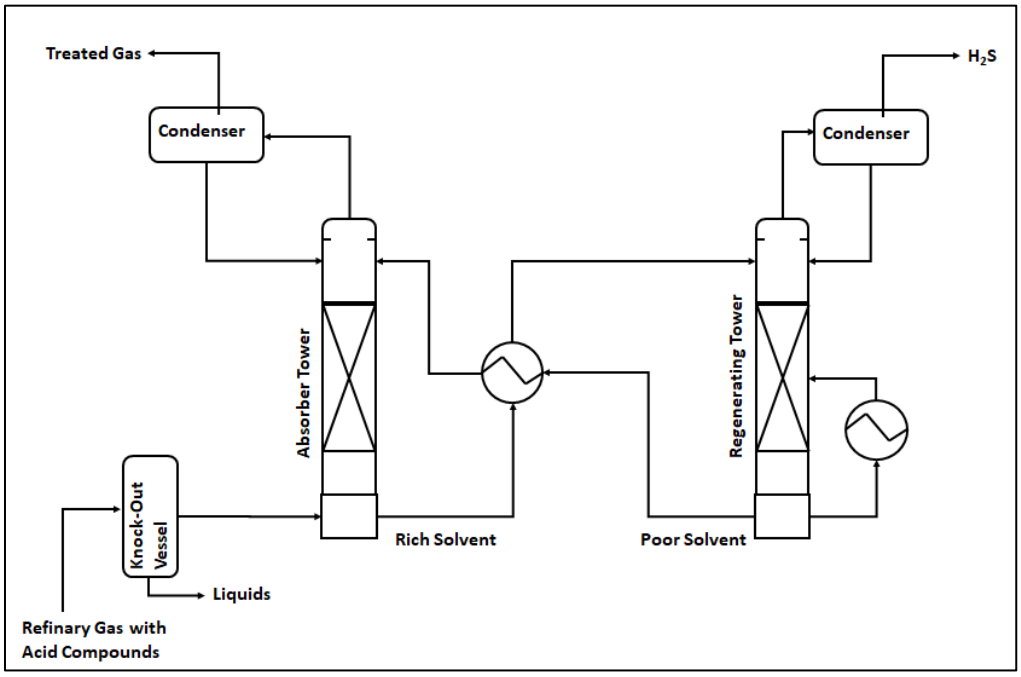

Figure 1 - Process Flow Chart - Amines Absorption (adapted from Petrobras Refinery Manual)

A critical step in the process is the amine solution regeneration containing the acidic compounds (this stream is called the rich stream). This current is preheated. The heating occurs in a heat exchanger whose heating fluid is the regenerated amine itself, which leaves the absorbing tower. This heat exchanger is a point of industrial unit´s energy integration, which decreases its overall energy demand. In the regenerating tower, due to the increase in temperature and decrease in pressure, the acid gas is released from the amine solution upon entering in with the steam generated by the reboiler. The acid solution then comes out over the regenerating tower together with the water vapor. This current passes through a condenser, where the vapor condenses. The acid gas is sent to the SRU (Sulphur Recovery Unit). If the process feed has a highly content of hydrogen, before passing through the sulfur recovery unit, it will pass through a hydrogen production unit.

The recovered amine, poor in acid gas, leaves the regenerator tower and is recirculated to the absorbing tower, completing the solvent cycle.

2.1.3 Amines Solvents

Alkanolamines are the main chemical solvents used in the treatment of gas streams containing H_2S. This group has an amine function that imparts an alkaline character to the group. Alkanolamines have a high affinity for polar compounds due mainly to the hydroxyl radical (-OH) present in their constitution (ZARE; MIRZAEI, 2009).

In this group, the most commonly employed alkanolamines are monoethanolamine (MEA), diethanolamine (DEA) and methyldiethanolamine (MDEA). Other less widely used alkanolamines are triethanolamine (TEA), 2-amino-2-methyl-1-propanol (AMP) and diglycolamine (DGA). The decision of which alkanolamine to be utilized in the absorption process depends on several factors such as process feed composition, system operating conditions and output current desired purity (KOHL; NIELSEN, 1997). Alkanolamines are an excellent choice of absorbents since they are relatively low in cost and are produced in the ethylene oxide industry (MEDEIROS; BARBOSA; ARAÚJO, 2013).

Amines can be classified into primary, secondary and tertiary amines depending on the amount of hydrogens presented into central nitrogen to be replaced by other radicals. The primary amines have higher affinity for acidic compounds but react almost irreversibly, making it difficult to regenerate the solvent. Secondary amines have moderate affinity to the acidic compounds (having a reversible reaction), which facilitates their regeneration (BULLIN; POLASEK; DONNELLY, 1990). Tertiary amines are the amines which have the lowest affinity with the acidic compounds and therefore their regeneration is the most facilitated (however, it is the alkanolamines that have the worst results for the acidic compounds removal). Thus, in general, the secondary amines present a better compromise between the ability to treat the gas stream and enable the solvent recovery. Figure 2 is an illustration of the main alkanolamines (KOHL; NIELSEN, 1997):

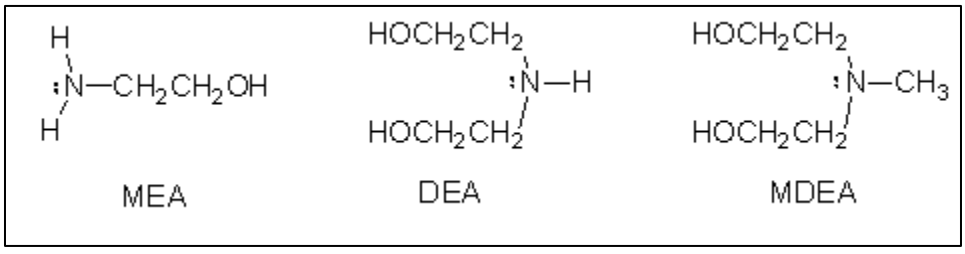

Figure 2 - Main alkanolamines used as solvents for gas absorption (adapted from Kohl, 1997)

2.1.4 Alkanolamine Selection

Some aspects should be taken into account when selecting an amine for the absorption of H_2S from a gas stream (POLASEK; BULLIN, 1994):

1º) Does the amine used conform to the reboiler and condenser ability to provide the energy needed for its purification?

2º) The absorption of H_2S can be optimized using a mixture of amines?

3º) Could the amine employed promote corrosion in the system? Is there an amine (or amine mixture) that will lessen this impact?

4º) Will the chosen amine need how much of the circulation rate? Is there any amine that will lessen this need?

In a gas absorption plant with amines, between 50% -70% of the costs related to the initial investment are associated with the solvent circulation rate size. Another 10%-20% is associated with the plant's energy demand. About the operating costs, 70% is related to solvent regeneration (POLASEK; BULLIN, 1994). In this way, the selection of the most appropriate amine (or amine mixture) for the process impacts the plant costs.

As already mentioned, each alkanolamine has its specific characteristics that influence the acid gas absorption. Because it has intermediary characteristics between primary and tertiary amines, DEA is often the alkanolamine chosen for industrial processes whose objective is the removal of primarily H_2S (INDIO DO BRASIL; ARAÚJO; SOUSA, 2012). Regularly the decision to choose the DEA is based on the MEA unfavorable characteristics (MEDEIROS; BARBOSA; ARAÚJO, 2013): high energy demand for recovery, corrosiveness, compound degradation and vapor losses. MDEA has among the three the lowest vaporization loss and the lowest energy demand for its recovery. However, it has the lowest affinity for the acidic compounds.

2.1.5 Chemical Reactions

The main chemical reaction involved in the absorption process of H_2S with DEA are presented in Equation 1:

$$(CH_2 - CH_2 - OH)_2NH + H_2S \leftrightarrow (CH_2 - CH_2 - OH)_2NH_2^+ + HS^- \quad (1)$$

H_2S, in aqueous solutions, dissociate forming a weak acidic solution. Its reactions with amines are exothermic. The reaction is favored by low temperatures. The reaction with H_2S occurs instantaneously and reversibly (MANDAL; BANDYOPADHYAY, 2006).

Secondary reactions that need to be taken into account are (BARREAU *et al.*, 2006) presented in Equations 2, 3 and 4.

Dissociation of water:

$$H^+ + OH^- \leftrightarrow H_2O \quad (2)$$

Dissociation of hydrogen sulphide:

$$H_2S + H_2O \leftrightarrow HS^- + H_3O^+ \quad (3)$$

Dissociation of disulphide:

$$HS^- + H_2O \leftrightarrow S^{2-} + H_3O^+ \quad (4)$$

Reactions occurring in the liquid phase can be categorized into equilibrium-controlled reactions and kinetic-controlled reactions. The chemical reactions determine the ionic species compositions in the liquid phase (ZARE; MIRZAEI, 2009).

2.2 Thermodynamic Basis related to EoS

2.2.1 Soave Redlich-Kwong EoS

The SRK EoS (SOAVE, 1972) is a successful modification of the original Redlich-Kwong EoS. This equation has great acceptance in the oil and gas industry mainly because of its relative simplicity and accuracy in VLE calculations. One complication with this EoS is the limitation in the prediction of liquid density values. The equation generally predicts higher values than those found in the literature (ECHEVERRY; ACHERMAN; LOPEZ, 2017; JAVANMARDI; NASRIFAR; MOSHFEGHIAN, 2005).

Some authors have already suggested changes in the equation in order to generate better results without compromising the simplificity of the Equation (JI; LEMPE, 1997).

It can be considered the system pressure as the sum of the pressure of attraction and repulsion. The SRK repulsion pressure (P_R) is expressed by the van der Waals equation for the rigid sphere, Equation 5.

$$\boldsymbol{P_R = \frac{RT}{v - b}} \qquad \mathbf{5}$$

The term b is related to the chemical species proper volume. In the case of hard-sphere molecules, b is represented in Equation 6.

$$\boldsymbol{b = \frac{2\pi N\sigma^3}{3}} \qquad \mathbf{6}$$

Where σ is the molecule diameter:

The pressure of attraction (P_A) can be expressed by the Equation 7.

$$\boldsymbol{P_A = \frac{a(T)}{v(v + b)}} \qquad \mathbf{7}$$

The term a is related to the intermolecular attraction forces (Equation 8).

$$\boldsymbol{a(T) = a_0\left[1 + c_1\left(1 - \sqrt{\frac{T}{T_c}}\right)\right]^2} \qquad \mathbf{8}$$

Where a_0, b and c_1 are parameters of EoS.

a and b can be obtained through the substance's critical properties. For pure substances, the Equations 9 and 10 represent the expressions a and b based on the critical parameters:

$$a = 0.4278\frac{R^2T_c^{2.5}}{P_c} \quad (9)$$

$$b = 0.0867\frac{RT_c}{P_c} \quad (10)$$

The parameter c_1 can be obtained by the compound's acentric factor, according to Equation 11:

$$c_1 = 0,48508 + 1,55171w - 0,15613w^2 \quad (11)$$

2.2.2 Peng-Robinson EoS

The Peng-Robinson (PENG; ROBINSON, 1976) equation is also a cubic state equation, which is widely accepted in the oil and gas industry due to the quality of the results generated and its simplicity (KONTOGEORGIS, GEORGIOS M.; ECONOMOU, 2010) .

The explicit equation in terms of pressure is given in Equation 12:

$$P = \frac{RT}{v-b} - \frac{a(T)}{v(v+b)+b(v-b)} \quad (12)$$

The PR EoS term $b(v-b)$ is considered as an improvement of the attraction forces representation, which would cause the model to generate better liquid density results (ECHEVERRY; ACHERMAN; LOPEZ, 2017).

In a noticeably complete review, Echeverry (ECHEVERRY; ACHERMAN; LOPEZ, 2017) presented the most important modifications of the parameters proposed for the Peng Robinson model over the years.

2.2.3 Binary Parameters for SRK and PR

The binary parameter k_{ij} is remarkably important to fit the EoS predictions against the experimental data. Ideally, this parameter is obtained through binary mixture experimental data. However, it is known that this type of data is limited and is not available

for all the binaries involved in the simulated process. One way to overcome this limitation is to use empirical correlation models for k_{ij} (COUTINHO; KONTOGEORGIS; STENBY, 1994).

The binary parameters can be a function of temperature and depends on the experimental data quality (COUTINHO; KONTOGEORGIS; STENBY, 1994).

Often the zero value for k_{ij} is used when mixing alkane pairs. However, for mixtures containing other types of compounds, these parameters are relevant.

2.2.4 Molecular Based EoS

Complex thermodynamic systems, such as the system under study, require modern approaches to their description. Local composition models (CHAO; LEET; LAFAYETTE, 1983) and cubic EoS are not robust enough to describe a wide range of complex systems. Among the modern approaches its indispensable to mention those based on the theory of perturbation, based on the chemical theory and based on lattice theory (KONTOGEORGIS, GEORGIOS M., 2013).

2.2.5 Perturbation Theory and SAFT

The molecular association profoundly affects the phase equilibrium and the thermodynamic properties. Plentiful authors have attempted to explain and model this phenomenon, which occurs in several situations, such as polymer phases equilibrium, under high pressure conditions and supercritical conditions. One of these attempts is the Statistical Associated-Fluid Theory (SAFT), proposed by Chapman (CHAPMAN *et al.*, 1990), based on the first order perturbation theory of Wertheim (WERTHEIM, 1984).

Adopting a well-defined approach from Wertheim's work, the Helmholtz energy is written as the sum of different terms according to Equation 13.

$$\mathbf{A_{SAFT} = A_{ideal\ gas} + A_{hard\ sphere} + A_{chain} + A_{dispersion} + A_{association}} \qquad \mathbf{13}$$

Equation 13 represents the EoS SAFT written as a sum of Helmholtz energy terms. The choice of explicitly specifying a term in the sum is particularly important for the quality of the results obtained in the research.

Depending on how complex the EoS is, it can be quite laborious to transform it into terms derived from the Helmholtz energy. Bell and Jager (BELL; JÄGER, 2016) presented a way to transform cubic EoS (using a generic equation for such) in terms of Helmholtz energy, which they call the Helmholtz-energy-explicit EoS.

A major literature review was made by Vegas and Llovell (VEGA; LLOVELL, 2016) on the modeling of water and aqueous solutions using molecular based EoS. In this article the difficulties in modeling and the great importance in obtaining accurate and precise data considering the great industrial application of water were exposed. Three important models were discussed: Statistical Association Fluid Theory (SAFT), CPA (KONTOGEORGIS, G. M *et al.*, 1996) and Group Contribution Plus Association (GPA) (GROS; BOTTINI; BRIGNOLE, 1996). The systems used as examples were those that currently have greater expressiveness in chemical and energy industries: binary mixtures of water with hydrocarbons, amines, CO_2, alkanols and ionic liquids. An interesting point of attention of this review is that despite the large amount of experimental data and molecular parameters available in the literature, varied authors preferred the adequacy of their equation in relation to the experimental data, disfavoring the molecular theory involved. In this way, special care needs to be taken into account when using preconceived models.

2.2.6 Association Sites

The classical association schemes (1A, 2B, 3B and 4C) are widely applied in the models that use as basis the SAFT theory. The definition of these schemes is a fundamental step in the system thermodynamic modeling (KONTOGEROGIS; FOLAS, 2010). The association scheme follows the recommendations of nomenclature suggested by Huang and Radosz (HUANG; RADOSZ, 1990). Some compounds already have established molecular schemes that correspond greatly to reality (an example is water whose 4C scheme is the most

used) (GRENNER *et al.*, 2007). However, for higher complex compounds, the need to apply further bold molecular schemes is open for debate (since the classic models consider only one, two, three or four association sites). Some authors have already proposed other schemes trying to overcome the classical structure limitations and approaching the proposed model of reality (AVLUND *et al.*, 2011).This subject is considered one of the association theory area that deserves better examination (MOGENSEN, 2014).

Eight types of association schemes were designed based on the number and types of active sites of each molecule. In general, Schemes 2B and 3B are applied for amines and alcohols. Scheme 4C is used for substances with high association rate, which have two receptor protons and donors per molecule (such as water) (KONTOGEORGIS, GEORGIOS M. *et al.*, 2006).

Understanding what types of association (cross-associating, self-associating and non-associating) are present in the system is imperative to avoid an excess of parameters to be estimated in addition to bad results. Getting this clear perception is not an easy task since the associations can be quite complex (KONTOGEORGIS, GEORGIOS M., 2013).

Once the types of associations present in the mixture are determined and understood, it is important to choose how these interactions will be reflected in the model. One way is through mixing rules.

2.2.7 CPA EoS

It is notable that currently the most used cubic EoS are Peng-Robinson (PR) (PENG; ROBINSON, 1976) and Soave-Redlich-Kwong (SRK) (SOAVE, 1972), which represent an improvement of the EoS proposed by van der Waals. Unfortunately, these EoS are not designed to deal with molecules that have associating interactions (regardless of whether they are self-associating or cross-associating). This function is performed efficiently for several systems by CPA EoS, proposed by Kontogeorgis (KONTOGEORGIS, G. M *et al.*, 1996). This EoS combines SRK EoS with an adaptation of SAFT to be able to take into account the association interactions. Considerable number of papers (FARAMARZI *et al.*, 2009; KONTOGEORGIS, GEORGIOS M *et al.*, 1999; LINDVIG *et al.*, 2004; MOGENSEN; KONTOGEORGIS; THOMSEN, 2013; SANTOS *et al.*, 2015; TSIVINTZELIS; ALI; KONTOGEORGIS, 2015) prove the effectiveness of CPA in describing the thermodynamic

equilibrium of numerous systems. However, for some other systems, there is a need not only to accurately describe associative interactions but also the description of electrostatic interactions. A role that CPA alone, by its very conception, does not describe considerably (LIN, 2007). If it is desired to obtain results with great precision is important then to construct a thermodynamic model that establishes explicit these interactions and quantifies them. However, this is not the purpose of this work.

The CPA considers the interactions between different molecules (cross-association and solvation) and between identical molecules (self-association). In systems that are cross-association, there are associations between different compounds. However, the compounds may not be self-associating. The CPA association term is based on Wertheim's first-order thermodynamic perturbation theory (TPT-1) (KONTOGEORGIS, GEORGIOS M. *et al.*, 2006).

The initial objectives of the CPA were to extend the cubic EoS for the modeling of compounds that associate / polar compounds (KONTOGEORGIS, GEORGIOS M., 2013). Another CPA objective was to properly model multicomponent mixtures based only on binary interaction parameters (KONTOGEORGIS, GEORGIOS M. *et al.*, 2006). EoS SRK was used as the model physical basis; however, PR could also have been used. For the insertion in the model of a term that took into account the associations between the compounds, the Wertheim's theory (or of the perturbation) was chosen, being considered more comprehensive than other theories (lattice-fluid or chemical theory) (KONTOGEORGIS, GEORGIOS M. *et al.*, 2006).

One question that can be asked is: "Why work with the CPA instead of another EoS?". The answer is that CPA has proven to well describe common oil and gas industry systems over a wide range of temperature and pressure (KONTOGEORGIS, GEORGIOS M.; TASSIOS, 1997; KONTOGEORGIS, GEORGIOS M *et al.*, 1999; LINDVIG *et al.*, 2004). Also, CPA can describe mixtures where the water is in substantially small amount solubilized in hydrocarbons (and vice versa) (KONTOGEORGIS, GEORGIOS M., 2013). In addition, CPA has been used in several industrial applications over the years (SANTOS *et al.*, 2015).

SRK and PR cannot describe systems with highly immiscible compounds using only 1 interaction parameter. EoS in general, however, tend not to present as good results as

activity coefficient models when it comes to the prediction of condensed phase behavior (FREY; MODELL; TESTER, 2013). Both SRK and PR do not present satisfactory results for liquid phase densities. The results become worse as the study interval approaches the critical point (JI; LEMPE, 1997). The CPA can describe these systems over a wide range of temperatures using an interaction parameter, which is not temperature dependent.

In this section it was discussed the theoretical aspects of CPA EoS. All the mathematical details of the equation are found in the Methodology chapter.

2.2.8 Selection of Mixing Rules

The application of CPA for mixtures requires the use of mixing rules for only the parameters of the SRK term. It applies the van der Waals rule one-fluid rules (Equations 14 and 15):

$$\boldsymbol{a} = \sum_{i}\sum_{j} \boldsymbol{x_i x_j a_{ij}} \qquad \textbf{14}$$

$$\boldsymbol{b} = \sum_{i}\sum_{j} \boldsymbol{x_i x_j b_{ij}} \qquad \textbf{15}$$

The classic combining rules are used (Equations 16 and 17):

$$\boldsymbol{a_{ij}} = \sqrt{\boldsymbol{a_i a_j}}(\mathbf{1} - \boldsymbol{k_{ij}}) \qquad \textbf{16}$$

$$\boldsymbol{b_{ij}} = \frac{\boldsymbol{b_i} + \boldsymbol{b_j}}{\mathbf{2}}(\mathbf{1} - \boldsymbol{l_{ij}}) \qquad \textbf{17}$$

l_{ij} is a binary parameter, which in nearly all cases is set to zero. These parameters are not studied in this work.

If there is a cross-association, it is necessary to use the combining rules. Studies (KONTOGEORGIS, GEORGIOS M. *et al.*, 2006) have led to the conclusion that the CR-1 and Elliot rules are satisfactory (Equations 18 and 19):

$$\epsilon^{A_iB_j} = \frac{\epsilon^{A_iB_i} + \epsilon^{A_jB_j}}{2} \quad (18)$$

$$\beta^{A_iB_j} = \sqrt{\beta^{A_iB_i} \cdot \beta^{A_jB_j}} \quad (19)$$

In Elliot's combining rule, the geometric mean is used (Equation 20):

$$\Delta^{A_iB_j} = \sqrt{\Delta^{A_iB_i} \cdot \Delta^{A_jB_j}} \quad (20)$$

For the application of EoS for mixtures it is essential to handle mixing rules to define the mixture parameters. It's definition is fundamental to the quality of the results obtained (MATHIAS; KLOTZ; PRAUSNITZ, 1991). The choice of the most appropriate mixing rule depends on the characteristics of the system studied (PATEL; ABOVSKY; WATANASIRI, 1998) and it should be evaluated, among other things, whether the system is non-associating, cross-associating, self-associating or a combination of these. It's already known that the classic mixing rules are no longer sufficient to describe complex mixtures (KONTOGEORGIS, GEORGIOS M., 2013).

There is a plethora of references (ADACHI; SUGIE, 1986; HURON; VIDAL, 1979; ORBEY; SANDLER, 1996; ZAVALA; AROCHE; BAZÚA, 1996) in the literature that have presented new ideas and strategies for mixing rules over the years.

Several authors have developed their own mixing rules in order to better describe equilibrium system. Patel (PATEL; ABOVSKY; WATANASIRI, 1998) developed a mixing rule for the van der Walls EoS attraction parameter through perturbation theory. Their results showed a better description of hydrocarbons-alcohol and hydrocarbons-water systems.

2.2.9 Derivative Properties

The choice of thermodynamic properties to be generated by the model are fundamental to be judicious. It is known that the derived properties calculation (such as C_v, C_p and sound velocity) does not offer the same reliability in the obtained information when compared with the information related to the phase equilibrium (ABILDSKOV; KONTOGEORGIS, 2004; MAIA *et al.*, 2012) and this signify a limitation of association

theory. Kontogeorgis (KONTOGEORGIS, GEORGIOS M., 2013) states that cubic EoS such as SRK and CPA do not well represent some derivative properties. Different ways to get better results for these properties are by adding extra parameters to be estimated or actually improving model theory.

2.2.10 Modeling of alkanolamines

For the modeling of Acid Gases Absorption System by Alkanolamines, hereafter AGASA, there are several approaches. The most formal approach is one that considers the system's mass and heat transfer coefficients and their non-equilibrium, as mentioned in the Motivation. Chemical and mass transfer reactions can then be modeled using the Higbie Penetration Theory (MANDAL; BANDYOPADHYAY, 2006). Another strategy is the approach considering that the system has already reached the thermodynamic equilibrium.

Among the various theories that can describe the absorption of acid gases by amines from the mass transfer point of view, the theories of penetration, film and renewable surface are the most expressive. These theories most often require the resolution of a system of partial or ordinary differential equations that describe the species' concentration profile (GLASSCOCK; ROCHELLE, 1993).

In AGASA there is a molecular vaporized phase and a reactive liquid phase containing ionic and molecular species.

The thermodynamic equilibrium approach is often chosen over a more formal (non-equilibrium) approach (MEDEIROS; BARBOSA; ARAÚJO, 2013). The formal approach requires a large amount of information, such as chemical, physical and geometric parameters of the system, besides equilibrium constants, mass and heat transfer coefficients, kinetic constants, mass transfer coefficients / interfacial heat, kinetic coefficients, among others. It is then a challenge to implement this amount of information in process simulators (MEDEIROS; BARBOSA; ARAÚJO, 2013).

For those who prefer to adopt the thermodynamic equilibrium approach, one option is to use an EoS to describe the vapor phase and an activity coefficient model to describe the liquid phase. In other words, the thermodynamic modeling can be homogeneous (phi-phi) or heterogeneous (gamma-phi). The first employs the same equation to describe both liquid and

vapor phases. In the second, an activity coefficient model is used to describe the liquid phase and an EoS to describe the vapor phase.

For a broader purpose, Kontogeorgis (KAARSHOLM *et al.*, 2005) first studied the behavior of pure amines and their binaries (with water, alcohols and alkanes). Knowing that amines are compounds that self-associate and that form hydrogen bonds when bound to alkanes, the author carried out a study with the intention of understanding better the behavior of these compounds. According to the author, primary and secondary amines are compounds that self-associate and form non-ideal solutions with organic compounds. Tertiary amines, on the other hand, are not capable of self-association. Given that the decision of which association scheme to be used in the amine studies is not conclusive, Kontogeorgis (KAARSHOLM *et al.*, 2005) proposed a study to verify if for primary amines which of the 2B or 3B schemes would be more appropriate. The results indicated a small difference when using either scheme. Other important results were that using any of the Elliott or CR-1 combining rules it was possible to well describe the behavior of the VLE mixture of amines with alcohols using CPA. For the amine mixture with water the results were not satisfactory and the rule CR-1 performed better than the Elliot rule. Good results were obtained in the mixture of amines with alkanes using low values of k_{ij} .

In his work, Barreau (BARREAU *et al.*, 2006) adopted the heterogeneous approach, using PR to model the gas phase and NRTL to model the liquid phase. This approach was considered more adequate to model strongly asymmetric systems due to the particles electrolytic interactions. Zare (ZARE; MIRZAEI, 2009) used Electrolyte NRTL (for the liquid phase) and Amine Experimental EoS (for the gas phase).

An alternative to modeling is to combine the rigorous approach (from mass transfer) and the less rigorous approach (based on thermodynamic equilibrium). This was done by Glasscock (GLASSCOCK; ROCHELLE, 1993), who modeled the equilibrium using Electrolyte NRTL and proposed a general methodology for the absorption of acid gases considering chemical reactions.

Another approach is to use EoS for the description of balance. In this context it is possible to implement different combining rules, such as Valleé (VALLÉE *et al.*, 1999), which used the SRK associated with the Wong-Sandler mixing rule considering the

electrolytic interactions through a term based on the Mean Spherical Association Theory (MSA).

Medeiros (MEDEIROS; BARBOSA; ARAÚJO, 2013) in his work applied SRK and PR EoS to describe the behavior of liquid and vapor phases. The author models the system using an approach based on the Chemical Theory. In this approach he considered the formation of hypothetical non-volatile complexes in the liquid phase.

In AGASA the liquid phase is composed primarily of water and alkanolamine. Thus, the ions present in the solution may influence its properties (MEDEIROS; BARBOSA; ARAÚJO, 2013). This ionic interaction can be translated as solvation energies and hydrogen bonds, for example.

Some authors have modeled systems containing alkanolamines using CPA (AVLUND *et al.*, 2011; AVLUND; KONTOGEORGIS; MICHELSEN, 2008; SANTOS *et al.*, 2015; TSIVINTZELIS; ALI; KONTOGEORGIS, 2015). Avlund suggested the need to use other information to get the best set of parameters. Kontogeorgis suggested that among the possible additional information, liquid-liquid equilibrium (LLE) data are the most adequate to guarantee the best results in parameter estimation.

However, there was not much discussion about the parameter estimation strategy to be used for modeling systems containing alkanolamines. Santos (SANTOS *et al.*, 2015) then in her paper suggested two approaches to this estimation procedure (considering the utilization of LLE data in parallel or consecutively to the VLE information in each of the approaches).

A difference in the approach adopted by Santos that is different from the one used by other authors (AVLUND *et al.*, 2011; AVLUND; KONTOGEORGIS; MICHELSEN, 2008) is that in older works only a few parameters were checked against LLE experimental data, whereas in the methodology proposed by Santos (SANTOS *et al.*, 2015), all parameters obtained through the VLE could be checked against the LLE data, and therefore is used here.

Chapter 3

Methodology

This chapter is dedicated to clarifying the mathematical models employed here. This chapter describes the optimization methods used, the parameter estimation strategy, the CPA mathematical model presented and the Moving Window methodology (used in the statistical treatment of operational data obtained).

3.1 Optimization Methods

3.1.1 Particle Swarm Method (PSO)

The PSO algorithm is based on the collective intelligence of swarms. The methodology was described in 1995 by James Kennedy and Russel C. Eberhart (EBERHART; KENNEDY, 1995).

For a determined problem, there is a number of pre-defined particles and interactions, which sought to find the best solution. For this, each particle has information of its current speed, its best position found and the best position found by the side.

The particles evaluate the best solution where they were (particle minimum) and the best solution of the whole flock (global minimum).

The model was generated considering a space where the particles have position and velocity. Its new position is determined according to a weighting of the inertial terms, individual and collective, according to Equations 21 and 22:

$$v_{id}^{t+1} = w.v_{id}^{t} + c_1.w_1.(p_{id}^{t} - x_{id}^{t}) + c_2.w_2.(p_{gd}^{t} - x_{id}^{t}) \quad 21$$

v_{id}^{t+1} is the particle new velocity which is a function of w_1 and w_2 (which are random numbers between 0 and 1), the particle current speed v_{id}^{t}, the particle best position p_{id}^{t}, the particle current position x_{id}^{t}, the particle flock best position p_{gd}^{t} , the acceleration factors c_1 and c_2 (which increases the particle tendency to follow its best solution or the one of the flock) and the inertia factor *w* which determines the particle's tendency to continue to explore a particular region of space and not to vary its velocity so much.

$$x_{id}^{t+1} = x_{id}^{t} + v_{id}^{t+1} \quad 22$$

x_{id}^{t+1} is the particle new position, which is a function of its current position x_{id}^{t} and its new velocity v_{id}^{t+1}.

A new value of *w* is calculated at each interaction to decrease the weight value of the inertial term, according to Equation 23:

$$w = \frac{w_0 + (w_f - w_0)(k-1)}{Niter - 1} \quad 23$$

$Niter$ is the number of iterations, w_0 is the initial inertia factor and w_f is the final inertia factor.

Larger inertia factors favor space exploration. Minor inertia factors cause the new particle positions to be determined primarily by the best individual and global positions.

In all interactions it is checked whether the boundaries of the search region have been exceeded. If yes, the velocity is then updated to a new velocity with half the magnitude of the previous velocity, in the same orientation but in opposite directions (in the direction to return to the limits).

3.1.2 Simplex Method

The Simplex method (NELDER; MEAD, 1965) is a technique applied to determine, numerically, the optimal solution of a Linear Programming model. Simplex was chosen because it is a deterministic method relatively easy to implement. This method is used in

sequence of the application of a stochastic method (PSO), so its initial conditions will already be in theory close to a possible global minimum, facilitating the method convergence.

In general, the simplex method considers a number of $n + 1$ points that form a geometric figure when considering a plane of dimension n. Each of these geometric figures (or spatial coordinates) is formed by reflecting, contracting and/or expanding one of the points according to the objective function best direction. For such purpose, the method has three parameters, which represent each of the possible movements described (reflection parameter, contraction parameter and expansion parameter).

3.2 Parameter Estimation

3.2.1 Objective Function

The objective function definition is crucial in order to obtain good results in parameter estimation (APIO; BOTELHO; TRIERWEILER, 2017). In this work, for the studies involving pure substance VLE data it was considered the objective function according to Equation 24:

$$\boldsymbol{F_{obj} = \frac{1}{N_{exp}}\left[\sum_{i=1}^{N\,exp}\frac{(P_i^{calc} - P_i^{exp})^2}{\left(P_i^{exp}\right)^2} + \sum_{i=1}^{N\,exp}\frac{(\rho_i^{calc} - \rho_i^{exp})^2}{\left(\rho_i^{exp}\right)^2}\right]} \qquad \mathbf{24}$$

Where P_i^{calc} and ρ_i^{calc} are the vapor pressure and liquid density, respectively, calculated by the EoS. P_i^{exp} and ρ_i^{exp} are the experimental information.

The metric used for VLE calculations in mixtures is based on the bubble pressure calculation (Equation 25)

$$\boldsymbol{F_{obj} = \frac{1}{N_{exp}}\left[\sum_{i=1}^{N\,exp}\frac{(P_i^{calc} - P_i^{exp})^2}{\left(P_i^{exp}\right)^2}\right]} \qquad \mathbf{25}$$

The metric used for LLE calculations is based on the alkanolamine composition in the organic phase and the hydrocarbon in the polar phase (Equation 26).

$$F_{obj} = \frac{1}{N_{exp}} \left[\sum_{i=1}^{N\,exp} \frac{(x_{o,i}^{DEA,calc} - x_{o,i}^{DEA,exp})^2}{\left(x_{o,i}^{DEA,exp}\right)^2} + \sum_{i=1}^{N\,exp} \frac{(x_{p,i}^{HC,calc} - x_{p,i}^{HC,exp})^2}{\left(x_{p,i}^{HC,exp}\right)^2} \right] \qquad 26$$

Where $x_{o,i}^{DEA,calc}$ is the alkanolamine composition in the organic phase and $x_{p,i}^{HC,calc}$ is the hydrocarbon composition in the polar phase, calculated by the CPA EoS. While $x_{o,i}^{DEA,exp}$ and $x_{p,i}^{HC,exp}$ are the experimental data. N_{exp} is the number of experiments.

The objective functions adopted in this work are the same as those adopted by Santos (SANTOS *et al.*, 2015), since it is seeking to apply the same parameter estimation methodology proposed by this author.

3.2.2 Equilibrium Calculations

Regarding the parameter estimation strategy, Kontogeorgis (KONTOGEORGIS, GEORGIOS M. *et al.*, 2006) assembles some observations: the energy of association can be considered equal to the enthalpy of hydrogen bonding (which can be obtained by spectroscopy or calorimetry). This information can be used to check association energy values. Another suggestion is the utilization of LLE data from binaries mixtures of associated compounds and non-associated compounds (such as hydrocarbons) to determine the best set of pure parameters of the associated compounds. Other information that may be handled is the second virial coefficient and the fraction of monomers (obtained by spectroscopy). However, the former does not always provide pure parameters that can easily be used in mixtures and the second presents insufficient data available.

Avlund (AVLUND; KONTOGEORGIS; MICHELSEN, 2008) simulated hydrocarbon binaries mixtures with alkanolamines (DEA, MEA and MDEA). In that work it was concluded that data related to VLE are not sufficient to satisfactorily model these mixtures. Thus, another type of information would be needed for the proper simulation of these mixtures.

The optimization method for EoS parameter estimation is not something that is widely discussed in the literature. Santos (SANTOS *et al.*, 2015) proposed two parameter estimation strategies, both considering the LLE data of binaries mixtures (in the case of MEA with benzene and MEA with heptane).

The calculation strategy to be used here for the VLE and LLE calculations is proposed by Santos (SANTOS *et al.*, 2015), who has already proven that this strategy is effective for systems containing amines (Figure 3).

In this the work, as the first step, the parameters for pure MEA were estimated, without LLE data, using saturation pressure and liquid density data. The MEA was chosen as a didactic example, since it was the same alkanolamine chosen by Santos (SANTOS *et al.*, 2015) and therefore experimental data were available for results comparison.

In a second step, for the DEA, the complete methodology was used, including the LLE data.

In this methodology, after the selection of the best result sets using LLE data, a new comparison with the VLE data is studied, based on AAP% and AAρ% values.

For this work, it was chosen the estimation strategy that considers the LLE data sequential to the estimation using VLE data. This strategy is shown in Figure 3:

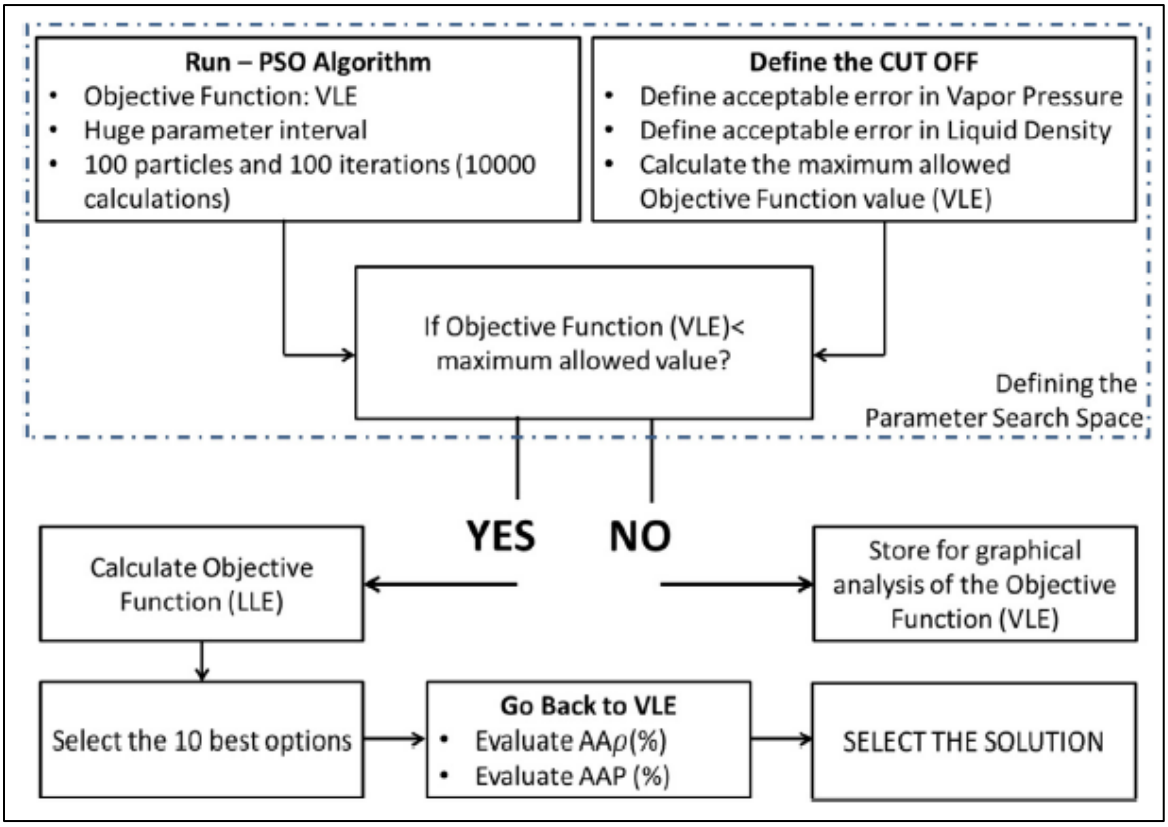

Figure 3 - Methodology chosen for the Estimation of Parameters
(obtained from (SANTOS *et al.*, 2015)**)**

Next, there is a detailed procedure on parameter estimation managed to obtain the best set of parameters:

1º) To define the parameter search region, apply the PSO using a large range for the parameters.

2º) According to the data experimental errors, define the maximum acceptable value for the objective function. For DEA, for example, DIPPR (Design Institute for Physical Properties) indicates errors less than 3% for vapor pressure and less than 5% for their liquid densities. As it is known, it is not possible for the model to present more reliable results than the experimental data. Therefore, if it is made the consideration that $P_i^{calc} = 1.05P_i^{exp}$ and $\rho_i^{calc} = 1.05\rho_i^{exp}$ and apply them in Equation 24, it is obtained Equation 27:

$$\boldsymbol{F_{obj} \leq 0.0050} \qquad \textbf{27}$$

Thus, objective function values below 0.0050 are statistically accepted (considering experimental errors).

3º) After obtaining the results using the VLE data, use the parameters considering the DEA and hydrocarbon LLE. The hydrocarbon is considered a compound that does not associate and its parameters are calculated based on its critical properties and acentric factor. An aliphatic hydrocarbon is the best solution because it can be considered an inert component, modeled by SRK. A consideration by Santos (SANTOS *et al.*, 2015) was that the association parameter β (Equation 28).

$$\boldsymbol{\beta_{ij} = \beta_{polar}} \qquad \mathbf{28}$$

At this stage, the binary parameter $k_{ij}$is equal to zero (Equation 29).

$$\boldsymbol{k_{ij} = 0} \qquad \mathbf{29}$$

4º) The 10 best results should be tested again using VLE data. The best selected one is used for k_{ij} estimation.

3.3 CPA Mathematical Model

The CPA Equation (KONTOGEORGIS, G. M *et al.*, 1996) is composed by a sum of two terms, one referring to the physical interactions, which is exactly the same as the SRK model. And the other term refers to the chemical association. The Equation 30 presents the equation:

$$\boldsymbol{P = \frac{RT}{V_m - b} - \frac{a(T)}{V_m(V_m + b)} - \frac{1}{2}\frac{RT}{V_m}\left(1 + \rho\frac{\partial lng(V_m)^{ref}}{\partial \rho}\right)\sum_i x_i \sum_{A_i}(1 - X_{A_i})} \qquad \mathbf{30}$$

Where *T* is the temperature, *P* is the pressure, *R* is the ideal gases universal constant, V_m is the molar volume, X_{A_i} is the mole fraction of molecules type i not bounded with site type A and x_i is the mole fraction of component i, $a(T)$ the energy parameter of the physical part and b is the covolume.

$a(T)$is calculated using Equation 31:

$$\boldsymbol{a(T) = a_0\left[1 + c_1\left(1 - \sqrt{T_R}\right)\right]^2} \quad \textbf{31}$$

$T_R$is the reduced temperature.

X_{A_i} is calculated using Equation 32:

$$\boldsymbol{X_{A_i} = \frac{1}{1 + \frac{1}{V_m}\sum_j x_j \sum_{B_j} \Delta^{A_i B_j}}} \quad \textbf{32}$$

Where $\Delta^{A_i B_j}$ is the intensity of association between the type *A* site on molecule *i* and the type B site on molecule *j*. This term is calculated using Equation 33:

$$\boldsymbol{\Delta^{A_i B_j} = g(V_m)^{ref}\left[\exp\left(\frac{\varepsilon^{A_i B_j}}{RT}\right) - 1\right] b_{ij}\beta^{A_i B_j}} \quad \textbf{33}$$

$\varepsilon^{A_i B_j}$ is the energy of association and $\beta^{A_i B_j}$ is the volume of association. $g(V_m)^{ref}$ is the radial distribution function for the reference fluid. The latter term can be calculated using Equations 34 and 35.

$$\boldsymbol{g(V_m)^{ref} = \frac{1}{1 - 1.9\xi}} \quad \textbf{34}$$

$$\boldsymbol{\xi = \frac{1}{4V_m} b} \quad \textbf{35}$$

ξ is the fluid reduced density.

3.4 Moving Window Methodology

The moving window methodology is related to the characterization of the process in terms of steady state information. In the thermodynamic study, this non-stationary information is undesirable, since it is preferable that the chemical species are near the steady state and operational transients do not have great influence on the results.

By calculating the variances and correlation coefficients of the data sets, the one with the lowest correlation coefficient is usually the best candidate of the analyzed period to

consider that the selected data set is near the steady state. It follows a numeric example for better understanding (Table 1).

Table 1 - Numerical example of hypothetical operational data to simplify the understanding of the calculation of the correlation coefficient and its interpretation in the analysis of the interdependence between data.

N°	Date	Temperature °C
1	13-Apr-18 22:00:00	43.368
2	13-Apr-18 22:20:00	43.185
3	13-Apr-18 22:40:00	43.002
4	13-Apr-18 23:00:00	42.966
5	13-Apr-18 23:20:00	42.980
6	13-Apr-18 23:40:00	42.993

Considering a window composed of five data, through Table 1, it is possible to consider two data windows, one starting at 22:00 and ending at 23:20 (number 1 through 5) and the second window starting at 22:20 and ending at 23:40 (number 2 through 6). Comparing the two windows, the correlation coefficient is 0.900. Thus, the data above indicate transience and therefore are not the most suitable for the steady state system study. The correlation coefficient calculation is facilitated by the Excel function CORREL.

The confidence interval indicates how close the obtained data is to the actual values (SCHWAAB; PINTO, 2007). When this range is large, numerous values are contained in these and the range of acceptable values is large. The results reliability is relatively low. When the confidence interval is narrower, the acceptable values are closer to the measured values and therefore their reliability is considerably high (SCHWAAB; PINTO, 2007).

Table 2 - Numerical example of hypothetical operational data to simplify the understanding of confidence interval calculation. 95% of confidence level was considered.

Moving Window	Average Values	Confidence Interval
1	43.100	[42.884; 43.316]
2	43.025	[42.913; 43.137]

Working with the already mentioned example, it is possible calculate the confidence intervals through the Excel's function INT.CONFIANÇA.T. For this, the Student's t corresponding to 95% confidence level is used.

According to Table 2, it can be concluded that the moving window 2 presents more reliable data than those of moving window 1, since its confidence interval is narrower. In other words, the difference between the upper and lower limits of moving window 2 (0.224) is smaller than the difference in moving window 1 (0.432).

It is important to mention that there are more complex and sophisticated statistical treatments to analyze the influence of transience on data, but nevertheless, for the industrial application, it was concluded that the moving window methodology was adequate for the operational data statistical treatment to be presented in Chapter 4.

3.5 Process Simulation in Petrox

The parameter estimation is performed in the ThermOptimizer software, which interface is according to Figure 4:

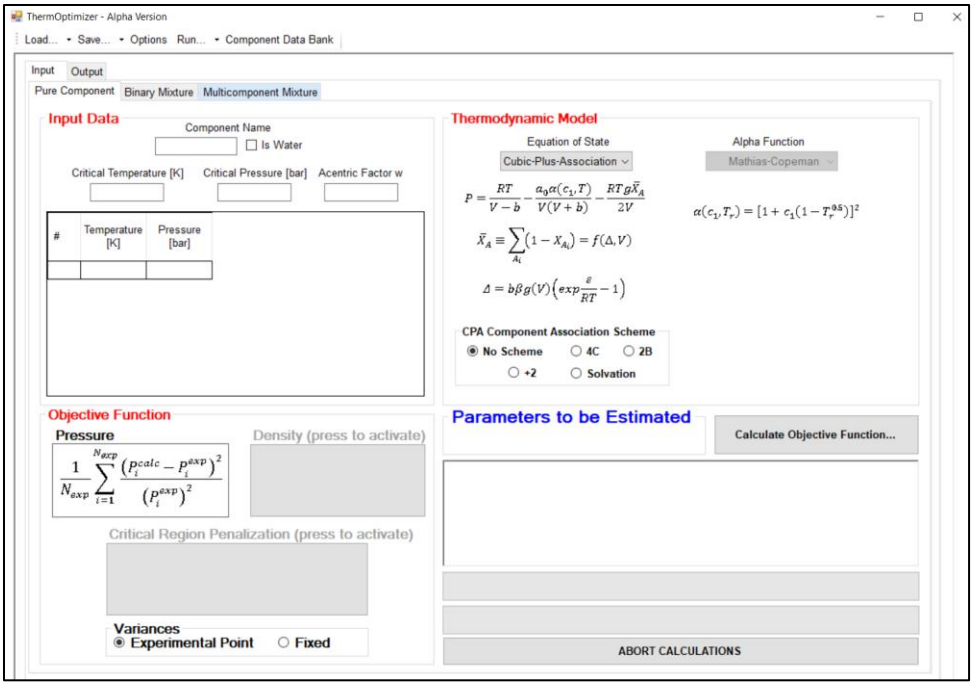

Figure 4 - ThermOptimizer Software Interface

(Software adopted in the parameter estimation in this work).

In order to proceed with parameter estimation, it was necessary to obtain experimental data from a reliable database. For this reason, data were extracted from the Design Institute for Physical Properties (DIPPR) database (DIADEM, 2004).

The mathematical strategy employed to obtain the global minimum of the objective function was to use a stochastic method (PSO) first with the subsequent application of a deterministic method (SIMPLEX). The PSO conducted a wide sweep in the parameters feasible region to search for the global minimum and map the local minimums. Thus, its best results were used as an initial condition so that the deterministic method could find the best set of values that minimized the objective function.

A problem in the search for the global minimum is the presence of local minimums. One way to overcome this difficulty is to use a stochastic search method that scans through large regions looking for the global minimum and identifies the presence of local minimas (SCHWAAB; PINTO, 2007). This long-range scanning is not something characteristic of the deterministic method. Thus, adopting only the SIMPLEX Method, it would be possible that the results obtained did not correspond to the global minimum of the search region.

The first modeled component was MEA, since there were available in the literature equilibrium data of this pure component associated to a proposed parameter estimation strategy. In addition, its parameter estimation procedure had a character of comparison between the different EoS (CPA, SRK and PR), adopting the same parameter estimation strategy for each EoS. It is important to note that the alkanolamine MEA is not present in the industrial gas absorption unit to be simulated. Its parameter estimation is didactic and comparative in relation to the efficiency of the thermodynamic equilibrium prediction using different EoS.

After that, the DEA compound was studied, taking into consideration its modeling using VLE and LLE data (details will be demonstrated in the next sections). The parameters obtained in this step were inserted in the Petrox simulator.

The Petrox software is a process simulator developed by Petrobras and in an article published in 2015 (SANTOS *et al.*, 2015), the authors present the structure of this tool and the implementation procedure of EdE CPA in the software using the CERE / DTU dll. During this development, the DEA parameters were inserted into the PETROx database to expand the previously incorporated model.

Chapter 4

Results and Discussion

4.1 Pure MEA Parameter Estimation

As mentioned, two optimization methods were adopted to estimate the parameters of the pure compounds (PSO and Simplex). In all simulations the same internal PSO parameters were used (excluding number of particles and number of iterations) and SIMPLEX. This information can be found in the

Table 3 and Table 4.

Table 3 - PSO parameters for EoS Analysis for Pure MEA parameter estimation.

PSO Parameters	
Maximum number of iterations	200
Maximum number of species	100
Individual Factor c_1	1
Global Factor c_2	0.1
Inertia Factor w_0	0.9
Inertia Factor w_f	0.001
Tolerance	0.0001

The PSO parameters and Simplex parameters used are those that are part of the ThermOptimizer default. It was not the scope of this study to evaluate the impact of these numbers on the results obtained in the thermodynamic parameter estimation.

In order to compare the results between the different EoS, the same parameter limits for the EoS equations were used (a_0, b and c_1). The epsilon and beta parameters are only found in CPA EoS. It was necessary for the parameter limits to satisfy the three EoS (enabling the optimization method to converge). For that, tests were carried out that led to the set of intervals presented in Table 5. There was concern that no parameter was limited by the mathematical range imposed. The limits presented in Table 5 are those of ThermOptmizer default.

Table 4 - SIMPLEX parameters for EoS Analysis for Pure MEA parameter estimation.

SIMPLEX Parameters	
Maximum number of iterations	1000
Reflection Factor Alpha	1
Contraction Factor Beta	0.5
Expansion Factor Gamma	2

Table 5 - Parameters Constraints for the Cubic EoS and CPA for Pure MEA parameter estimation. Parameters a_0, b and $c_1$were used for all equations and epsilon and beta parameters were used only for CPA. Equilibrium data from DIPPR(DIADEM, 2004).

Parameters	Lower Bounds	Upper Bounds
a_0 (bar.L^2/mol^2)	8	40
b (L/mol)	0.01	0.1
c_1	0.1	2.0
ε/R (K)	100	2500
β.10^3	0.1	100

As an additional way to compare the results of the executions using the different EoS, common in literature (AVLUND; KONTOGEORGIS; MICHELSEN, 2008; SANTOS *et al.*, 2015; TSIVINTZELIS *et al.*, 2011) and therefore managed in this work as a metric, is the Average Absolute Deviation of the Pressures (AAP%), defined according to Equation 36:

$$\boldsymbol{AAP\%} = \left(\frac{\boldsymbol{100}}{\boldsymbol{N_{exp}}}\right)\sum_{\boldsymbol{k=1}}^{\boldsymbol{N_{exp}}}\left|\frac{(\boldsymbol{P_k^{exp}} - \boldsymbol{P_k^{calc}})}{\boldsymbol{P_k^{exp}}}\right| \qquad \textbf{36}$$

N_{exp} is the number of experiments.

P is the saturation pressure.

Superscript exp means experimental and $calc$ means calculated.

The MEA parameters were estimated using the three EoS (CPA, SRK and PR) and the results are presented in Table 6:

Table 6 - Comparison between three different EoS (CPA, SRK and PR). Pure MEA parameter estimation. Equilibrium data from DIPPR(DIADEM, 2004).

EoS	Optimization Method	Parameters					
		a_0 $\left(\frac{bar \cdot L^2}{mol^2}\right)$	b $\left(\frac{L}{mol}\right)$	c_1	F_{obj}	AAP%	Iterations
PR	PSO	17.670	0.055	1.218	$5.150.E^{-3}$	-	76
	Simplex	17.671	0.055	1.218	$5.150.E^{-3}$	5.276%	69
SRK	PSO	15.497	0.055	1.261	$3.285.E^{-3}$	-	73
	Simplex	15.468	0.055	1.262	$3.279.E^{-3}$	4.521%	79
CPA	PSO	9.332	0.055	1.338	$2.089.E^{-3}$	-	74
	Simplex	13.874	0.056	0.946	$5.620.E^{-4}$	1.694%	981

According to Table 6, it can be concluded that CPA presented better results than the other two EoS, which means that CPA can possibly better predict MEA equilibrium behavior than the other equations. Therefore, the study continued using CPA EoS. One point of attention is that the parameters estimation using CPA required a greater number of Simplex iterations than SRK and PR. An explanation for this fact may be the need to adjust 2 extra parameters (epsilon and beta) compared to the other two EoS.

In order to validate the results generated in the chosen parameter estimation strategy, the results generated for MEA were compared with the literature (SANTOS, *et al.*, 2015). Table 7 presents the results of this comparison.

The comparison with the literature was satisfactory and thus validate the Pure MEA parameter estimation results. According to Table 7, the results were slightly better (1.694 %) than those in the literature (3.905 %), regarding the AAP% values.

Table 7 - Pure MEA parameter estimation results comparison with literature data (SANTOS *et al.*, 2015). Parameter estimation applying the CPA EoS. Equilibrium data from DIPPR(DIADEM, 2004).

	a_0 $\left(\frac{bar \cdot L^2}{mol^2}\right)$	b $\left(\frac{L}{mol}\right)$	c_1	ε $\left(\frac{bar \cdot L^2}{mol}\right)$	1000* β	AAP%
MEA Estimate	13.874	0.056	0.946	140.060	11.600	1.694%
MEA Literature	14.382	0.055	0.627	184.210	4.730	3.905%

Next some graphs generated for the thermodynamic modeling contemplating the calculations of saturation pressure curves, liquid density and parametric analysis.

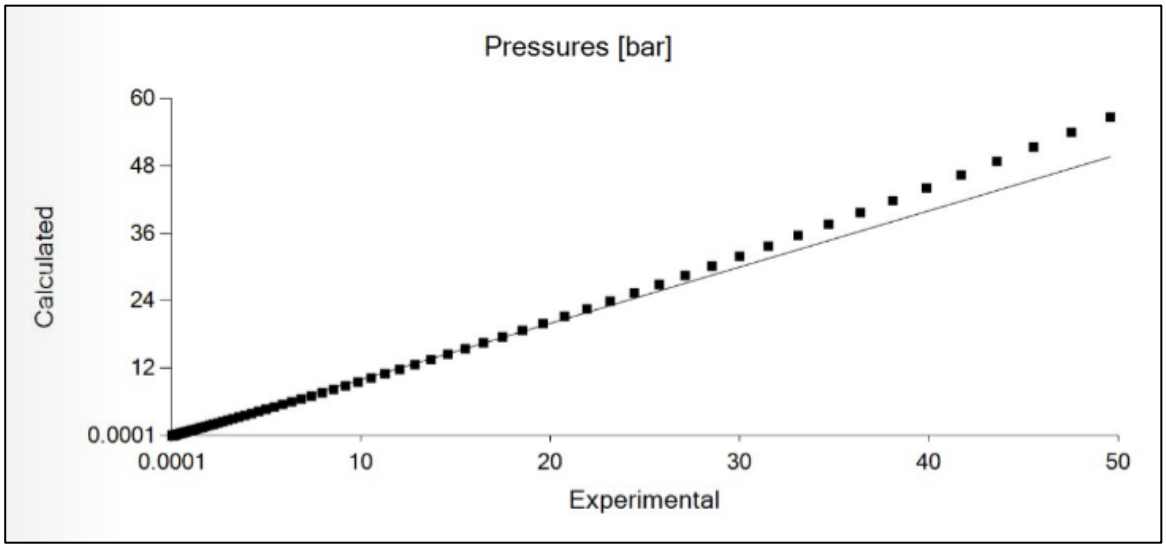

(a)

Figure 5 - Pure MEA using PR EoS. a) Saturation pressures b) Liquid Densities c) Saturation Curve. Solid line represents the data calculated by the thermodynamic model. The dotted line represents the experimental data. 100 experimental points were used between 0.42 - 0.90 T_R. MEA experimental data from DIPPR(DIADEM, 2004).

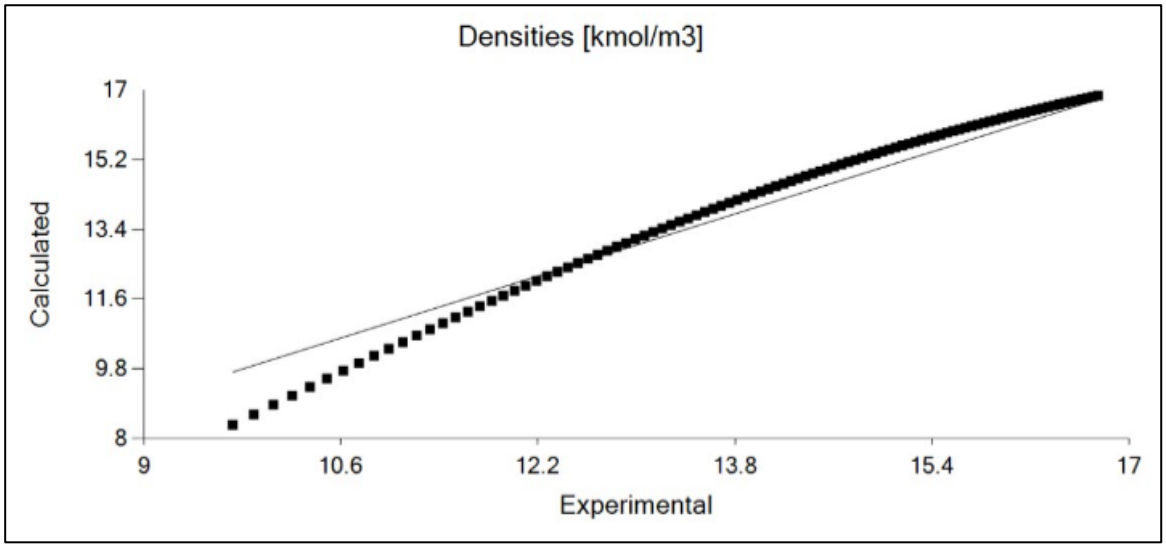

(b)

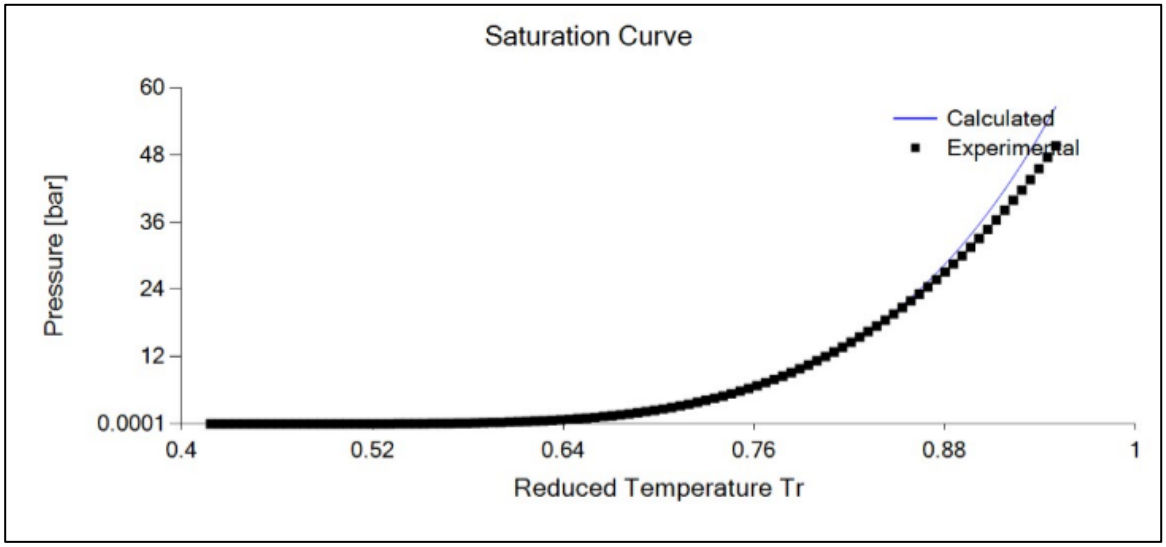

(c)

Figure 5 (continuation)- Pure MEA using PR EoS. a) Saturation pressures b) Liquid Densities c) Saturation Curve. Solid line represents the data calculated by the thermodynamic model. The dotted line represents the experimental data. 100 experimental points were used between 0.42 - 0.90 T_R. MEA experimental data from DIPPR(DIADEM, 2004).

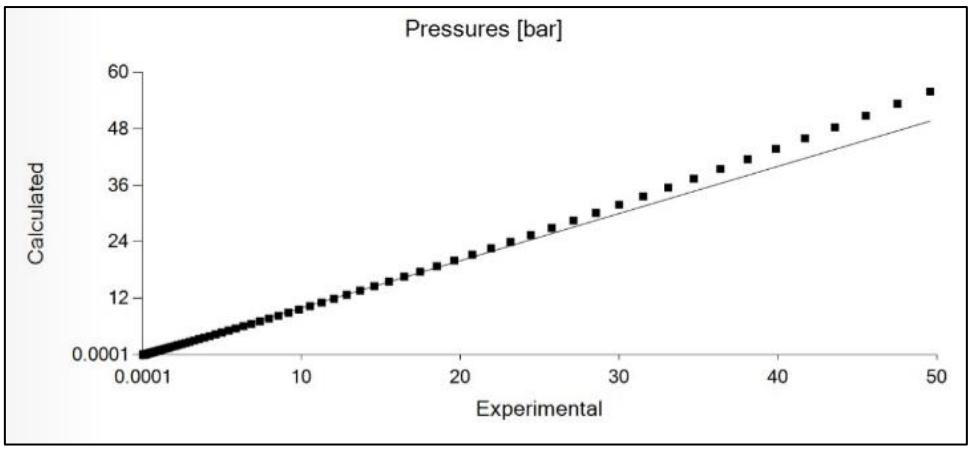

(a)

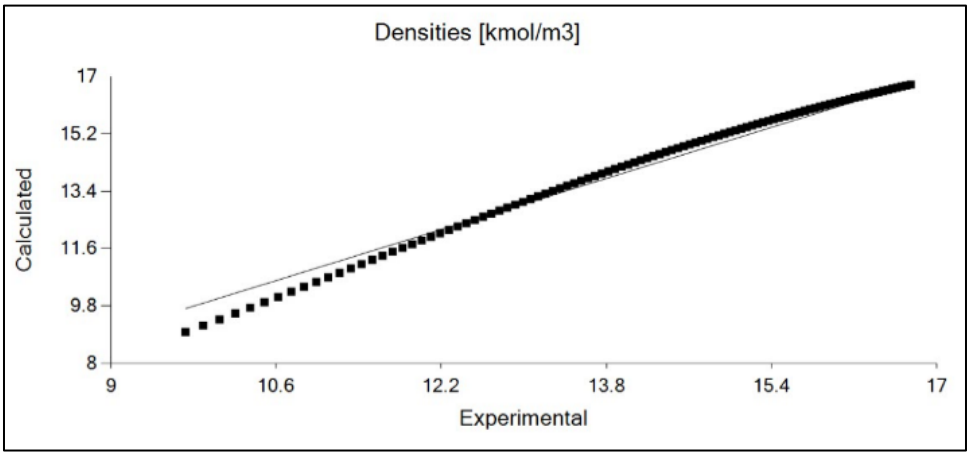

(b)

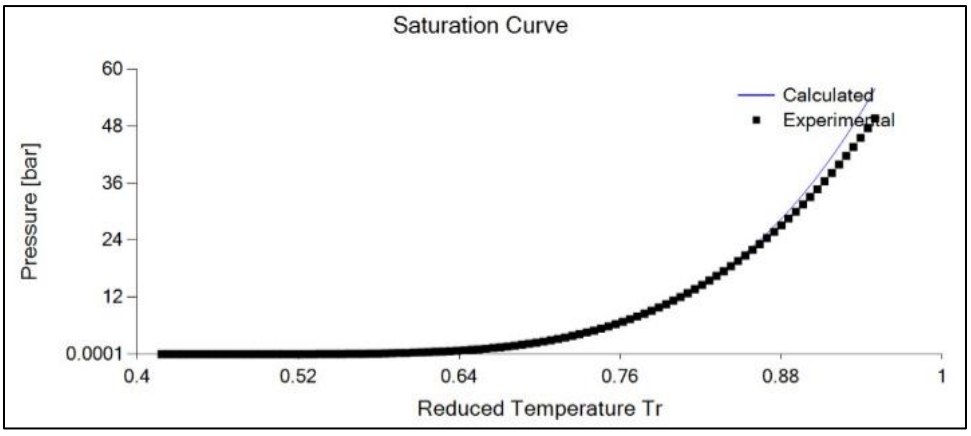

(c)

Figure 6 - Pure MEA using SRK EoS. a) Saturation pressures b) Liquid Densities c) Saturation Curve. The solid line represents the data calculated by the thermodynamic model. The dotted line represents the experimental data. 100 experimental points were used between 0.42 - 0.90 T_R. MEA experimental data from DIPPR(DIADEM, 2004).

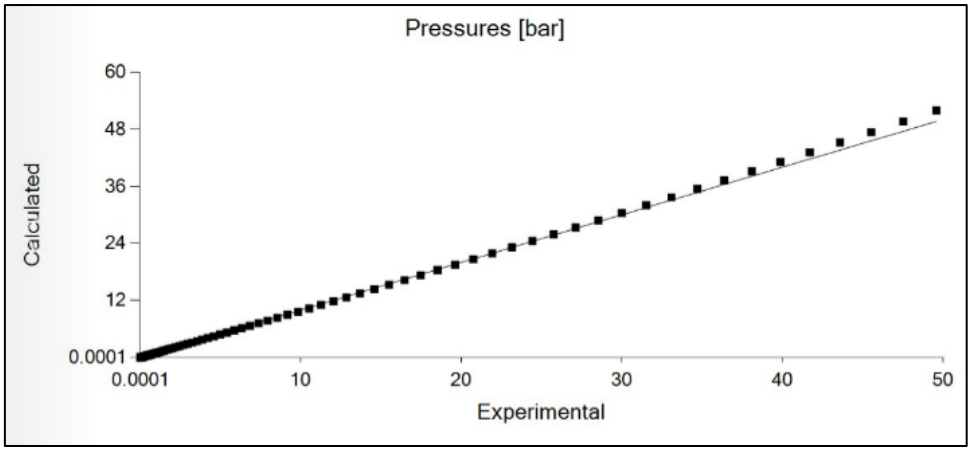

(a)

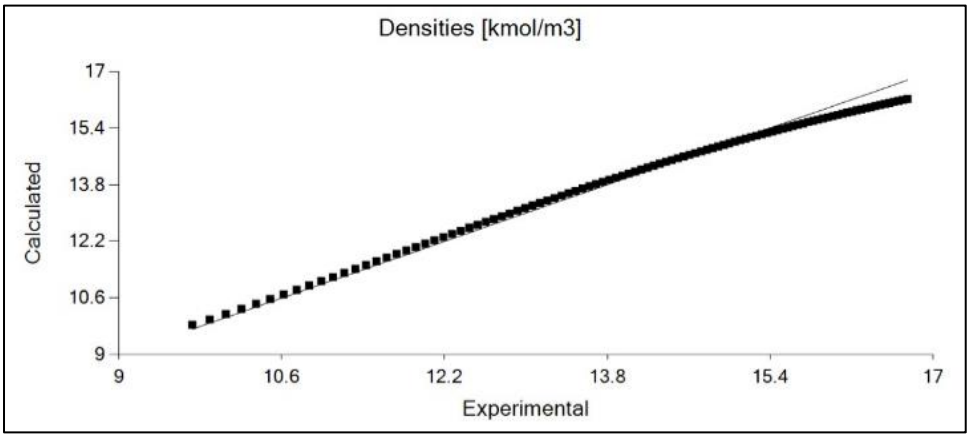

(b)

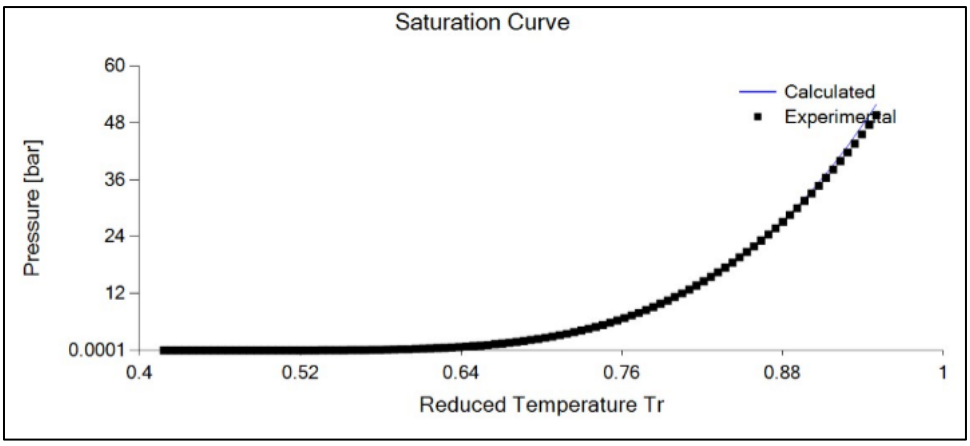

(c)

Figure 7 - Pure MEA using CPA EoS a) Saturation pressures b) Liquid Densities c) Saturation Curve. The solid line represents the data calculated by the thermodynamic model. The dotted line represents the experimental data. 100 experimental points were used between 0.42 - 0.90 T_R. MEA experimental data from DIPPR(DIADEM, 2004).

Based on Figure 5, Figure 6 and Figure 7, it is possible to observe visually, not only by the numerical values commented on in the Table 7, that CPA has the potential to model polar compound, since it presents satisfactory results, compared with the other EoS.

According to Santos(SANTOS *et al.*, 2015), The DIPPR database indicates for MEA errors less than 10% in the vapor pressure and less than 3% in the liquid densities. Since it is not expected to have a model with more reliable data than the experimental data, assuming that the limit values for the experimental pressure is $P_i^{sat,calc} = 1.1P_i^{exp}$ and for the experimental liquid density is $\rho_i^{sat,calc} = 1.03\rho_i^{exp}$, the maximum acceptable value for the objective function is 0.0109 (applying this concept in Equation 36).

Here are the graphs (Figure 8) generated with the CPA parametric analysis. These graphs were generated in the region where the maximum objective function is 0.0109, then all points in the graph are possible regions mathematically and thermodynamically speaking.

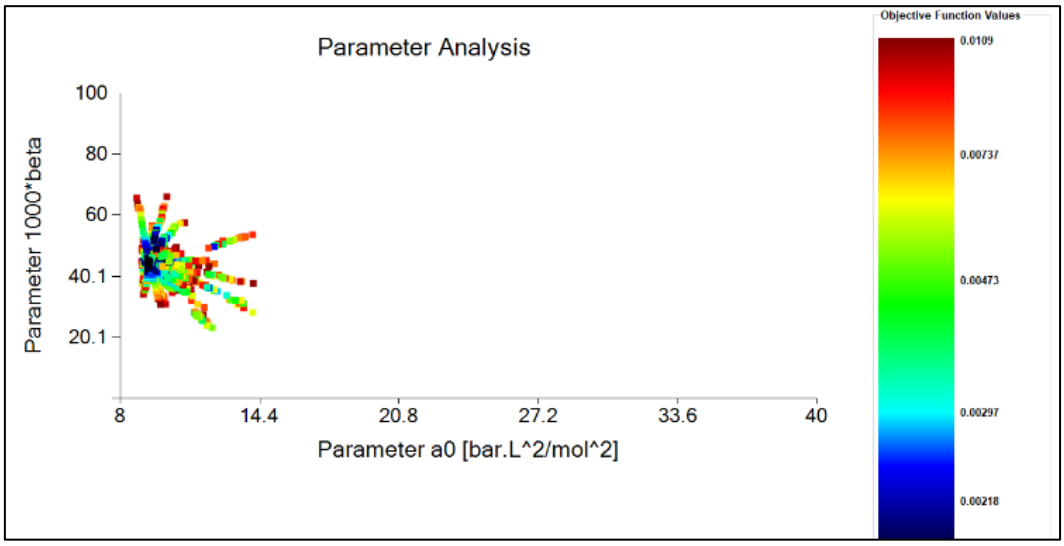

(a)

Figure 8 - Parametric Analysis of Pure MEA parameter estimation with CPA. (a) beta – a_0; (b) b – a_0; (c) c_1– a_0; (d) eps/R – a_0; (e) beta – b; (f) c_1– b; (g) eps/R – b; (h) beta – c_1; (i) eps/R – c_1; (j) beta – eps/R. Parameters estimated using optimization method PSO. Maximum number of 200 iterations and 200 particles. The maximum objective function value considered is 0.0190. 100 experimental points were used between 0.42 - 0.90 T_R. Experimental data from DIPPR (DIADEM, 2004).

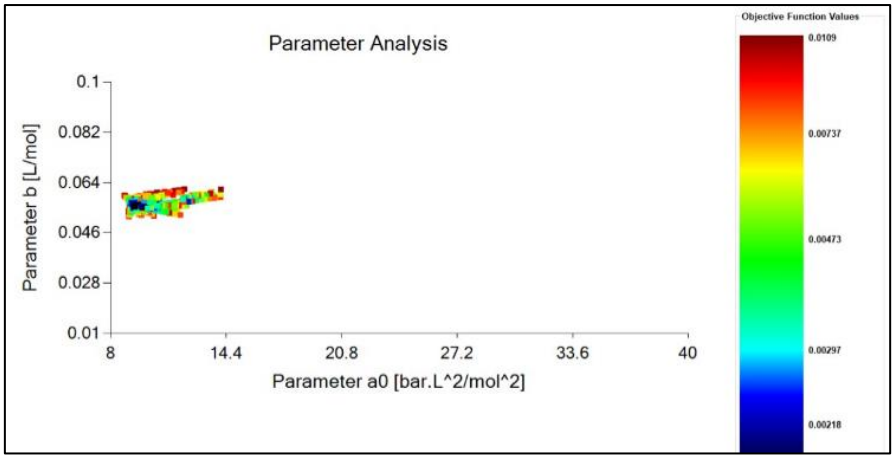

(b)

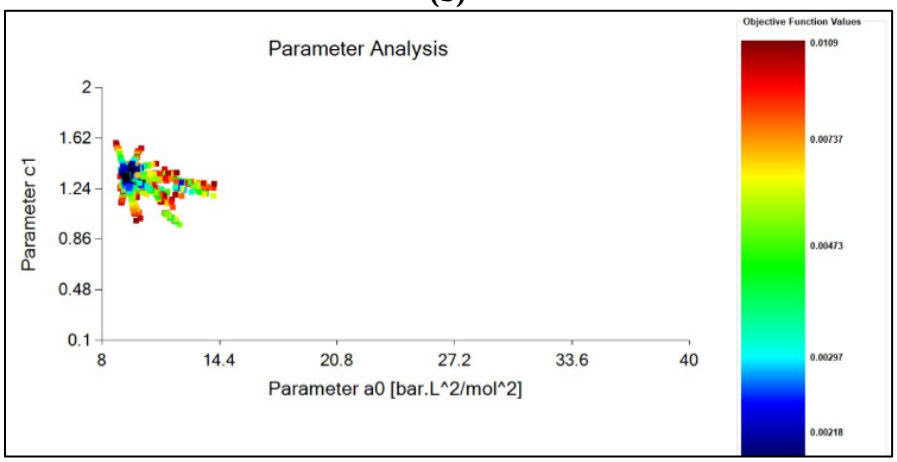

(c)

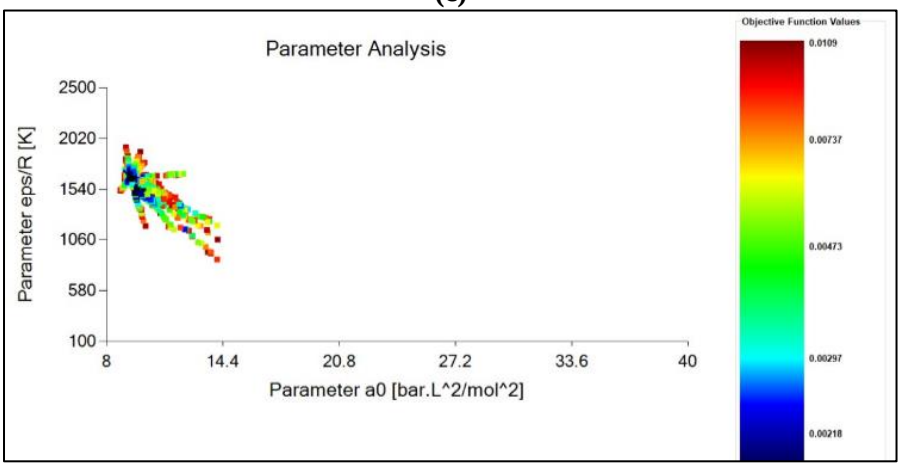

(d)

Figure 8 (continuation) - Parametric Analysis of Pure MEA parameter estimation with CPA. (a) beta – a_0; (b) b – a_0; (c) c_1– a_0; (d) eps/R – a_0; (e) beta – b; (f) c_1– b; (g) eps/R – b; (h) beta – c_1; (i) eps/R – c_1; (j) beta – eps/R. Parameters estimated using optimization method PSO. Maximum number of 200 iterations and 200 particles. The maximum objective function value considered is 0.0190. 100 experimental points were used between 0.42 - 0.90 T_R. Experimental data from DIPPR (DIADEM, 2004).

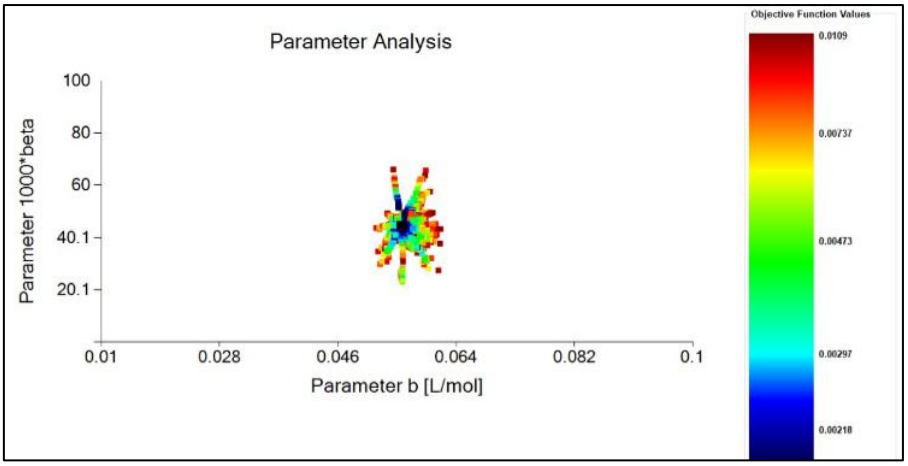

(e)

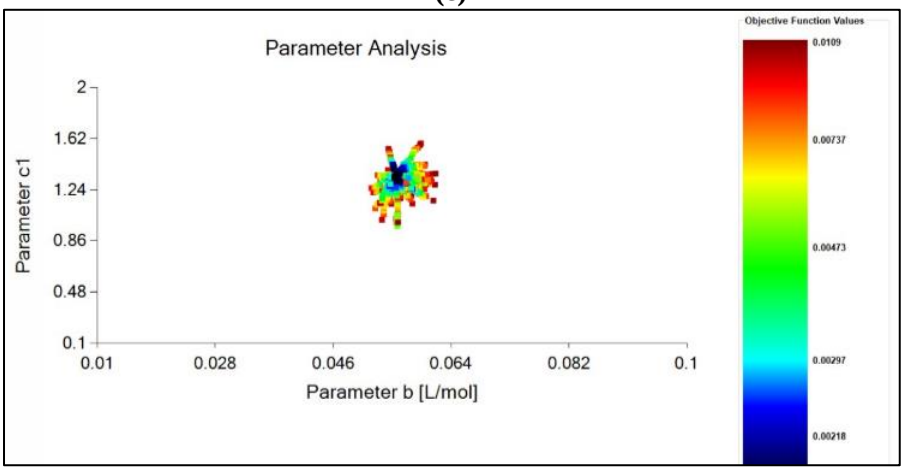

(f)

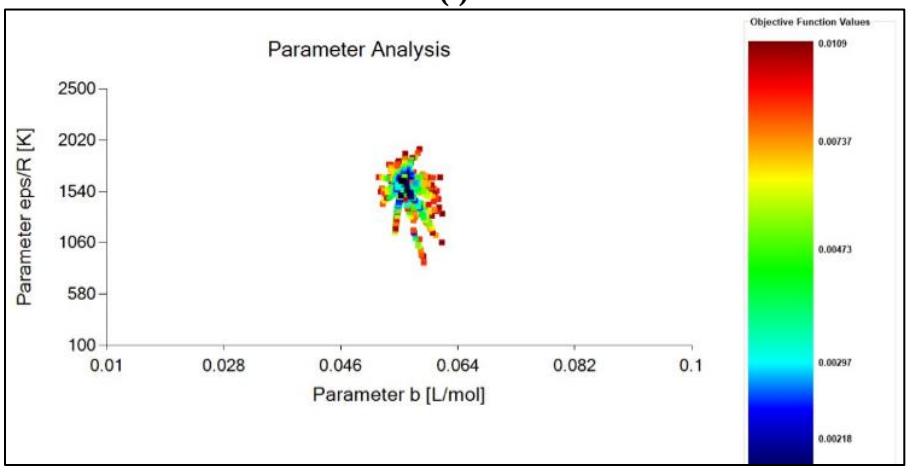

(g)

Figure 8 (continuation) - Parametric Analysis of Pure MEA parameter estimation with CPA. (a) beta – a_0; (b) b – a_0; (c) c_1– a_0; (d) eps/R – a_0; (e) beta – b; (f) c_1– b; (g) eps/R – b; (h) beta – c_1; (i) eps/R – c_1; (j) beta – eps/R. Parameters estimated using optimization method PSO. Maximum number of 200 iterations and 200 particles. The maximum objective function value considered is 0.0190. 100 experimental points were used between 0.42 - 0.90 T_R. Experimental data from DIPPR (DIADEM, 2004).

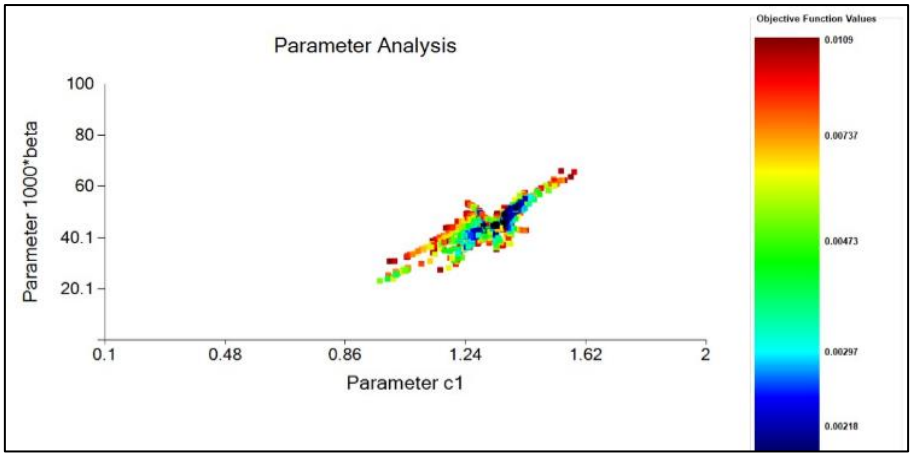

(h)

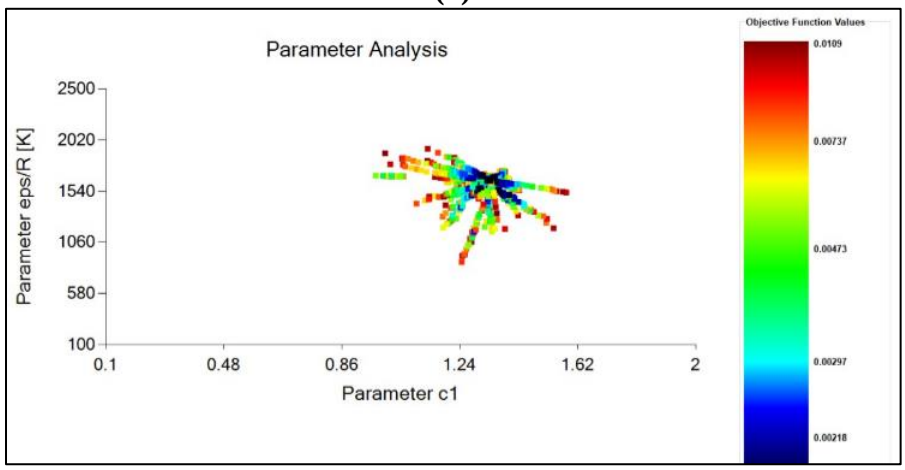

(i)

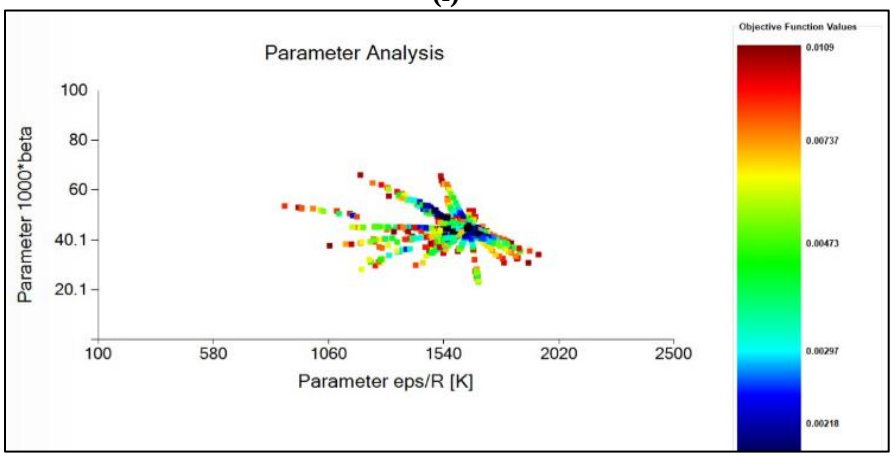

(j)

Figure 8 (continuation) - Parametric Analysis of Pure MEA parameter estimation with CPA. (a) beta – a_0; (b) b – a_0; (c) c_1– a_0; (d) eps/R – a_0; (e) beta – b; (f) c_1– b; (g) eps/R – b; (h) beta – c_1; (i) eps/R – c_1; (j) beta – eps/R. Parameters estimated using optimization method PSO. Maximum number of 200 iterations and 200 particles. The maximum objective function value considered is 0.0190. 100 experimental points were used between 0.42 - 0.90 T_R. Experimental data from DIPPR (DIADEM, 2004).

In Figure 9 (a, c, d and e) it is possible to visualize the presence of local minimas. If only the Simplex method were used, it could find a local minima region and the method would converge in this area; unlike the PSO, which, through its various particles, searches for the best individual and flock result and thus is able to identify these regions. Hence it is clear the importance of using a stochastic method before using a deterministic one to identify these local minima and to find the global minimum.

Once Pure MEA parameter estimation and its validation with the literature were completed, the DEA parameter estimation were then followed.

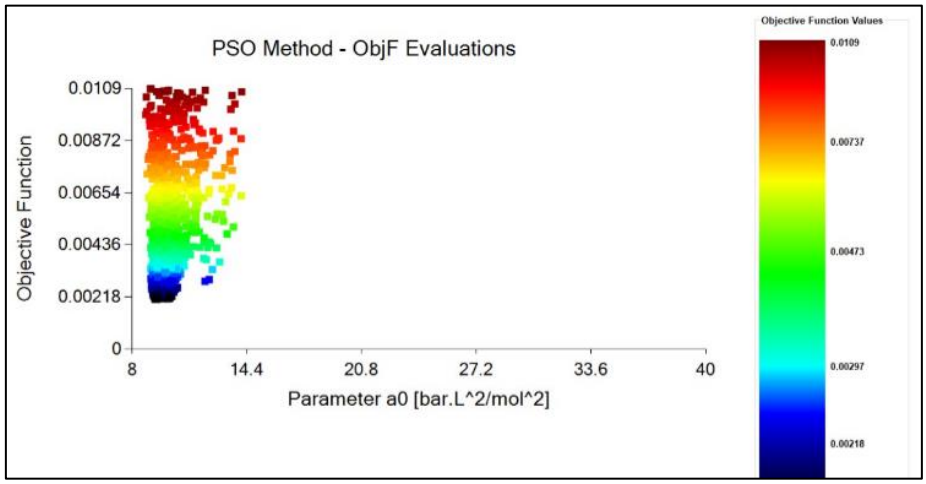

(a)

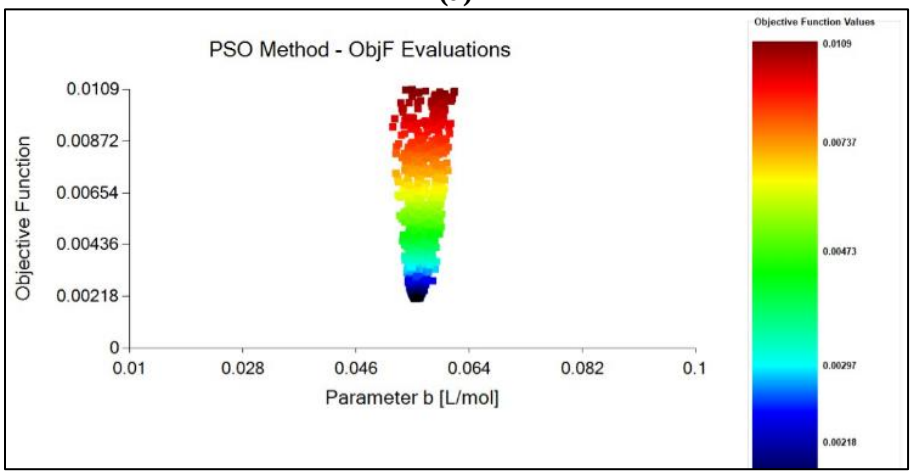

(b)

Figure 9 - Parametric Analysis of Pure MEA parameter estimation with CPA. (a) $F_{obj} - a_0$; (b) $F_{obj}-b$; (c) $F_{obj}-c_1$; (d) F_{obj}– eps/R; (e) F_{obj}– beta. Parameters estimated using optimization method PSO. Maximum number of 200 iterations and 200 particles. The maximum objective function value considered is 0.0190. 100 experimental points were used between 0.42 - 0.90 T_R. Experimental data from DIPPR(DIADEM, 2004).

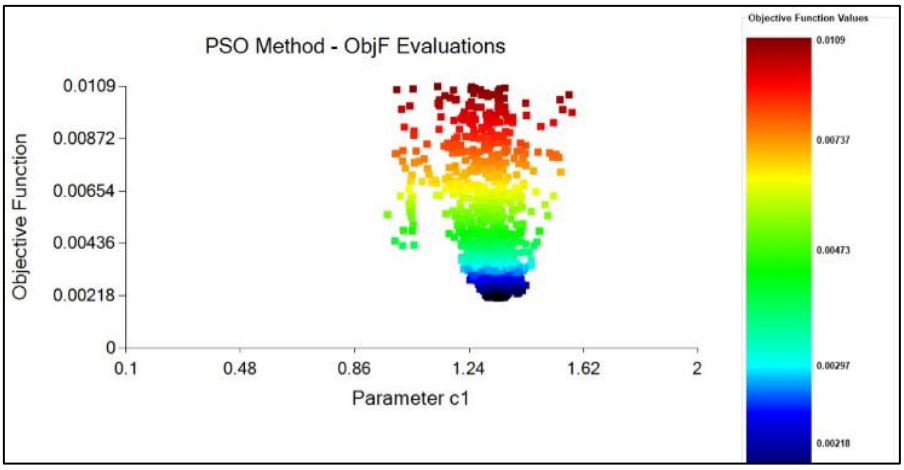

(c)

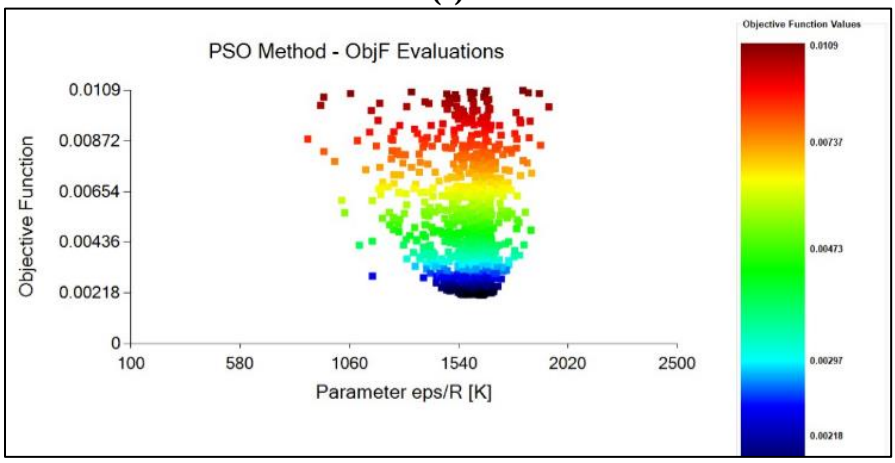

(d)

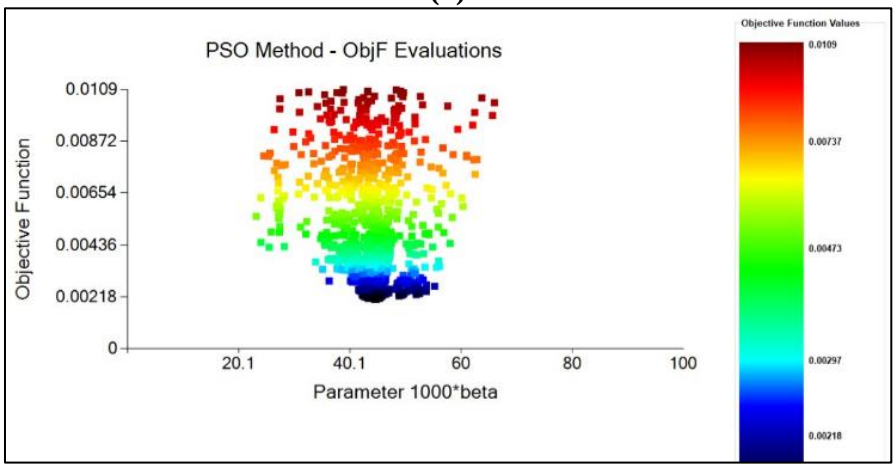

(e)

Figure 9 (continuation)- Parametric Analysis of Pure MEA parameter estimation with CPA. (a) $F_{obj} - a_0$; (b) $F_{obj}- b$; (c) $F_{obj}- c_1$; (d) $F_{obj}-$ eps/R; (e) $F_{obj}-$ beta. Parameters estimated using optimization method PSO. Maximum number of 200 iterations and 200 particles. The maximum objective function value considered is 0.0190. 100 experimental points were used between 0.42 - 0.90 T_R. Experimental data from DIPPR(DIADEM, 2004).

4.2 Pure DEA Parameter Estimation

In order to obtain the pure DEA final parameters, several simulations were carried out aiming to guarantee a global minimum. For this, the first estimates considered wide intervals of the parameters. In this way, the stochastic method, PSO, could search for a wide area, searching for the global minimum and also identifying local minima (which were visually recognized). At each new simulation, the parameter intervals became smaller and smaller, and so did the objective function.

Once the final parameter interval was determined, a new simulation was carried out with a large number of particles and interactions, in order to guarantee greater accuracy in the estimated final parameters.

4.2.1 A didactic way of understanding the simulations workflow

In the parameter estimation step, hundreds of simulations were performed until the final parameters of each compound could be obtained. For the presentation in this work, key simulations were selected, which facilitate the step-by-step understanding of the methodology used to obtain the final ones.

The 12 main simulations performed to estimate the pure DEA parameters are presented next. They can be sectorized into three types:

1º) Initial simulations (simulations 1, 2 and 3), using several particles and iterations in the PSO, considering large parameters intervals. Its purpose is to map favorable search intervals and identify local minimas.

2º) Simulations of trial and error (simulations 4, 5, 6, 7, 8, 9 and 10), where the intervals obtained through the initial simulations results is explored. This simulation provides possible better ranges for the parameters.

3º) Final simulations (simulations 11 and 12), where a large number of particles and iterations is used in the PSO, using small intervals obtained through the trial and error simulations. Its objective is to obtain central values for the parameters, which is inserted in a range that takes into account the confidence interval based on the experimental errors.

4.2.2 Initial simulations

The initial simulations, hereafter SIM (in tables), were routed in order to scan a large search area. These simulations used the following parameters of PSO and Simplex (Table 8 and Table 9):

Table 8 - PSO parameters for EoS Analysis for Pure DEA parameter estimation.

Parameters	SIM1	SIM2 and SIM3
Maximum number of iterations	250	200
Maximum number of species	1000	1000
Individual Factor c_1	1	1
Global Factor c_2	0.1	0.1
Inertia Factor w_0	0.9	0.9
Inertia Factor w_f	0.1	0.1
Tolerance	0.0001	0.0001

Table 9 - Simplex parameters for EoS Analysis for Pure DEA parameter estimation.

SIMPLEX Parameters	
Maximum number of iterations	1000
Reflection Factor Alpha	1
Contraction Factor Beta	0.5
Expansion Factor Gamma	2
Tolerance	10^{-7}

The parameters restrictions are presented in the Table 10, Table 11 and Table 12.

Table 10 - SIM1 parameter constraints for pure DEA parameter estimation using CPA EoS considering only VLE data. Equilibrium data from DIPPR(DIADEM, 2004).

Parameters	Lower Bounds	Upper Bounds
a_0 (bar.L^2/mol^2)	5	100
b (L/mol)	0.01	5
c_1	1	5
ε/R (K)	100	3000
$\beta.10^3$	10	200

Table 11 - SIM2 parameter constraints for pure DEA parameter estimation using CPA EoS considering only VLE data. Equilibrium data from DIPPR(DIADEM, 2004).

Parameters	Lower Bounds	Upper Bounds
a_0 (bar.L^2/mol^2)	5	50
b (L/mol)	0.001	2
c_1	1	2
ε/R (K)	300	1800
$\beta.10^3$	20	100

Table 12– SIM3 parameter constraints for pure DEA parameter estimation applying CPA EoS considering only VLE data. Equilibrium data from DIPPR(DIADEM, 2004).

Parameters	Lower Bounds	Upper Bounds
a_0 (bar.L^2/mol^2)	16.0	32.0
b (L/mol)	0.0001	1.0
c_1	1.2	2.0
ε/R (K)	1100	2200
$\beta.10^3$	20	60

A further way of comparing the parameter estimation results, which is also adopted here, is the Average Absolute Deviation of the Liquid Density (AAρ%), defined according to Equation 38:

$$\boldsymbol{AA\rho\%} = \left(\frac{\mathbf{100}}{\boldsymbol{N_{exp}}}\right)\sum_{\boldsymbol{k=1}}^{\boldsymbol{N_{exp}}}\left|\frac{(\boldsymbol{\rho_k^{exp}} - \boldsymbol{\rho_k^{calc}})}{\boldsymbol{\rho_k^{exp}}}\right| \qquad \mathbf{37}$$

The parameter estimation results are shown in Table 13:

Table 13 - SIM1, SIM2 and SIM3 Pure DEA parameter estimation results applying CPA EoS considering only VLE data. Equilibrium data from DIPPR(DIADEM, 2004).

Parameters	SIM1		SIM2		SIM3	
	PSO	Simplex	PSO	Simplex	PSO	Simplex
a_0 (bar.L^2/mol^2)	26.560	31.962	23.504	30.418	21.324	16.020
b (L/mol)	0.096	0.093	0.095	0.094	0.095	0.093
c_1	1.643	1.477	1.600	1.530	1.730	2.000
ε/R (K)	876.878	100.011	1555.805	310.313	1574.023	1928.824
1000* β	78.921	10	41.961	89.805	54.772	58.428
F_{obj}	4.68.E^{-4}	2.05.E^{-4}	6.25.E^{-4}	2.45.E^{-4}	5.86.E^{-4}	4.44.E^{-4}
AAP%	1.16%	1.13%	1.48%	1.05%	1.42%	1.34%
AAρ%	1.40%	0.43%	1.54%	0.82%	1.50%	1.20%

From Figure 10 to Figure 11 it can be seen the PSO graphs for SIM1 and SIM3 that indicate the large search zone managed by the method:

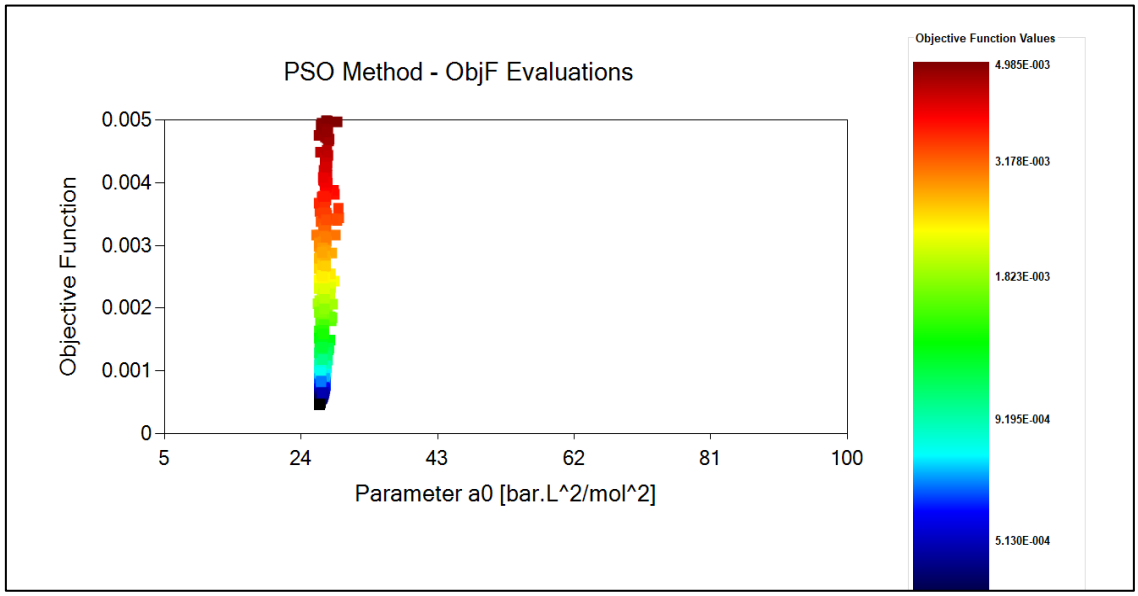

(a)

Figure 10 - Parametric Analysis of the Initial Simulations (SIM1). (a) F_{obj}– a_0; (b) F_{obj}– b; (c) F_{obj}– c_1; (d) F_{obj}– eps/R; (e) F_{obj}– beta. Parameters estimated using CPA and optimization method PSO. Maximum number of 200 iterations and 1000 particles. The maximum objective function value considered is 0.005. 100 experimental points were used between 0.55 - 0.90 T_R. Experimental data from DIPPR(DIADEM, 2004) .

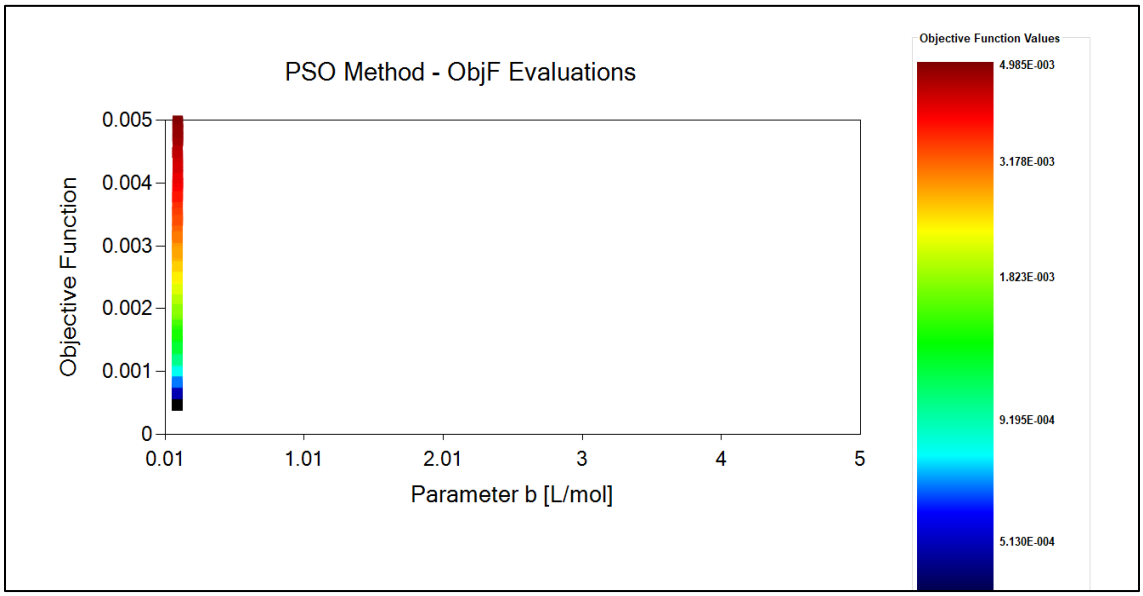

(b)

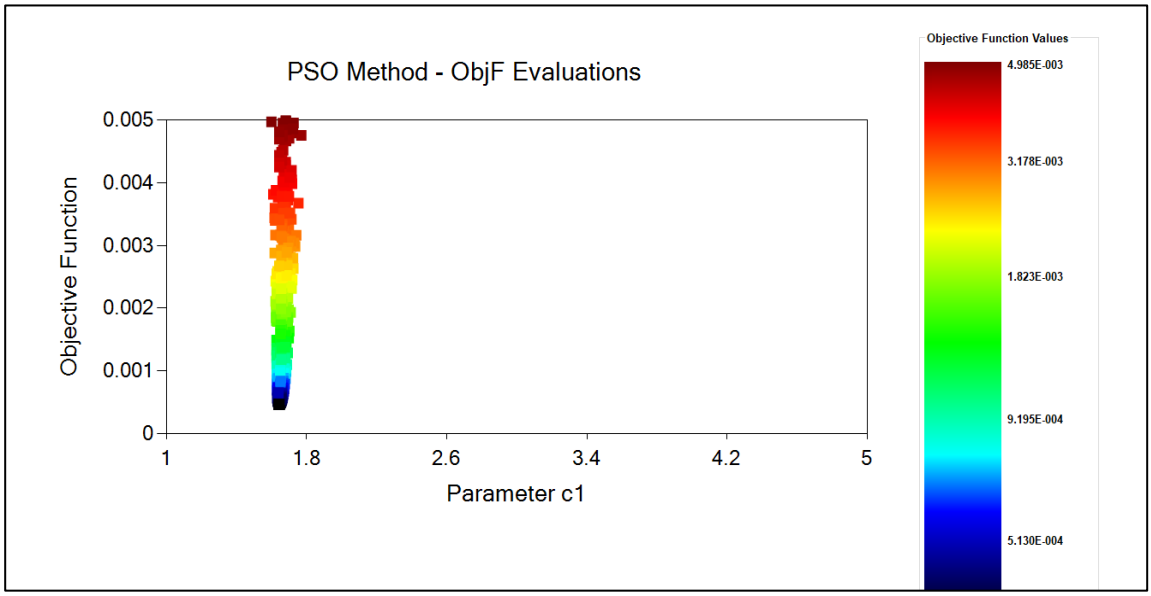

(c)

Figure 10 (continuation)- Parametric Analysis of the Initial Simulations (SIM1). (a) F_obj– a_0; (b) F_obj– b; (c) F_obj– c_1; (d) F_obj– eps/R; (e) F_obj– beta. Parameters estimated using CPA and optimization method PSO. Maximum number of 200 iterations and 1000 particles. The maximum objective function value considered is 0.005. 100 experimental points were used between 0.55 - 0.90 T_R. Experimental data from DIPPR(DIADEM, 2004) .

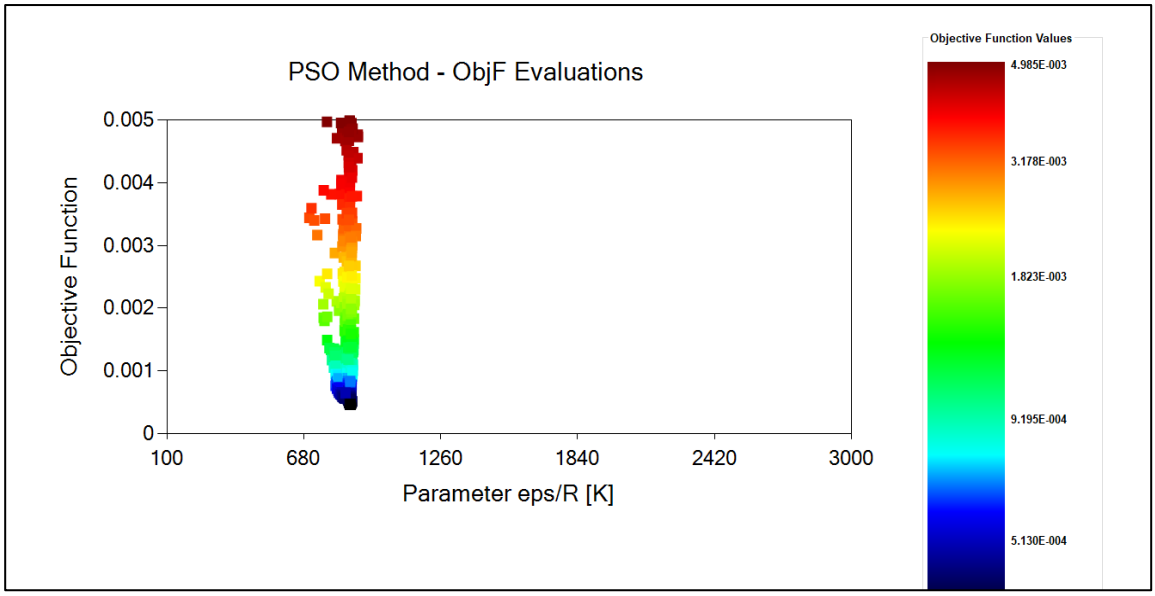

(d)

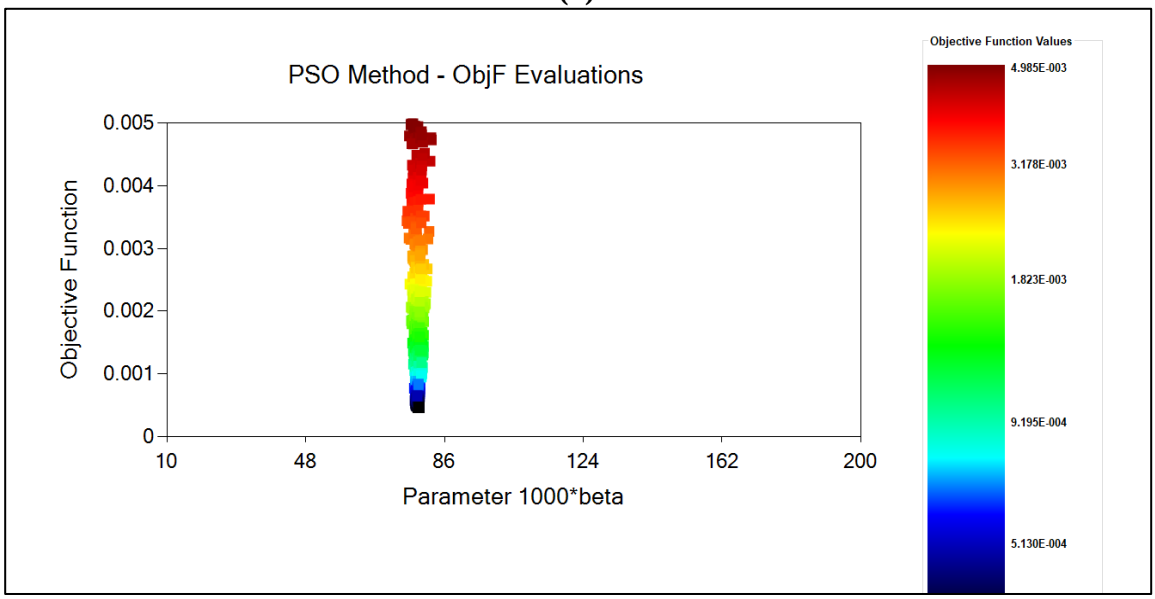

(e)

Figure 10 (continuation)- Parametric Analysis of the Initial Simulations (SIM1). (a) $F_{obj}-a_0$; (b) $F_{obj}-b$; (c) $F_{obj}-c_1$; (d) $F_{obj}-$ eps/R; (e) $F_{obj}-$ beta. Parameters estimated using CPA and optimization method PSO. Maximum number of 200 iterations and 1000 particles. The maximum objective function value considered is 0.005. 100 experimental points were used between 0.55 - 0.90 T_R. Experimental data from DIPPR(DIADEM, 2004) .

Based on the possible global minimum obtained by simulations 1, 2 and 3, it was proceeded to the trial and error simulations. Special attention was given to the β and epsilon parameters, since the simulations in Figure 11 indicated the presence of local minima. Thus, different ranges of intervals were studied for these parameters.

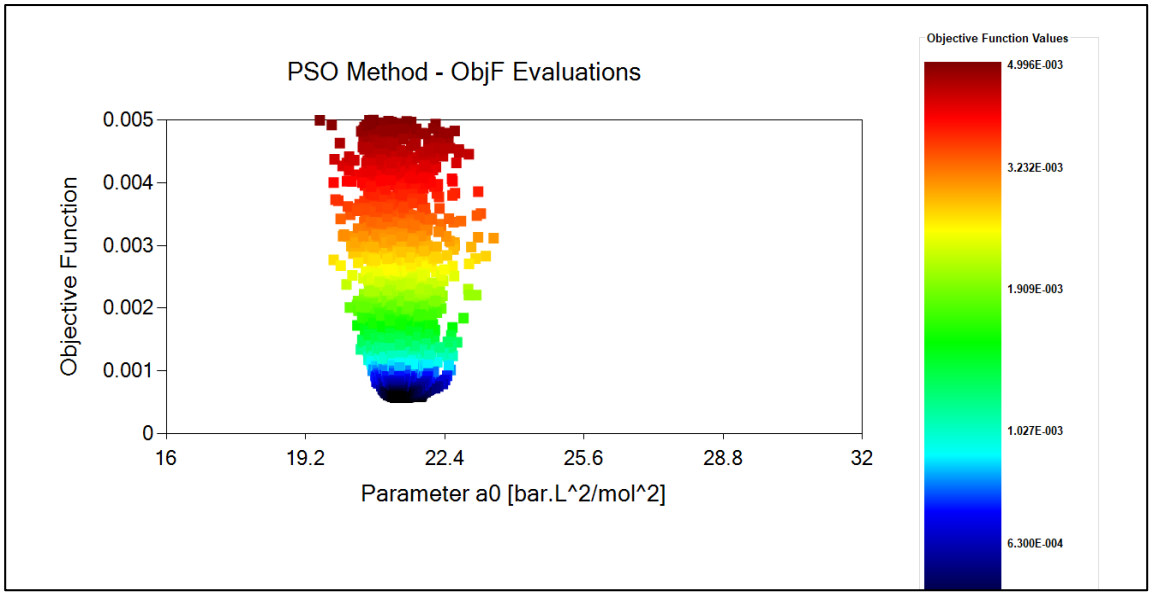

(a)

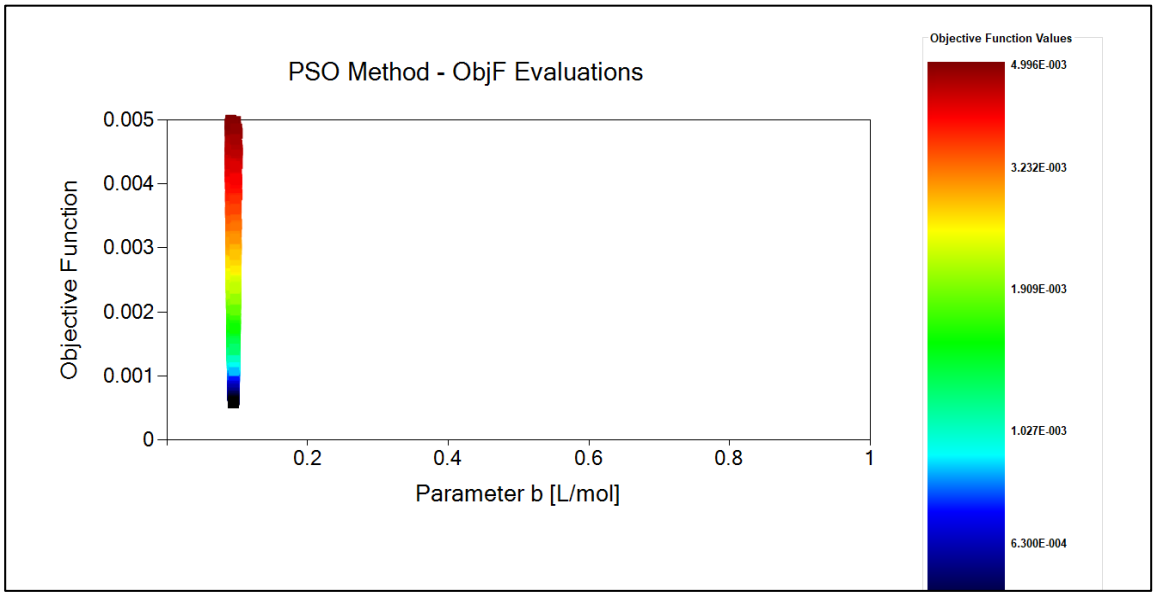

(b)

Figure 11 - Parametric Analysis of the Initial Simulations (SIM3). (a) $F_{obj}-a_0$; (b) $F_{obj}-b$; (c) $F_{obj}-c_1$; (d) $F_{obj}-$ eps/R; (e) $F_{obj}-$ beta. Parameters estimated using CPA and optimization method PSO. Maximum number of 200 iterations and 1000 particles. The maximum objective function value considered is 0.005. 100 experimental points were used between 0.55 - 0.90 T_R. Experimental data from DIPPR(DIADEM, 2004).

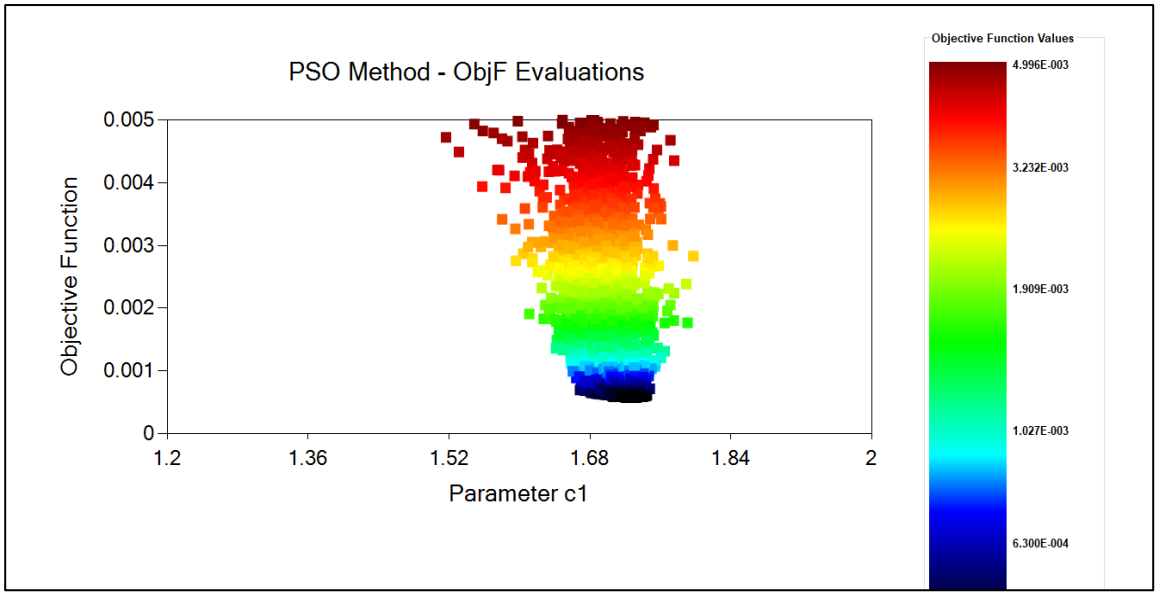

(c)

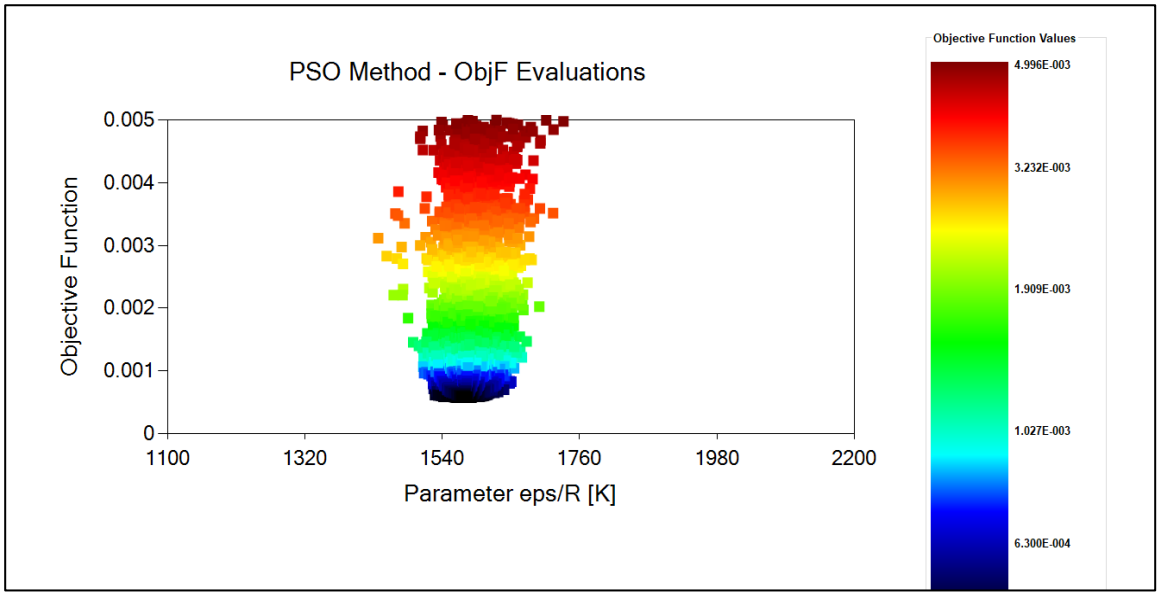

(d)

Figure 11 (continuation)- Parametric Analysis of the Initial Simulations (SIM3). (a) $F_{obj}-a_0$; (b) $F_{obj}-b$; (c) $F_{obj}-c_1$; (d) $F_{obj}-$ eps/R; (e) $F_{obj}-$ beta. Parameters estimated using CPA and optimization method PSO. Maximum number of 200 iterations and 1000 particles. The maximum objective function value considered is 0.005. 100 experimental points were used between 0.55 - 0.90 T_R. Experimental data from DIPPR(DIADEM, 2004).

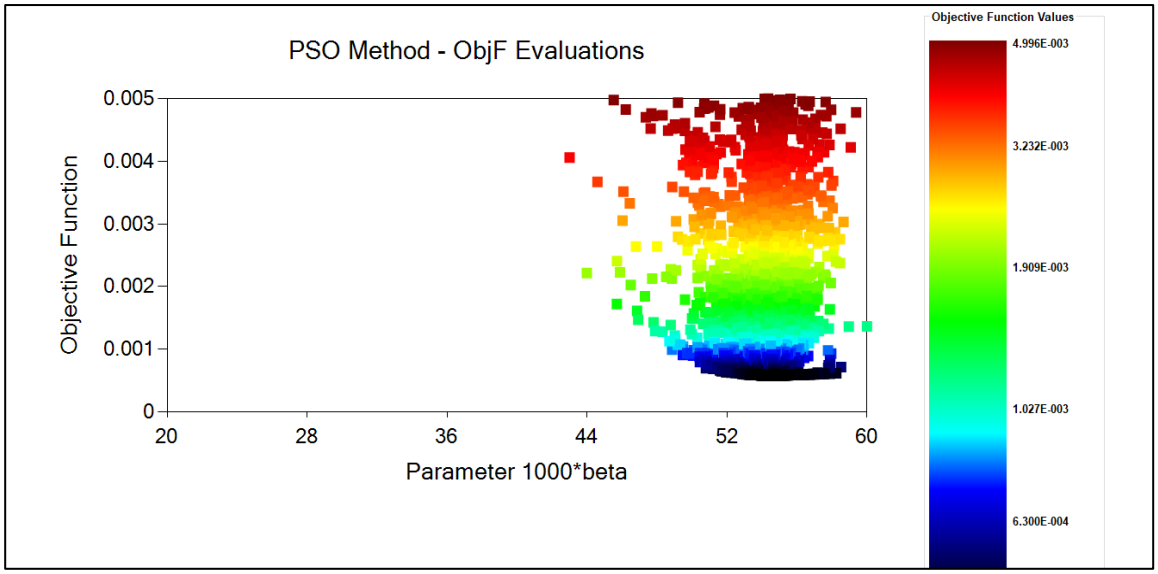

(e)

Figure 11 (continuation)- Parametric Analysis of the Initial Simulations (SIM3). (a) $F_{obj}-a_0$; (b) $F_{obj}-b$; (c) $F_{obj}-c_1$; (d) $F_{obj}-$ eps/R; (e) $F_{obj}-$ beta. Parameters estimated using CPA and optimization method PSO. Maximum number of 200 iterations and 1000 particles. The maximum objective function value considered is 0.005. 100 experimental points were used between 0.55 - 0.90 T_R. Experimental data from DIPPR(DIADEM, 2004).

4.2.3 Simulations of trial and error

Simulations 4, 5, 6, 7, 8, 9 and 10 are considered trial and error simulations, where the regions indicated by simulations 1, 2 and 3 were tested. In these simulations, depending on each case, a different number of particles and iterations was applied for each interval studied.

For simulations 4, 5, 6 and 7 the following sets of parameters for the PSO were used in Table 14.

Table 14 - PSO parameters for the trial and error simulations SIM4, SIM5, SIM6 and SIM7 considering Pure DEA parameter estimation.

PSO Parameters	
Maximum number of iterations	1000
Maximum number of species	1000
Individual Factor c_1	1
Global Factor c_2	0.1
Inertia Factor w_0	0.9
Inertia Factor w_f	0.1
Tolerance	0.0001

The parameters set for the SIMPLEX method are the same as those set in simulations 1, 2 and 3. In Table 15 are the results obtained for the 4 mentioned simulations.

Table 15 - Results of trial and error simulations SIM4, SIM5, SIM6 and SIM7 considering Pure DEA parameter estimation applying CPA EoS considering only VLE data. Equilibrium data from DIPPR(DIADEM, 2004).

Simulation		a_0 $\left(\frac{bar \cdot L^2}{mol^2}\right)$	b $\left(\frac{L}{mol}\right)$	c_1	ε/R (K)	1000* β	F_{obj}	AAP	AAρ
SIM4	PSO	22.226	0.094	1.733	1418.766	61.971	5.72.E^{-4}	1.39%	1.50%
	Simplex	18.600	0.094	1.785	1876.310	47.977	5.39.E^{-4}	1.39%	1.42%
SIM5	PSO	23.470	0.095	1.610	1534.035	43.871	6.21.E^{-4}	1.46%	1.54%
	Simplex	25.375	0.095	1.673	1005.463	76.109	4.82.E^{-4}	1.23%	1.42%
SIM6	PSO	25.270	0.095	1.645	1128.696	62.534	5.11.E^{-4}	1.29%	1.44%
	Simplex	28.500	0.095	1.567	750.326	61.228	3.63.E^{-4}	1.15%	1.16%
SIM7	PSO	24.286	0.095	1.717	1088.616	78.944	5.11.E^{-4}	1.27%	1.46%
	Simplex	28.500	0.095	1.602	500.000	110.000	3.24.E^{-4}	1.04%	1.14%

In Figure 12 it can be seen the PSO graphs for SIM7 that indicate the most restricted intervals set and the application of a relatively large number of particles in the global minimum search:

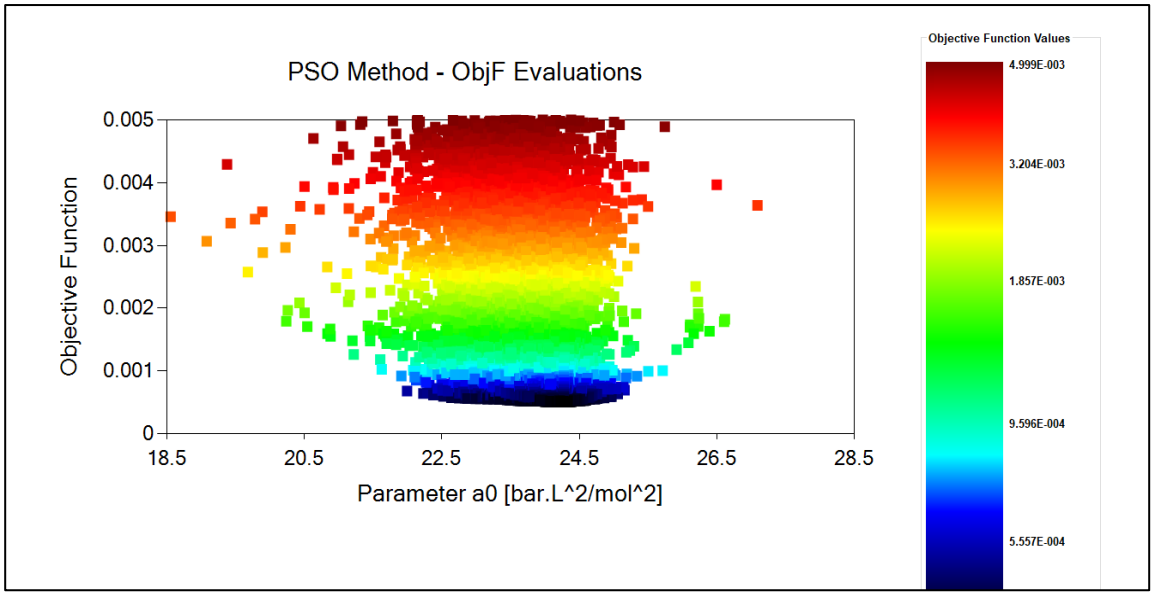

(a)

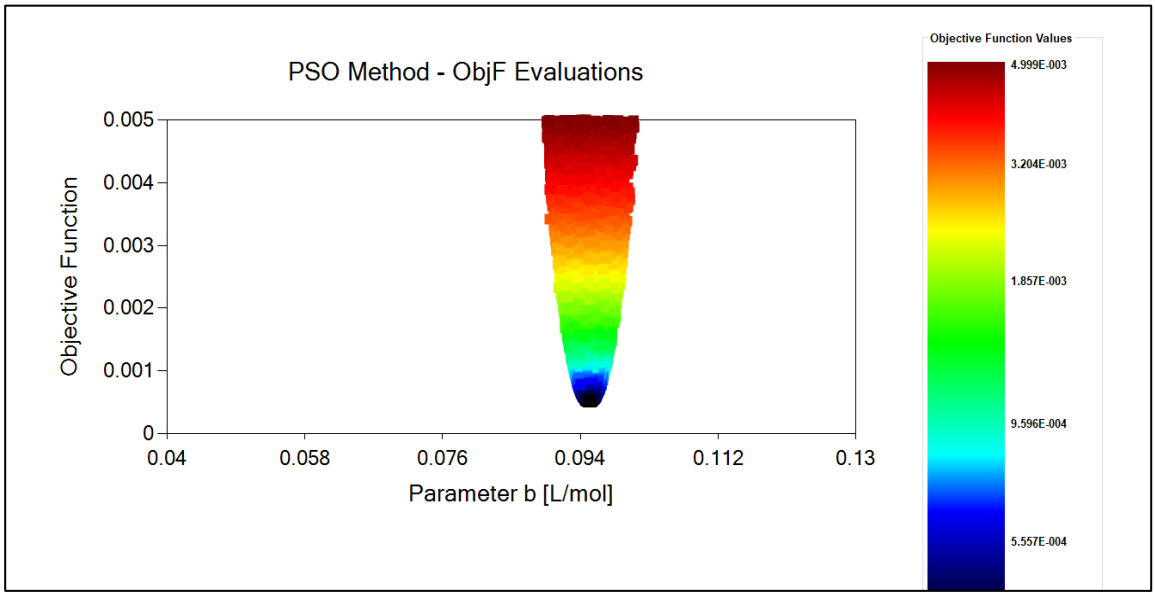

(b)

Figure 12 - Parametric Analysis of the Trial and Error Simulation (SIM7). (a) $F_{obj}-a_0$; (b) $F_{obj}-b$; (c) $F_{obj}-c_1$; (d) $F_{obj}-$ eps/R; (e) $F_{obj}-$ beta. Parameters estimated using CPA and optimization method PSO. Maximum number of 1000 iterations and 1000 particles. The maximum objective function value considered is 0.005. 100 experimental points were used between 0.55 - 0.90 T_R. Experimental data from DIPPR(DIADEM, 2004).

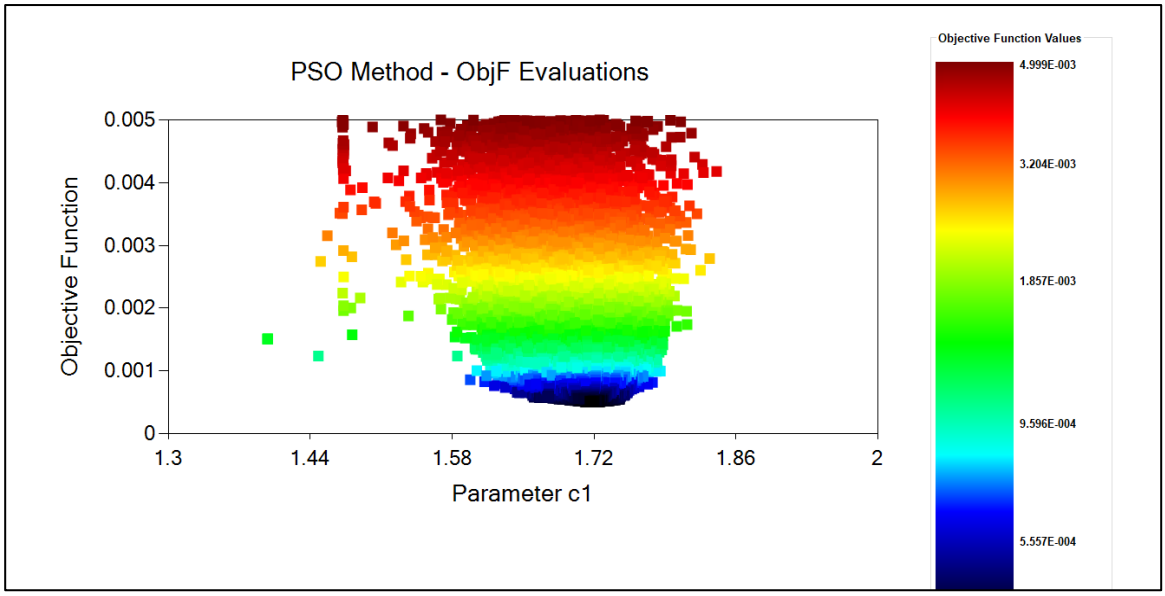

(c)

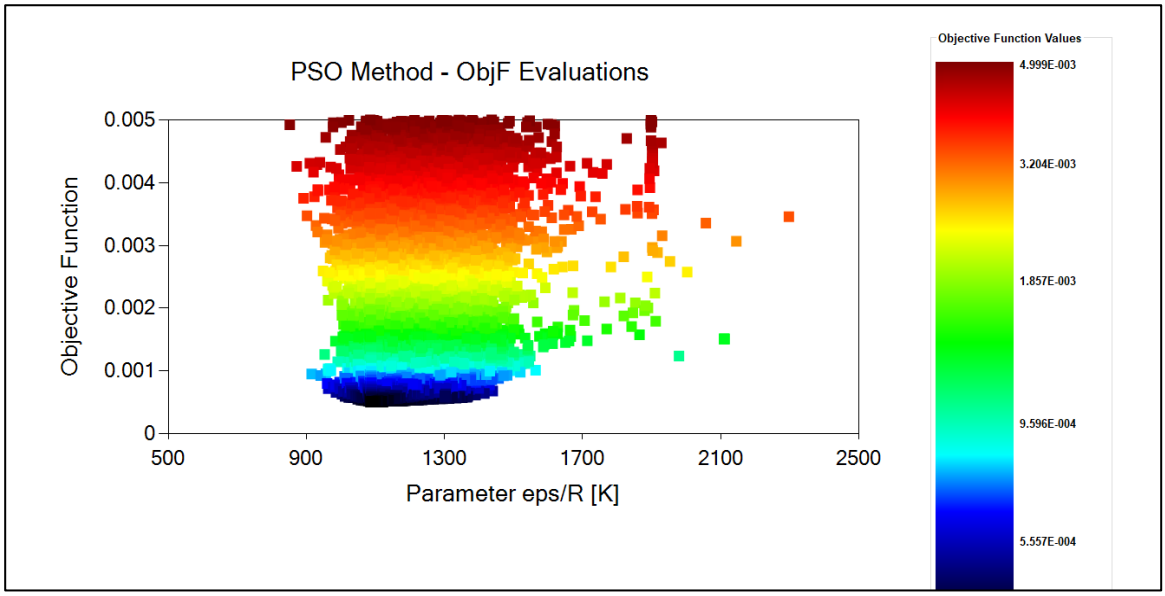

(d)

Figure 12 (continuation)- Parametric Analysis of the Trial and Error Simulation (SIM7). (a) F_{obj}– a_0; (b) F_{obj}– b; (c) F_{obj}– c_1; (d) F_{obj}– eps/R; (e) F_{obj}– beta. Parameters estimated using CPA and optimization method PSO. Maximum number of 1000 iterations and 1000 particles. The maximum objective function value considered is 0.005. 100 experimental points were used between 0.55 - 0.90 T_R. Experimental data from DIPPR(DIADEM, 2004).

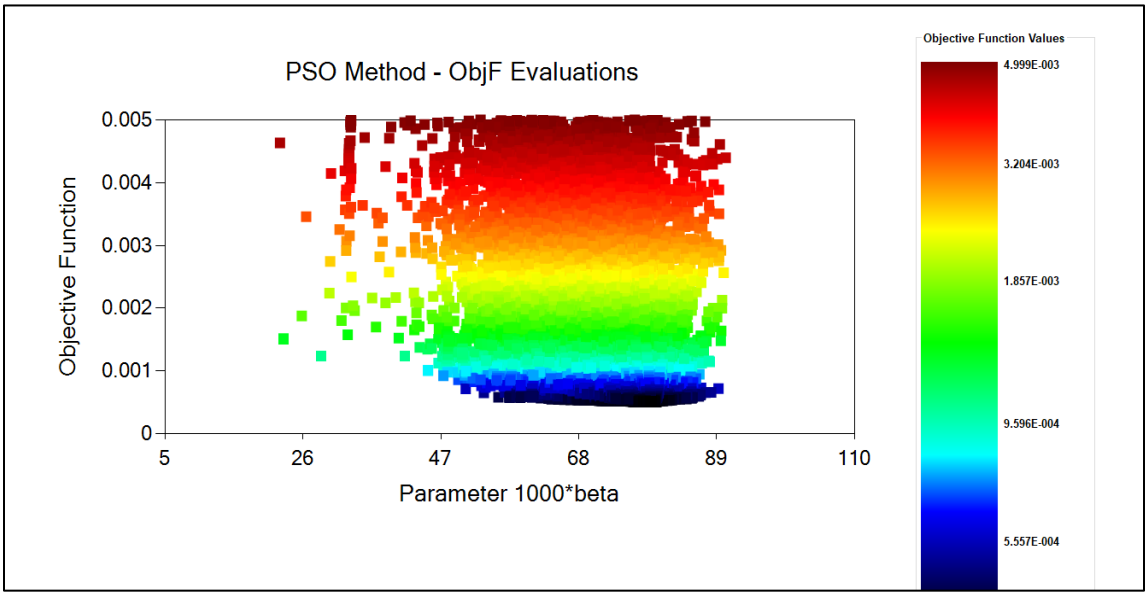

(e)

Figure 12 (continuation)- Parametric Analysis of the Trial and Error Simulation (SIM7). (a) F_{obj}– a_0; (b) F_{obj}– b; (c) F_{obj}– c_1; (d) F_{obj}– eps/R; (e) F_{obj}– beta. Parameters estimated using CPA and optimization method PSO. Maximum number of 1000 iterations and 1000 particles. The maximum objective function value considered is 0.005. 100 experimental points were used between 0.55 - 0.90 T_R. Experimental data from DIPPR(DIADEM, 2004).

It is evident the presence of different minima for the parameters a_0, c_1, epsilon and beta in the intervals established for simulation SIM7. This can be visualized in the modified Figure 13 (d), where it is possible to visualize these minimas (purple circles).

The large number of particles allows a large area to be swept and thus both the possible global minimum and local minima are identified.

Simulation 7 was the one that led to the lowest values of F_{obj}, AAP% and AAρ%. The parameters estimated by this simulation were the basis of the intervals used in simulations 8, 9, and 10. These simulations used the following parameters of PSO and Simplex (Table 16).

Table 16 - PSO parameters for the trial and error simulations SIM8, SIM9 and SIM10 considering Pure DEA parameter estimation.

PSO Parameters			
Simulation	**SIM8**	**SIM9**	**SIM10**
Maximum number of iterations	500	300	200
Maximum number of species	500	300	500
Individual Factor c_1	1	1	1
Global Factor c_2	0.1	0.1	0.1
Inertia Factor w_0	0.9	0.9	0.9
Inertia Factor w_f	0.1	0.1	0.1
Tolerance	0.0001	0.0001	0.0001

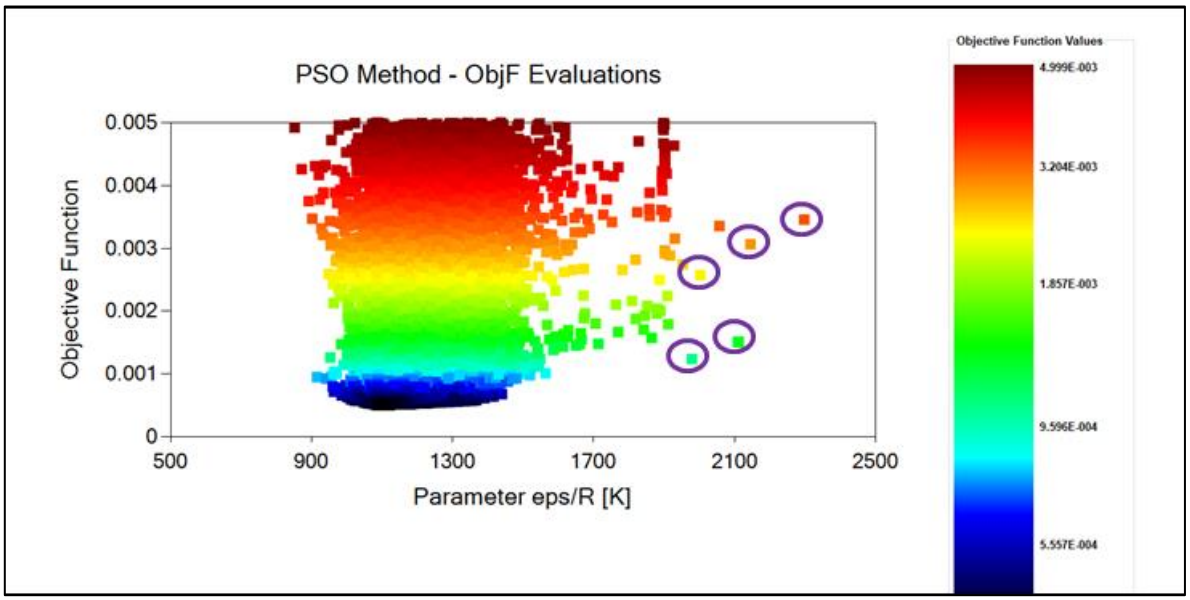

Figure 13 - Modified Figure 12 (d) - F_{obj}– eps/R. Highlights of the presence of local minimas (purple circles) in pure DEA parameter estimation. Parameters estimated using CPA and optimization method PSO. Maximum number of 1000 iterations and 1000 particles. The maximum objective function value considered is 0.005. 100 experimental points were used between 0.55 - 0.90 T_R. Experimental data from DIPPR(DIADEM, 2004).

The results of simulation 8, 9 and 10 are shown in Table 17.

Table 17 - Results of trial and error simulations SIM8, SIM9 and SIM10 considering Pure DEA parameter estimation applying CPA EoS considering only VLE data. Equilibrium data from DIPPR(DIADEM, 2004).

Simulation		a_0 $\left(\frac{bar \cdot L^2}{mol^2}\right)$	b $\left(\frac{L}{mol}\right)$	c_1	ε/R (K)	1000* β	F_{obj}	AAP	AAρ
SIM8	PSO	26.381	0.95	1.626	977.435	66.126	$4.61.E^{-4}$	1.23%	1.37%
	Simplex	30.000	0.94	1.508	750.000	35.053	$3.21.E^{-4}$	1.22%	0.94%
SIM9	PSO	27.536	0.095	1.635	621.575	104.928	$3.70.E^{-4}$	1.10%	1.24%
	Simplex	31.970	0.093	1.477	1.867	469.947	$2.05.E^{-4}$	1.13%	0.43%
SIM10	PSO	9.925	0.089	2.121	2728.828	32.757	$5.25.E^{-5}$	0.33%	0.50%
	Simplex	7.862	0.087	2.440	2825.685	34.430	$1.10.E^{-5}$	0.14%	0.23%

Simulation 10 presented the best results among the three simulations (SIM8, SIM 9 and SIM10), obtaining satisfactory objective function, AAP% and AAρ% values. The parameters intervals determined in simulation 10 were the basis for the intervals used in the final simulations. It is worth to notice that the value of ε/R is quite different in all the presented simulations, not clearly showing the convergence of the parameter to a definitive value (leading to a global minimum).

In Figure 14, it can be seen the PSO graphs for SIM10 that indicate even more restricted intervals and lower objective function values:

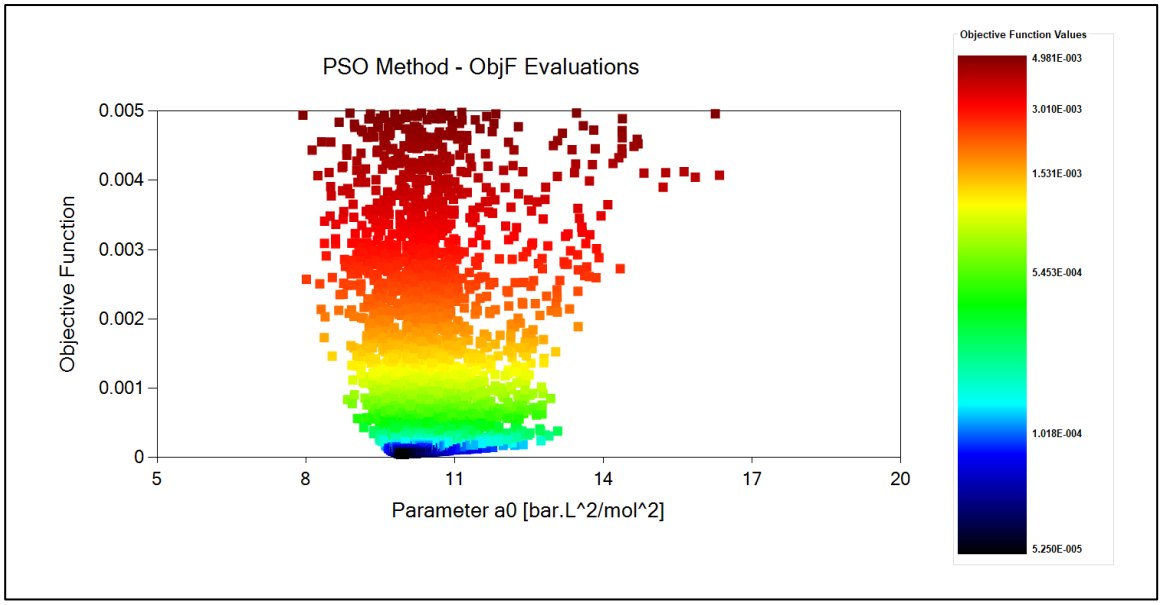

(a)

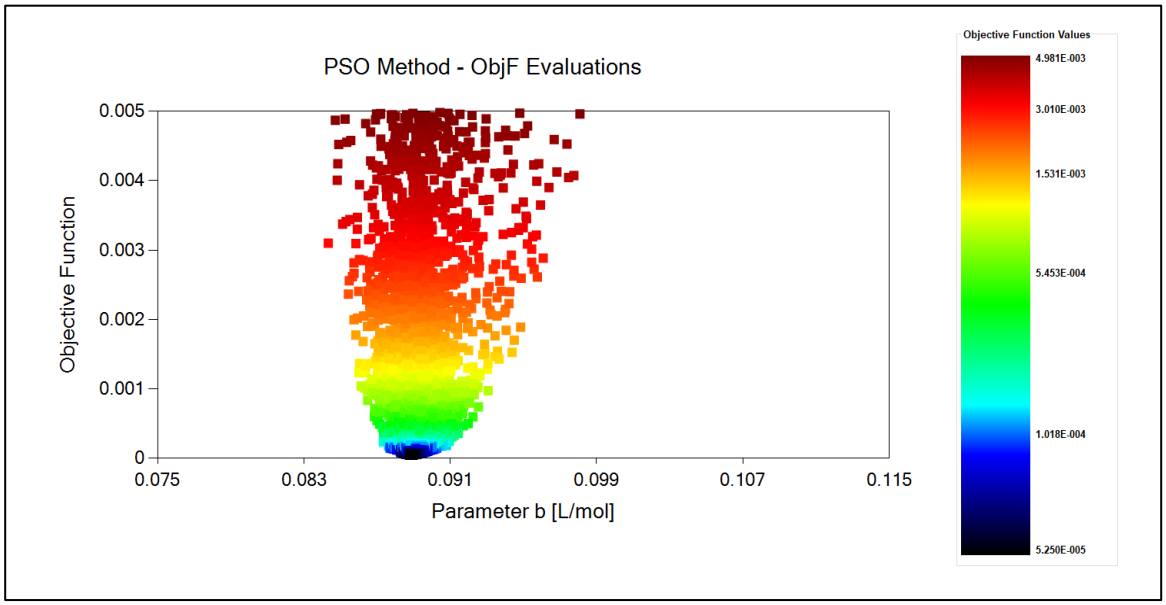

(b)

Figure 14 - Parametric Analysis of the Trial and Error Simulation (SIM10). (a) F_{obj}– a_0; (b) F_{obj}– b; (c) F_{obj}– c_1; (d) F_{obj}– eps/R; (e) F_{obj}– beta. Parameters estimated using CPA and optimization method PSO. Maximum number of 1000 iterations and 1000 particles. The maximum objective function value considered is 0.005. 100 experimental points were used between 0.55 - 0.90 T_R. Experimental data from DIPPR(DIADEM, 2004).

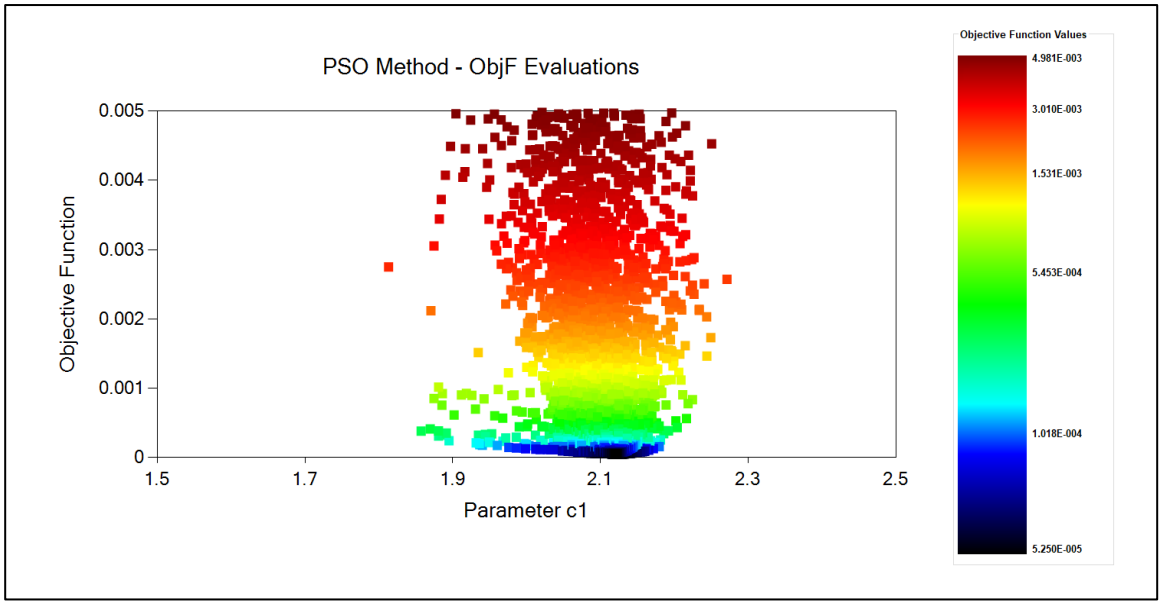

(c)

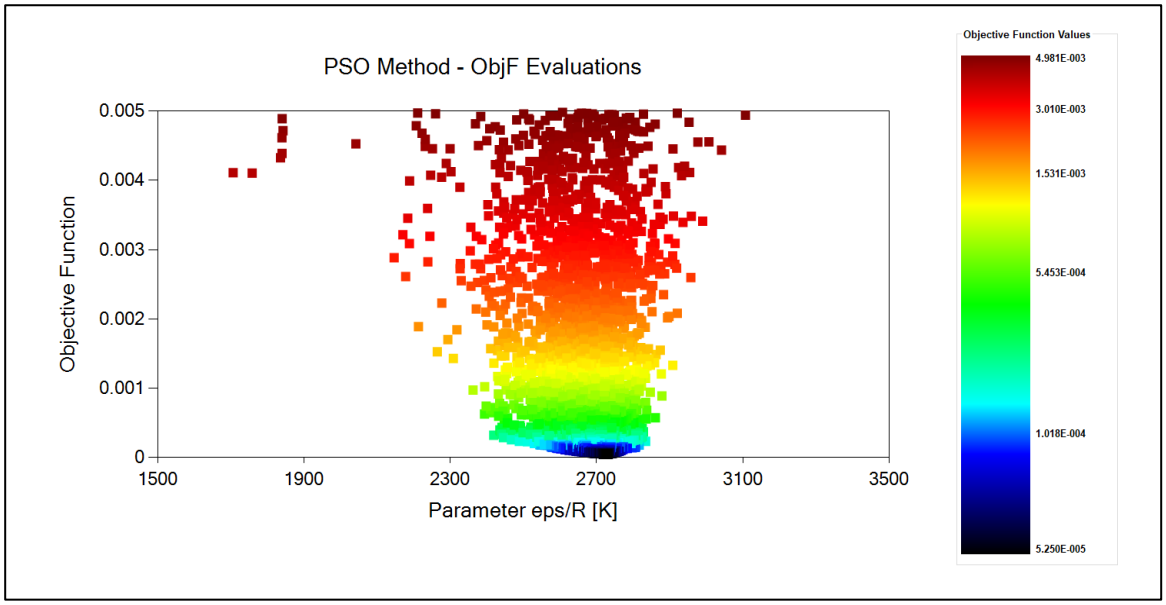

(d)

Figure 14 (continuation)- Parametric Analysis of the Trial and Error Simulation (SIM10). (a) $F_{obj}-a_0$; (b) $F_{obj}-b$; (c) $F_{obj}-c_1$; (d) $F_{obj}-$ eps/R; (e) $F_{obj}-$ beta. Parameters estimated using CPA and optimization method PSO. Maximum number of 1000 iterations and 1000 particles. The maximum objective function value considered is 0.005. 100 experimental points were used between 0.55 - 0.90 T_R. Experimental data from DIPPR(DIADEM, 2004).

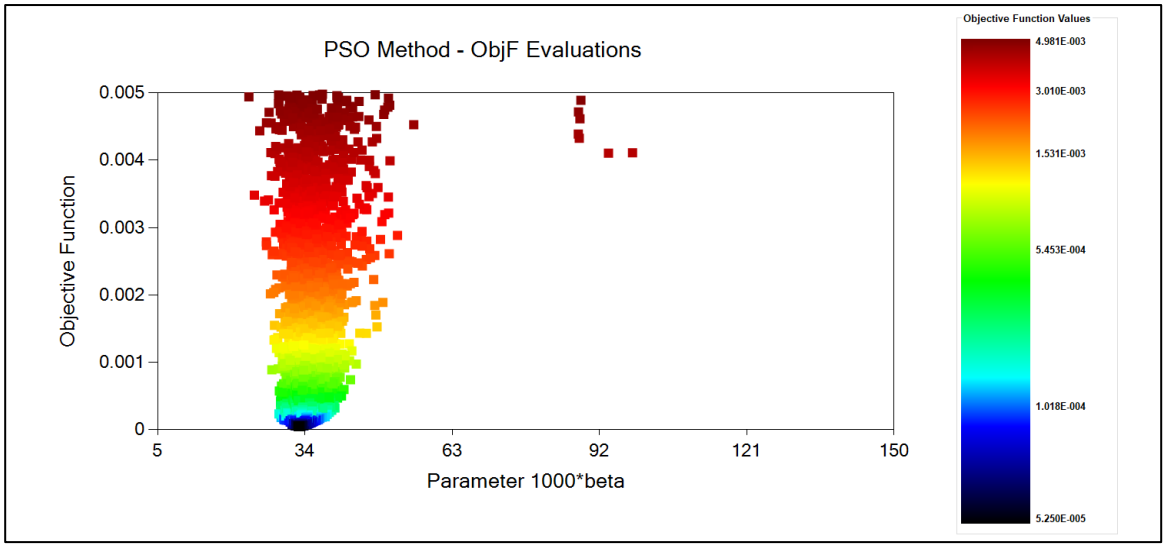

(e)

Figure 14 (continuation)- Parametric Analysis of the Trial and Error Simulation (SIM10). (a) F_{obj}– a_0; (b) F_{obj}– b; (c) F_{obj}– c_1; (d) F_{obj}– eps/R; (e) F_{obj}– beta. Parameters estimated using CPA and optimization method PSO. Maximum number of 1000 iterations and 1000 particles. The maximum objective function value considered is 0.005. 100 experimental points were used between 0.55 - 0.90 T_R. Experimental data from DIPPR(DIADEM, 2004).

4.2.4 Final Simulations

Simulations 11 and 12 aimed to obtain the final set of parameters for pure DEA, considering only VLE data. For this, a large number of particles (500) and iterations (1000) of the PSO associated with a narrow range of parameters were used.

Table 18 - SIM11 and SIM12 parameter constraints for pure DEA parameter estimation applying CPA EoS considering only VLE data. Equilibrium data from DIPPR(DIADEM, 2004).

Parameters	SIM11		SIM12	
	Lower Bounds	Upper Bounds	Lower Bounds	Upper Bounds
a_0 (bar.L^2/mol^2)	5.000	20.000	5.000	12.000
b (L/mol)	0.075	0.115	0.080	0.110
c_1	1.000	4.000	1.500	3.500
ε/R (K)	1250.000	3500.000	2000.000	3500.000
β.10^3	5.000	150.000	20.000	80.000

The best results obtained in the trial and error simulations served as a basis for the intervals of simulation 11. The intervals obtained in simulation 11 served as the basis for the determination of the intervals set in simulation 12 (intervals which are more restrictive). In Table 18 are the intervals used in each simulation.

The mentioned simulations results are in Table 19:

Table 19 - Results of final simulations SIM11 and SIM12 considering Pure DEA parameter estimation applying CPA EoS considering only VLE data. Equilibrium data from DIPPR(DIADEM, 2004).

Simulation		a_0 $\left(\frac{bar \cdot L^2}{mol^2}\right)$	b $\left(\frac{L}{mol}\right)$	c_1	ε/R (K)	1000* β	F_{obj}	AAP	AAρ
SIM11	PSO	8.184	0.088	2.867	2455.415	57.308	$1.09.E^{-4}$	0.84%	0.24%
	Simplex	7.946	0.087	2.392	2843.879	33.281	$1.06.E^{-5}$	0.15%	0.23%
SIM12	PSO	9.447	0.0890	2.441	2542.973	44.790	$7.17.E^{-5}$	0.63%	0.33%
	Simplex	7.948	0.087	2.392	2843.811	33.280	$1.06.E^{-5}$	0.15%	0.23%

The F_{obj}, APP% and AAρ% values are the same up to the fifth decimal place. Since the results of the simulation SIM12 are similar to those of the simulation SIM11 but with a more restrictive interval, it was decided to consider the parameters estimated in SIM12 as the final parameters of the pure DEA, when considering only VLE data.

Figure 15 represents the graphs of simulation 12. The maximum value indicated in the graphs is 0.0050 (highest statistically acceptable value for the objective function). Thus, all the points presented in these graphs are statistically correct.

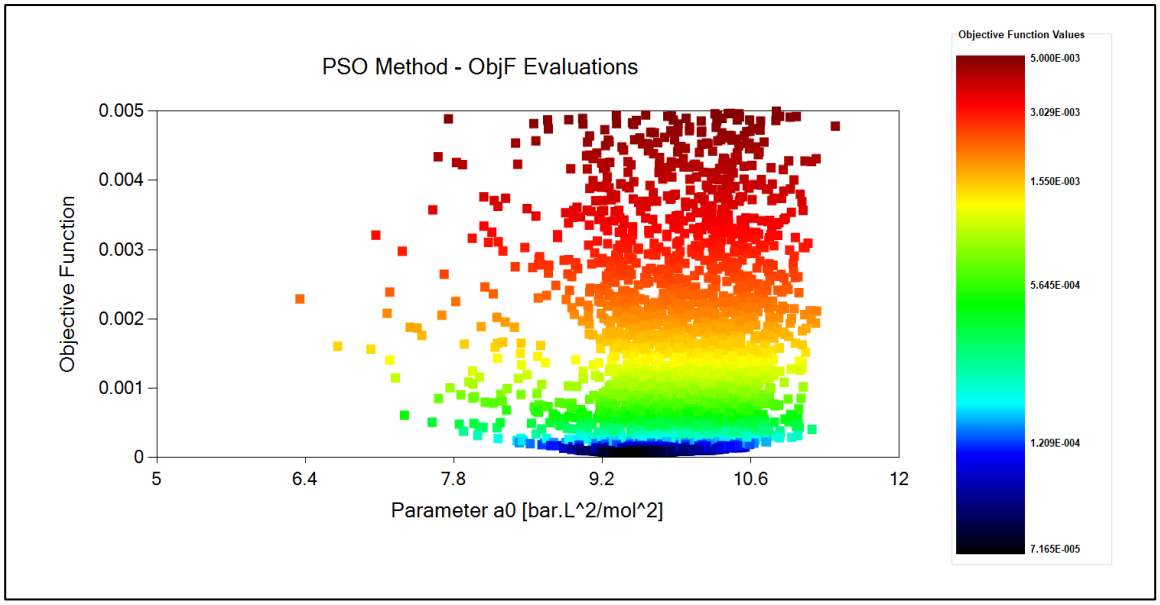

(a)

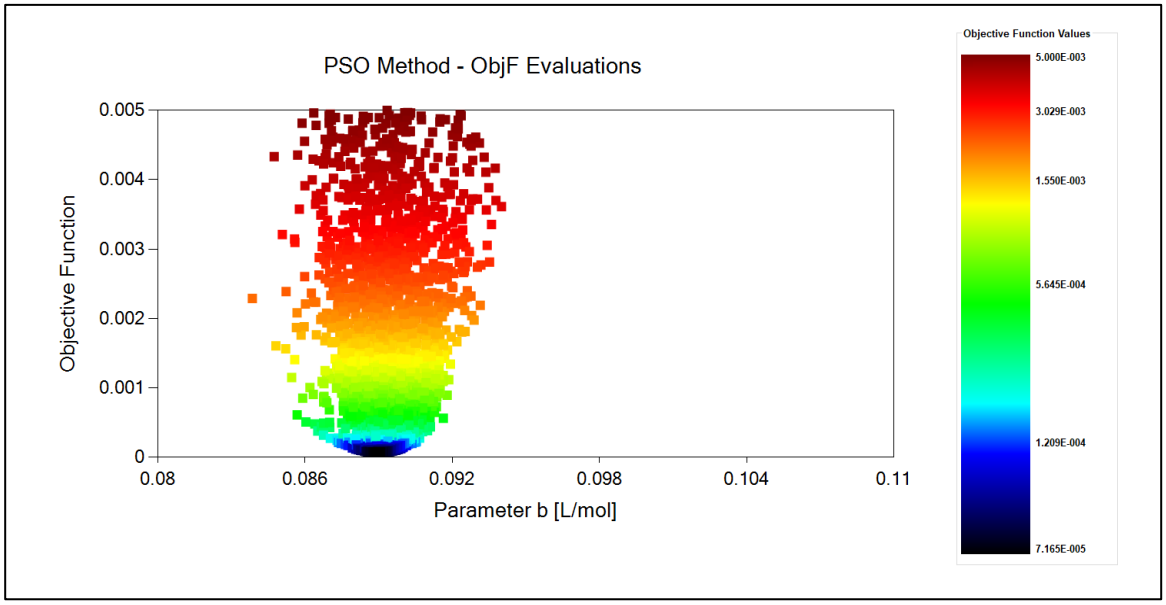

(b)

Figure 15 - Parametric Analysis of the Final Simulation (SIM12). (a) F_{obj}– a_0; (b) F_{obj}– b; (c) F_{obj}– c_1; (d) F_{obj}– eps/R; (e) F_{obj}– beta. Parameters estimated using CPA and optimization method PSO. Maximum number of 1000 iterations and 200 particles. The maximum objective function value considered is 0.005. 100 experimental points were used between 0.55 - 0.90 T_R. Experimental data from DIPPR(DIADEM, 2004).

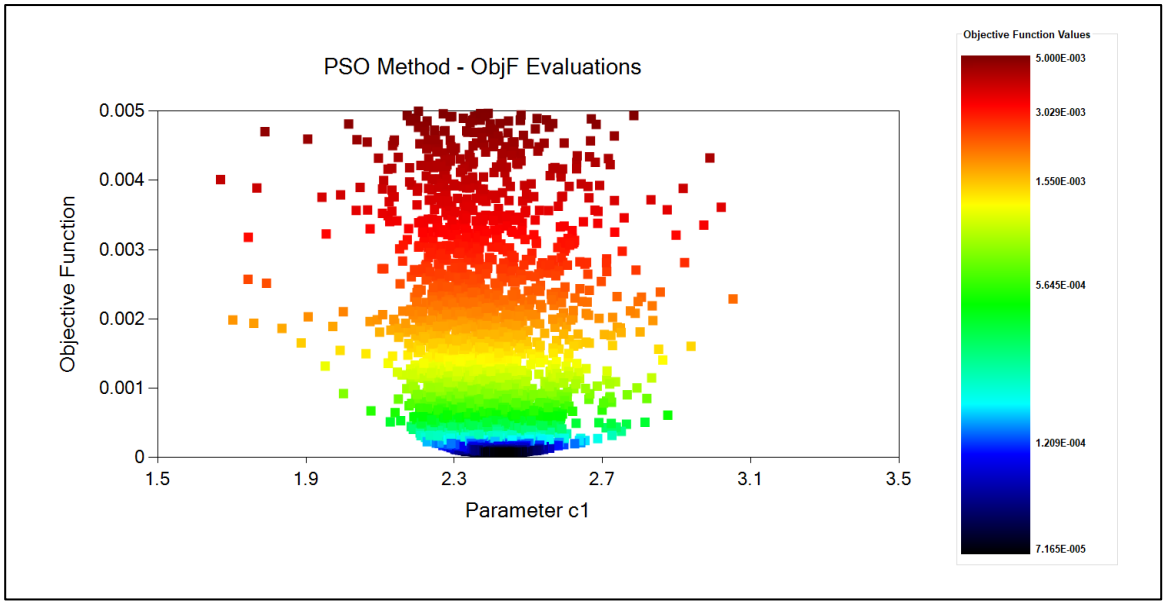

(c)

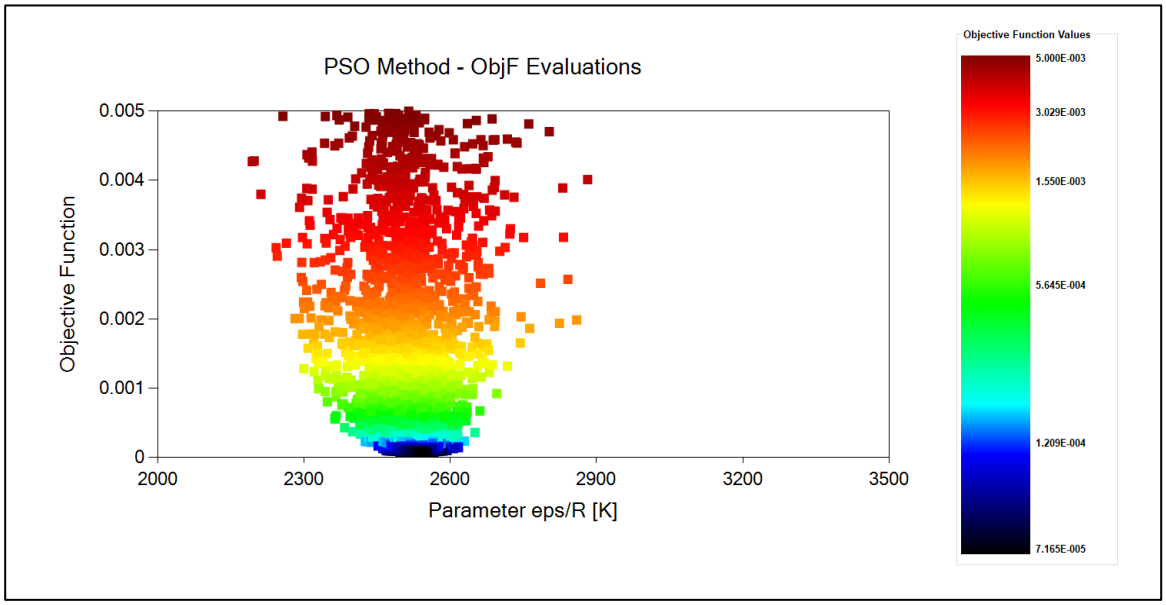

(d)

Figure 15 (continuation)- Parametric Analysis of the Final Simulation (SIM12). (a) $F_{obj}-a_0$; (b) $F_{obj}-b$; (c) $F_{obj}-c_1$; (d) $F_{obj}-$ eps/R; (e) $F_{obj}-$ beta. Parameters estimated using CPA and optimization method PSO. Maximum number of 1000 iterations and 200 particles. The maximum objective function value considered is 0.005. 100 experimental points were used between 0.55 - 0.90 T_R. Experimental data from DIPPR(DIADEM, 2004).

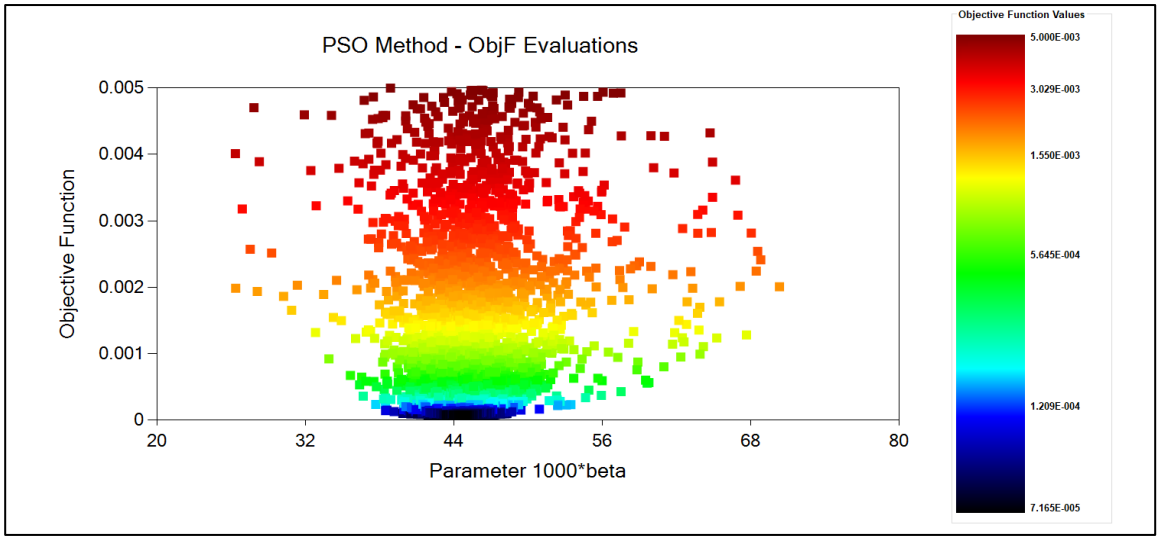

(e)

Figure 15 (continuation)- Parametric Analysis of the Final Simulation (SIM12). (a) F_{obj}– a_0; (b) F_{obj}– b; (c) F_{obj}– c_1; (d) F_{obj}– eps/R; (e) F_{obj}– beta. Parameters estimated using CPA and optimization method PSO. Maximum number of 1000 iterations and 200 particles. The maximum objective function value considered is 0.005. 100 experimental points were used between 0.55 - 0.90 T_R. Experimental data from DIPPR(DIADEM, 2004).

All the parameters presented in Figure 15 are statistically accepted since they lead to an objective function smaller than 5.10^{-3}. A parametric analysis of the estimated parameters allows the identification of the range of statistically accepted parameters, indicated by the red simulated ellipse present in the graphs (Figure 16).

Considering to the experimental errors of saturation pressure and liquid density, it is possible to obtain a statistically accepted region based on the results found in SIM12 (Table 20).

Table 20- Final parameter intervals generated from pure DEA parameter estimation applying CPA considering only VLE data. The parameter interval was generated considering the pure DEA experimental data error.

Parameters	Lower Bounds	Upper Bounds
a_0 (bar.L^2/mol^2)	6.349	11.399
b (L/mol)	0.084	0.094
c_1	1.669	3.052
ε/R (K)	2193.840	2881.620
$\beta.10^3$	26.343	70.328

These ranges of the pure DEA parameters are used in the next simulations, which also consider the LLE data, in accordance with the proposed complete methodology.

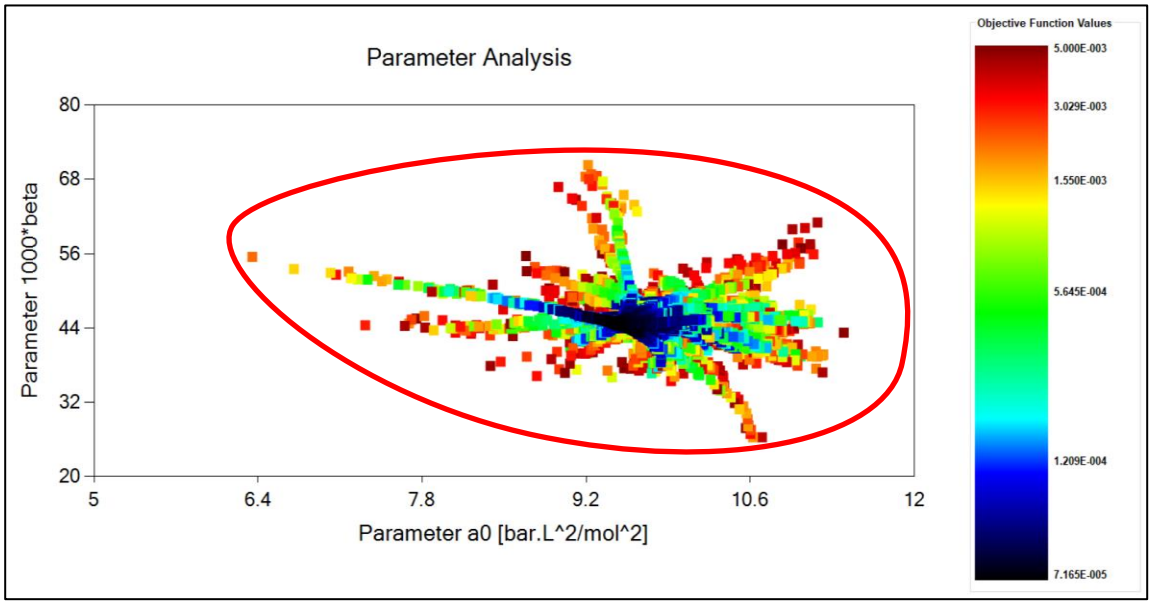

(a)

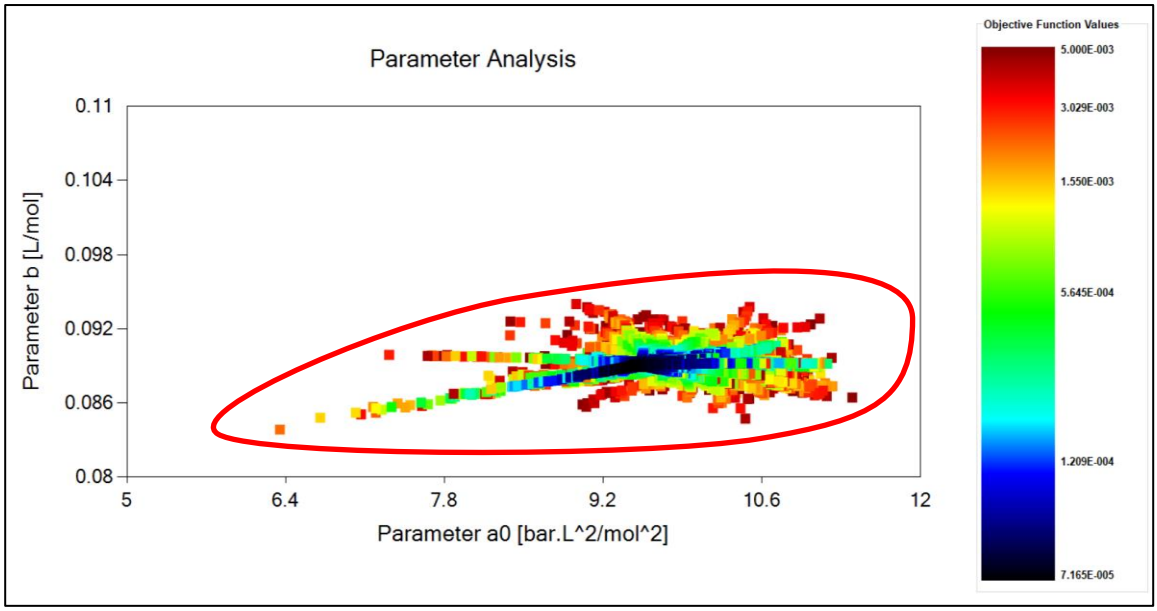

(b)

Figure 16 - Parametric Analysis of the Final Simulation (SIM12). (a) beta – a_0; (b) b – a_0; (c) c_1– a_0; (d) eps/R – a_0; (e) beta – b; (f) c_1– b; (g) eps/R – b; (h) beta – c_1; (i) eps/R – c_1; (j) beta – eps/R. Parameters estimated using CPA and optimization method PSO. Maximum number of 1000 iterations and 200 particles. The maximum objective function value considered is 0.005. 100 experimental points were used between 0.55 - 0.90 T_R. Experimental data from DIPPR(DIADEM, 2004).

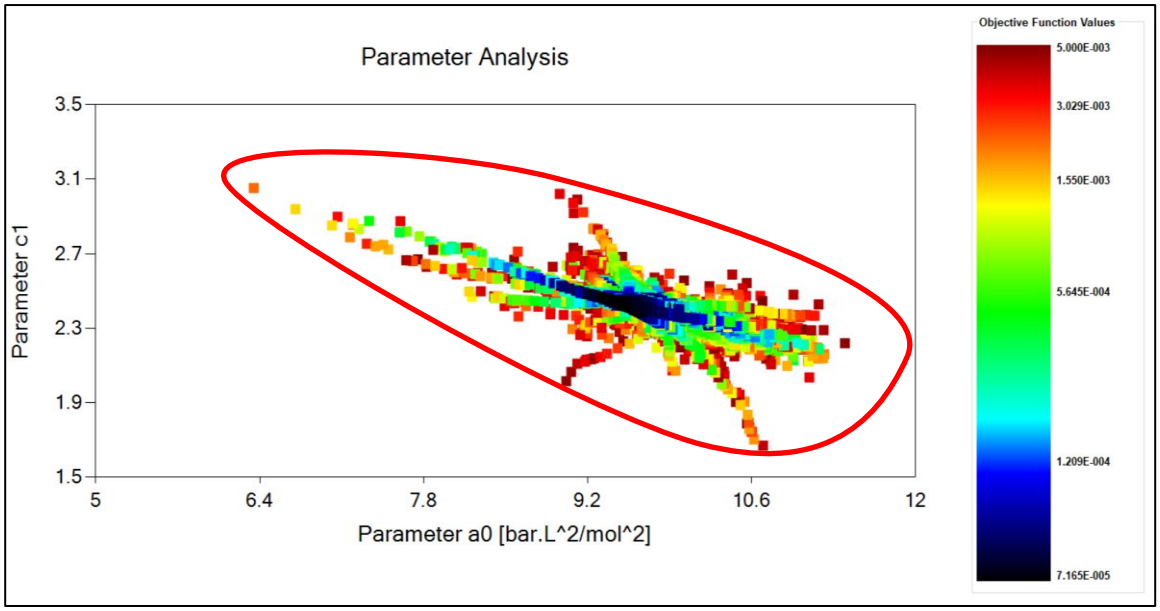

(c)

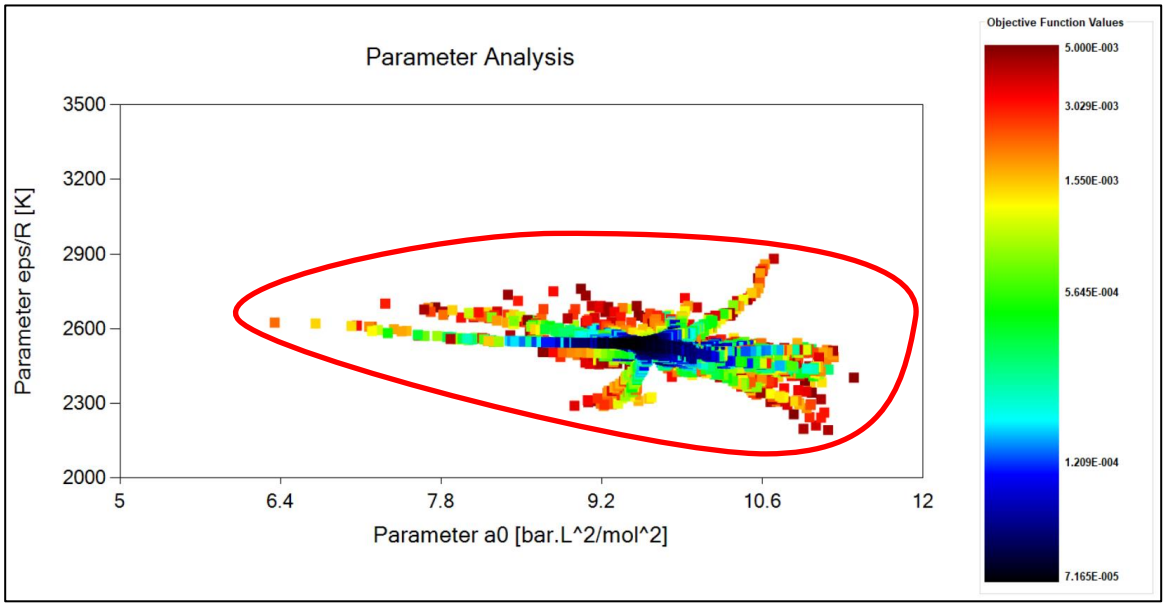

(d)

Figure 16 (continuation) - Parametric Analysis of the Final Simulation (SIM12). (a) beta – a_0; (b) b – a_0; (c) c_1– a_0; (d) eps/R – a_0; (e) beta – b; (f) c_1– b; (g) eps/R – b; (h) beta – c_1; (i) eps/R – c_1; (j) beta – eps/R. Parameters estimated using CPA and optimization method PSO. Maximum number of 1000 iterations and 200 particles. The maximum objective function value considered is 0.005. 100 experimental points were used between 0.55 - 0.90 T_R. Experimental data from DIPPR(DIADEM, 2004).

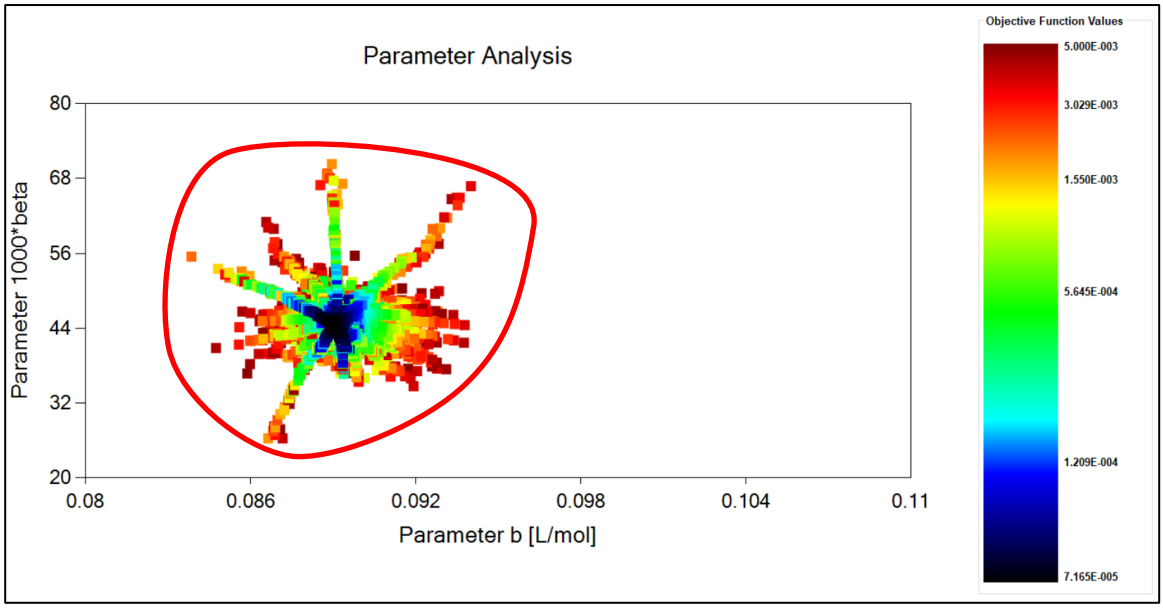

(e)

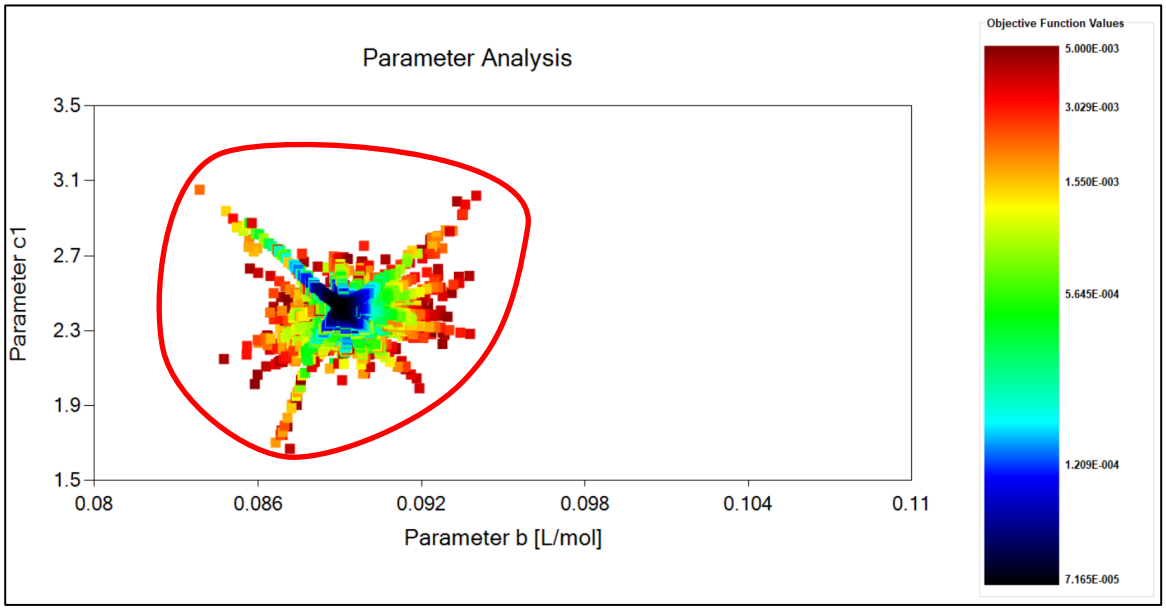

(f)

Figure 16 (continuation) - Parametric Analysis of the Final Simulation (SIM12). (a) beta – a_0; (b) b – a_0; (c) c_1– a_0; (d) eps/R – a_0; (e) beta – b; (f) c_1– b; (g) eps/R – b; (h) beta – c_1; (i) eps/R – c_1; (j) beta – eps/R. Parameters estimated using CPA and optimization method PSO. Maximum number of 1000 iterations and 200 particles. The maximum objective function value considered is 0.005. 100 experimental points were used between 0.55 - 0.90 T_R. Experimental data from DIPPR(DIADEM, 2004).

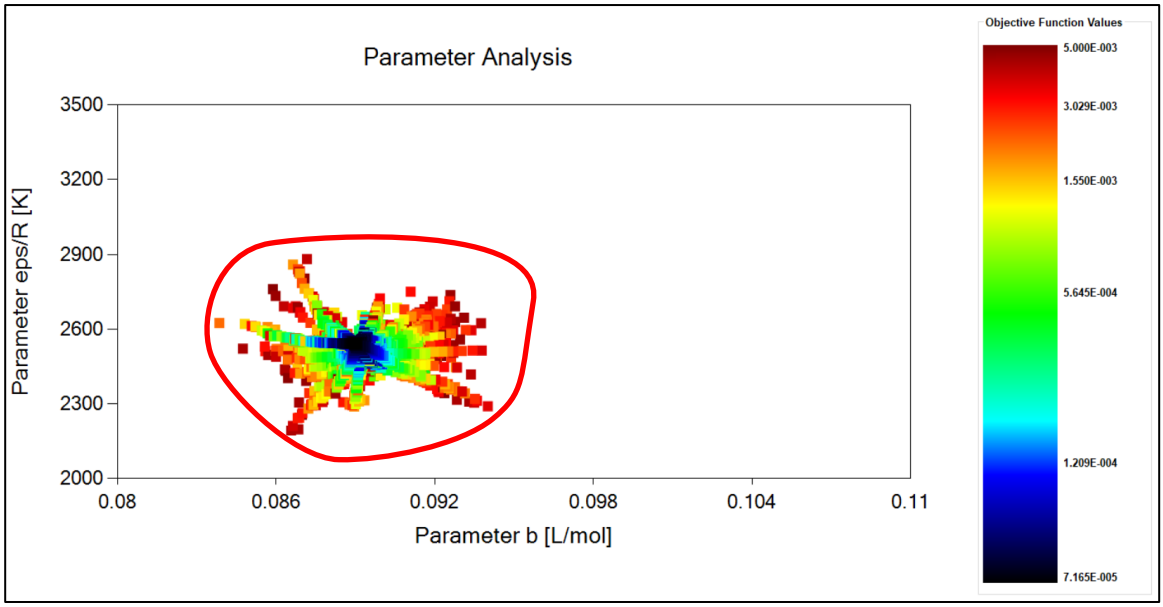

(g)

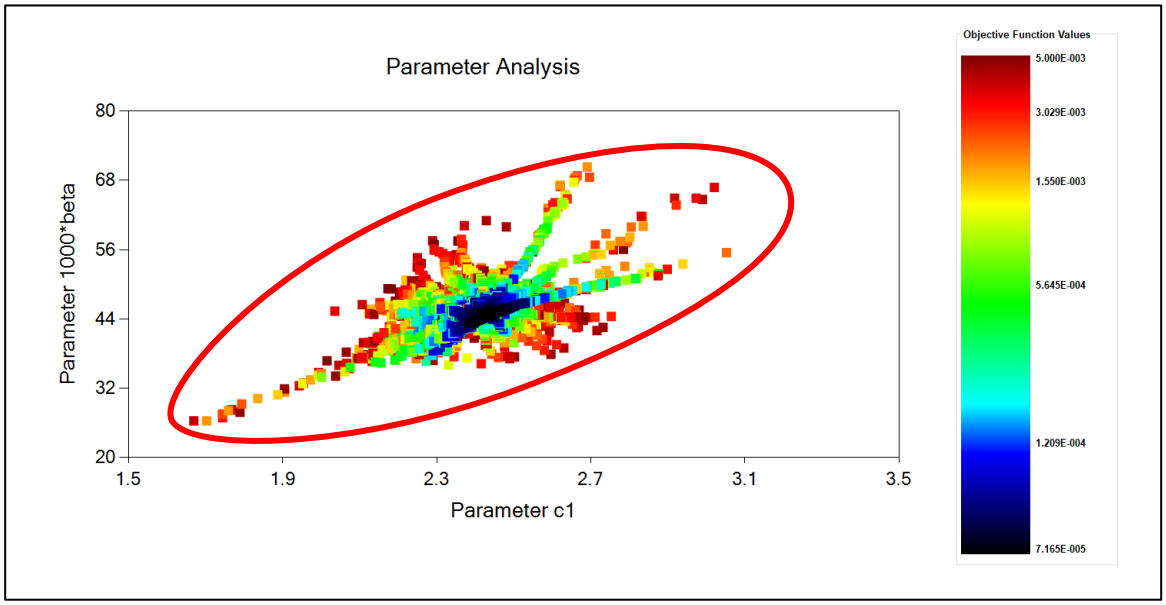

(h)

Figure 16 (continuation) - Parametric Analysis of the Final Simulation (SIM12). (a) beta – a_0; (b) b – a_0; (c) c_1– a_0; (d) eps/R – a_0; (e) beta – b; (f) c_1– b; (g) eps/R – b; (h) beta – c_1; (i) eps/R – c_1; (j) beta – eps/R. Parameters estimated using CPA and optimization method PSO. Maximum number of 1000 iterations and 200 particles. The maximum objective function value considered is 0.005. 100 experimental points were used between 0.55 - 0.90 T_R. Experimental data from DIPPR(DIADEM, 2004).

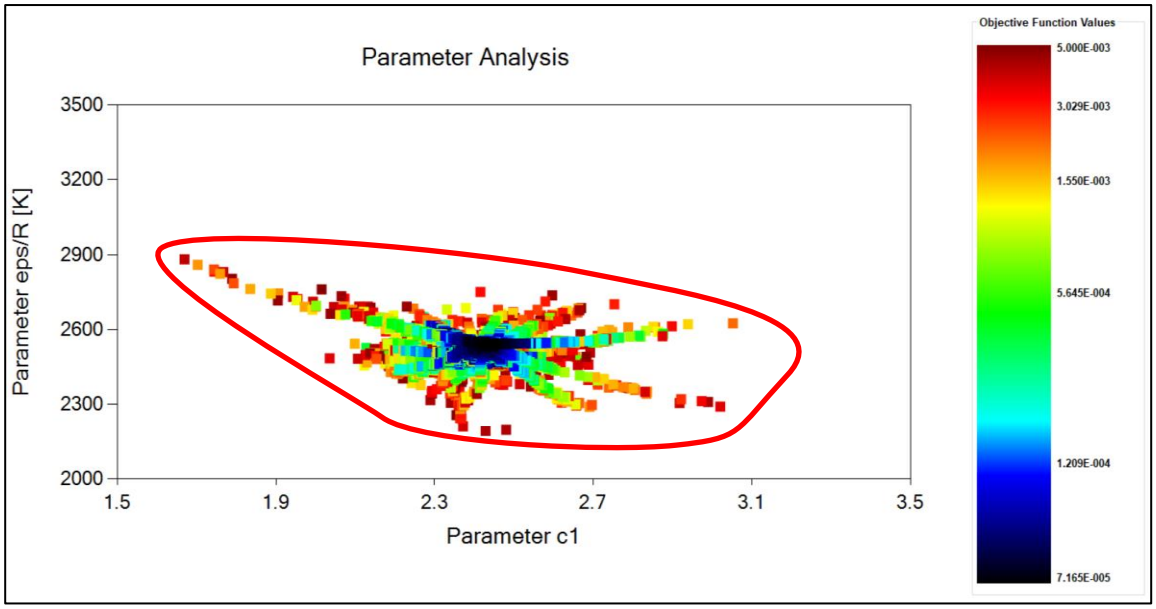

(i)

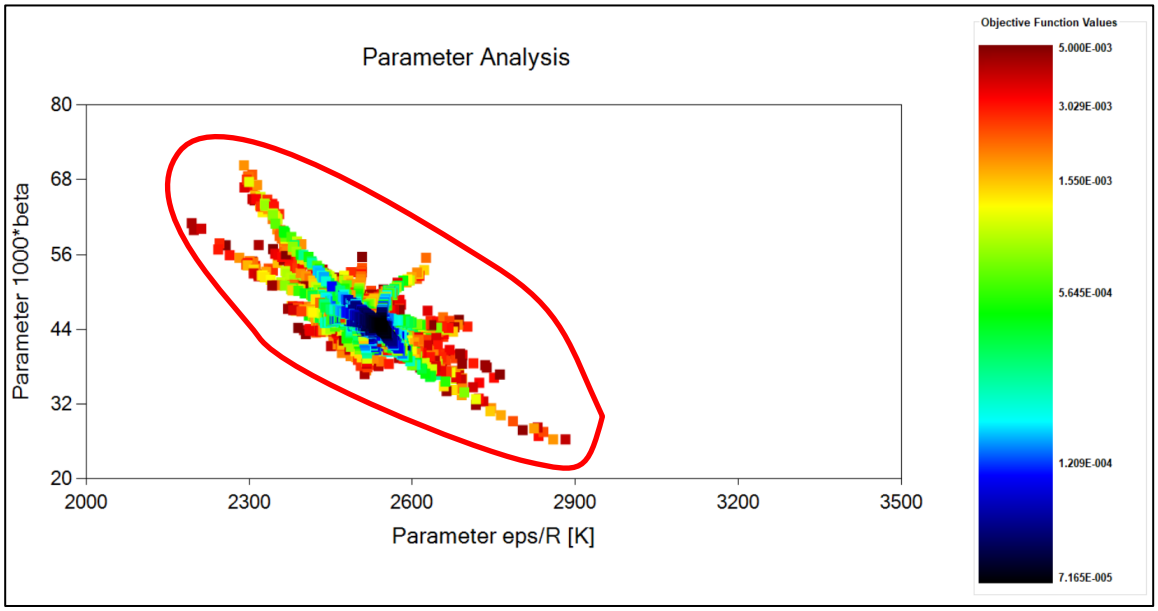

(j)

Figure 16 (continuation) - Parametric Analysis of the Final Simulation (SIM12). (a) beta – a_0; (b) b – a_0; (c) c_1– a_0; (d) eps/R – a_0; (e) beta – b; (f) c_1– b; (g) eps/R – b; (h) beta – c_1; (i) eps/R – c_1; (j) beta – eps/R. Parameters estimated using CPA and optimization method PSO. Maximum number of 1000 iterations and 200 particles. The maximum objective function value considered is 0.005. 100 experimental points were used between 0.55 - 0.90 T_R. Experimental data from DIPPR(DIADEM, 2004).

4.3 Liquid-Liquid Equilibrium Simulation

In order to comply with all the steps indicated in the parameter estimation methodology proposed, the parameter estimation was performed considering a binary mixture of DEA and Hexadecane. Any hydrocarbon could be utilized, since they do not associate. Hexadecane was used because of its availability for LLE experimental data with DEA.

The pure hexadecane data were obtained through their critical conditions. It would be possible to estimate them through CPA (that would be reduced to SRK EoS, since this compound does not originate hydrogen bonds), however it is not this work's objective to study the details of this compound simulation.

4.3.1 Liquid-Liquid Equilibrium Simulations for mixing DEA and Hexadecane

For the parameters estimation using both VLE and LLE data, it was decided to work with a multiobjective function, which is be the sum of the Equations 24 and 26, weighted by a factor w, multiplied by the LLE objective function, according to Equation 38.

$$\boldsymbol{F_{obj} = F_{obj_{ELV}} + w.F_{obj_{ELL}}} \qquad \textbf{38}$$

In this new procedure, adopting only the Simplex method, 5 parameters of pure DEA were estimated (a_0,b,c_1,$\frac{\epsilon}{R}$ and $beta$) and the binary parameter (k_{ij}) was set to zero. The weight w was varied from 10^{-3} to 1. The solely Simplex method application as the optimization method in this case occurred since it was considered that the intervals generated in Section 4.2 would provide good initial estimates. Despite this, this consideration is analyzed since the alkanolamines are especially complex compounds to be modeled(AVLUND; KONTOGEORGIS; MICHELSEN, 2008; SANTOS *et al.*, 2015).

The estimation of parameters using the weight (w) is considered a sensitivity analysis, since the weights are set by the user and the influence of it in the estimation procedure as a whole is evaluated.

After determining the best cases in the sensitivity analysis, the k_{ij} for these cases were estimated. It is important to explain the reason for not estimating k_{ij} at first. The objective of using the LLE data (in addition to adopting the proposed methodology completely) is to verify the quality of the estimated parameters by comparing the parameter estimation using as metric Equation 24 and Equation 26. As in pure DEA parameter estimation using VLE data, only 5 parameters were estimated, the number of estimated parameters should be maintained in the estimation with VLE and LLE data, for a fair comparison.

The simulations generated a large dataset, but often when evaluating the objective function considering only the VLE data, it presented values above 5.10^{-3} (above the maximum statistically acceptable value, based on the quality of the pure DEA experimental data). Thus, the chosen metric is the acceptance of the set of parameters that minimizes the multiobjective function but that maintains the objective function of the VLE in a maximum of 5.10^{-3}. Table 21 is a real example that illustrates the situation:

Table 21 - Example of how best results of the multiobjective function do not generate a statistically acceptable result for the objective function VLE

Example	w	F_{obj} (VLE+LLE)	F_{obj} (VLE)	F_{obj} (LLE)	AAP	AAρ	AAXI-II	AAXII-I
Example 1	0.1	0.991	0.004	0.991	0.104%	1.609%	6.732%	95.012%
Example 2	0.2	0.987	0.006	0.987	0.203%	2.590%	6.770%	94.939%

In Table 21, AAXI-II and AAXII-I are the average absolute deviation for the compositions in LLE. They are defined by Equations 39 and 40:

$$AAXI - II\ \% = \left(\frac{100}{N_{exp}}\right) \sum_{i=1}^{N\,exp} \frac{(x_{o,i}^{DEA,calc} - x_{o,i}^{DEA,exp})^2}{(x_{o,i}^{DEA,exp})} \quad 39$$

$$AAXII - I\ \% = \left(\frac{100}{N_{exp}}\right) \sum_{i=1}^{N\,exp} \frac{(x_{p,i}^{HC,calc} - x_{p,i}^{HC,exp})^2}{(x_{p,i}^{HC,exp})} \quad 40$$

Note that Example 2 leads to lower multiobjective function (Equation 38) value (0.987) while the VLE objective function value (0.006) is higher than the statistically accepted upper limit (0.005). Thus, the set of parameters estimated in Example 2 does not meet the criteria that establishes maximum value for the VLE objective function and thus the set of parameters estimated considering this weight are discarded. Example 1 however generates higher multiobjective function values (0.991) but lower VLE objective function value (0.004), which are in accordance with the acceptable limit and therefore the set of parameters are taken into account in the decision of the best set of parameters. The flowchart (Figure 17) illustrates the decision process for the best set of parameters.

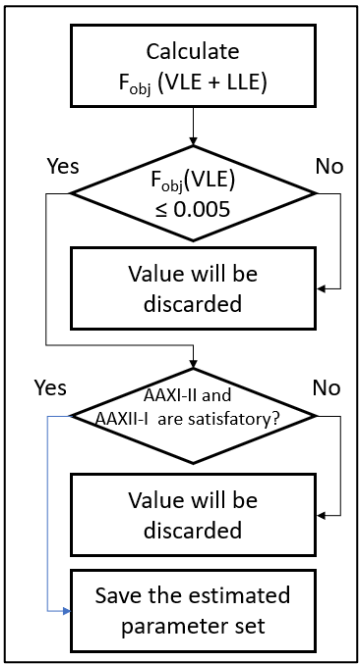

Figure 17- Decision flow diagram of the choice of the best sets of parameters based on the maximum value of the objective function VLE and on the analysis of the AAXI-II and AAXII-I values.

While the objective function VLE has a maximum numerical limit (5.10^{-3}), the AAXI-II and AAXII-I quality analysis is based on the set of parameters that minimizes these variables.

In order to begin the sensitivity analysis, it is fundamental to define the parameter limits and to do this, the intervals presented in Table 20 are adopted. It was necessary to provide initial estimates for the parameters to be estimated. These initial values are deeply important because they can lead the optimization method to different convergence areas. Due to this fact, it was decided to use nine sets of values that approached the whole statistically accepted interval. Among these nine sets, four stand out because they were based on: 1. Statistically accepted interval lower values (Set A); 2. Statistically accepted interval higher values (Set B); 3. Statistically accepted interval mean values (Set C); and 4. Best set of parameters found in the last simulation performed in the estimation of the parameters of the pure DEA (using only VLE data), SIM12 (Set D). The other five sets of parameters are a combination of the values of the first four sets. All nine parameter sets are in accordance with the ranges informed in Table 20. This information is presented in Table 22:

Table 22 - Initial guesses for the parameters to be estimated in the sensitivity analysis using VLE and LLE data

Parameter Set	a_0 (bar.L^2/mol^2)	b (L/mol)	c_1	ε/R (K)	1000* β
Set A	6.349	0.084	1.669	2193.840	26.343
Set B	11.399	0.094	3.052	2881.620	70.328
Set C	9.673	0.091	2.722	2862.716	51.804
Set D	7.948	0.087	2.392	2843.811	33.280
Set E	7.000	0.087	2.000	2500.000	30.000
Set F	9.200	0.092	2.500	2300.000	40.000
Set G	8.000	0.087	2.300	2500.000	30.000
Set H	7.000	0.092	2.700	2300.000	50.000
Set I	10.000	0.090	2.700	2300.000	60.000

The sensitivity analysis generated a considerable amount of results and each result presented the five estimated parameters and calculations of the multiobjective function, VLE objective function, LLE objective function, AAP%, AAρ%, AAXI-II% and AAXII-I%.

Table 23 is an example of a sensitivity analysis, varying the weight from 10^{-3} to 1, considering as initial values the lowest of the statistically accepted range.

Table 23 - Example of a sensitivity analysis, varying the weight of 10^{-3} to 1, considering as initial estimates the smallest values of the statistically accepted interval determined. Equilibrium data from DIPPR(DIADEM, 2004) and Abdi (ABEDINZADEGAN ABDI; MEISEN, 1998).

Weight	**0.001**	**0.005**	**0.01**	**0.05**	**0.1**	**0.5**	**1**
a_0 (bar.L^2/mol^2)	9.829	7.383	7.485	9.976	6.350	7.992	8.047
b (L/mol)	0.089	0.087	0.088	0.092	0.089	0.094	0.094
c_1	1.956	2.495	2.476	1.992	3.052	3.050	3.053
ε/R (K)	2876.98	2881.56	2881.49	2881.61	2783.31	2395.65	2331.71
1000* β	26.716	33.242	32.947	26.343	42.125	64.823	70.323
F_{obj}VLE	5.E^{-05}	6.E^{-05}	2.E^{-04}	2.E^{-03}	1.E^{-03}	9.E^{-03}	2.E^{-02}
F_{obj}LLE	1.163	1.124	1.111	1.055	1.070	0.977	0.961
F_{obj} (VLE+LLE)	0.001	0.006	0.011	0.054	0.108	0.497	0.981
AAP%	0.202	0.179	0.189	0.437	0.714	5.471	10.326
AAρ%	0.547	0.633	1.158	3.972	3.599	6.769	6.775
AAXI-II%	96.198	97.254	97.214	96.121	97.282	94.549	93.893
AAXII-I%	45.394	38.923	37.774	33.247	31.530	25.922	25.304

In Table 23 only a few values of weights are presented between the interval of 10^{-3} to 1 (because it is only an illustrative example). However, in ThermOptimizer software was possible for the user to set the desirable amount of points between the inferior interval and the superior interval. In this work, 100 points were used between the lowest weight (10^{-3}) and the highest weight (1).

It is possible to notice that as the weight is increased the VLE F_{obj} values are increased, due to the greater significance of the LLE F_{obj} term influenced by the higher weight. Thus, an increase in AAP% and AAρ% and a decrease of AAXI-II% and AAXII-I% (liquid phase modeling improvement), with the increase in the weight conferred, can be observed.

Aiming to illustrate the weight sensitivity according to the chosen metric, it follows the graphs of weights versus VLE objective function and versus the best results of AAXI-II and AAXII-I (Figure 18):

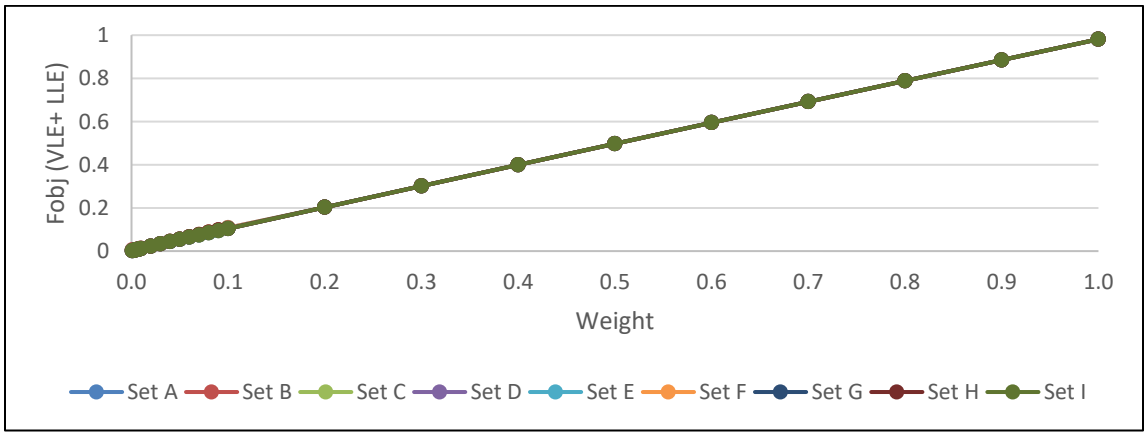

(a)

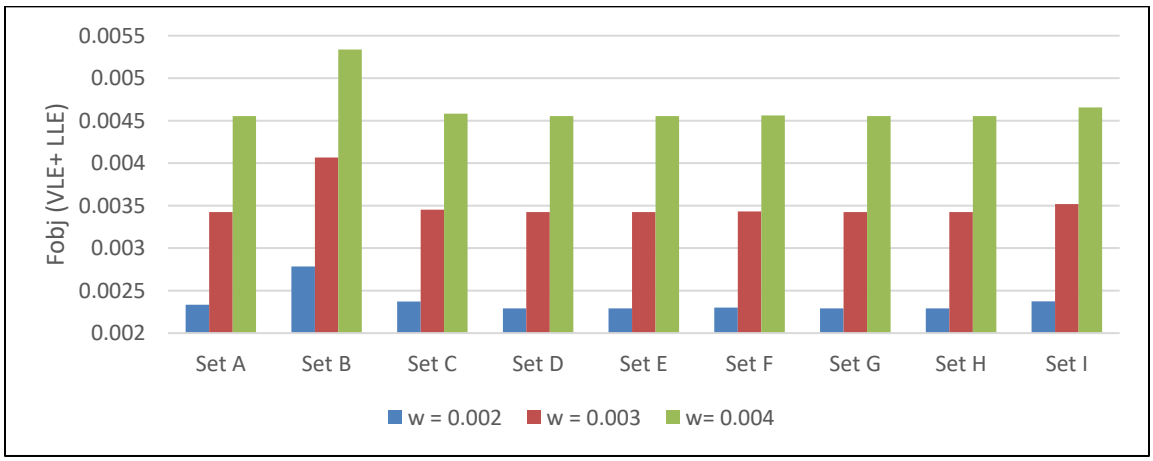

(b)

Figure 18 - Results of the Sensitivity Analysis, using the 9 sets of initial estimates: (a) Multiobjective Function (b) Weight range selected for checking the difference in Multiobjective Function values depending on each weight (c) VLE F_{obj} (d) AAXI-II% (e) AAXII-I%. Equilibrium data from DIPPR(DIADEM, 2004) and Abdi(ABEDINZADEGAN ABDI; MEISEN, 1998).

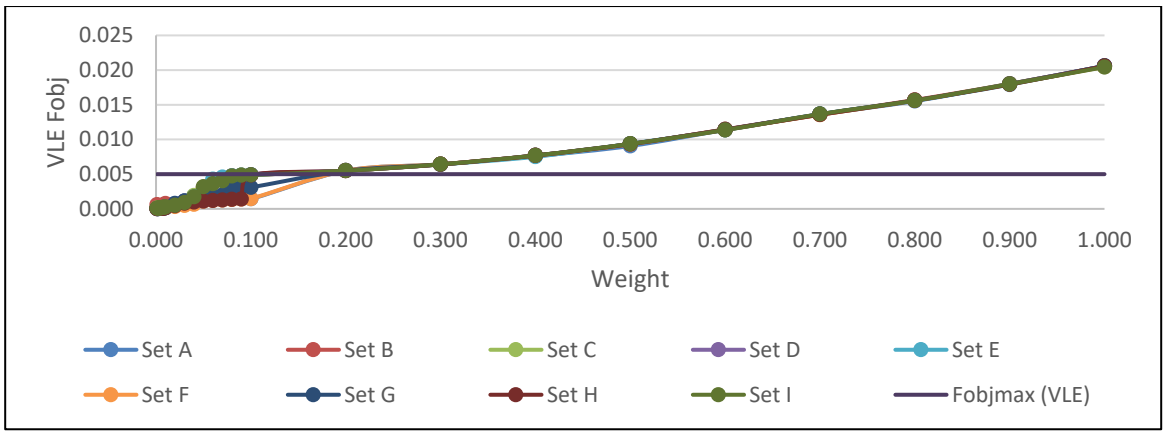

(c)

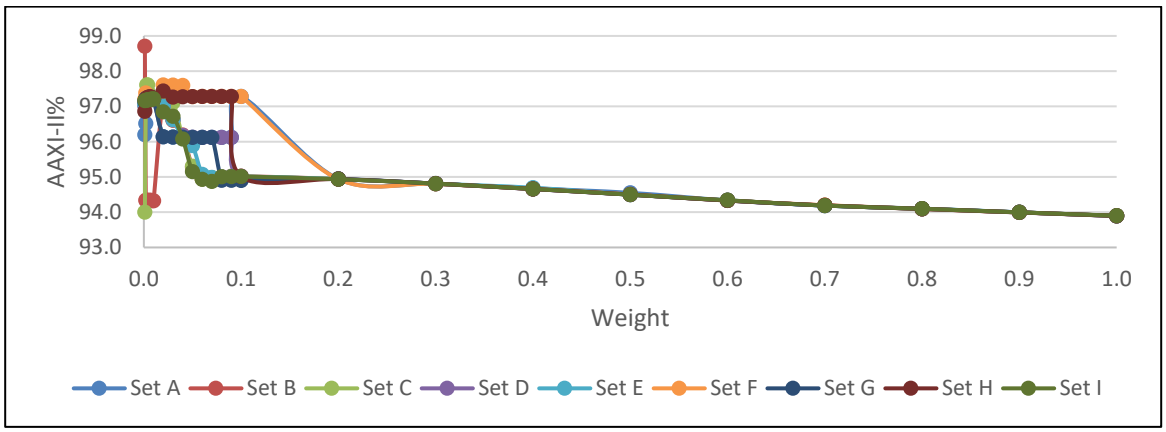

(d)

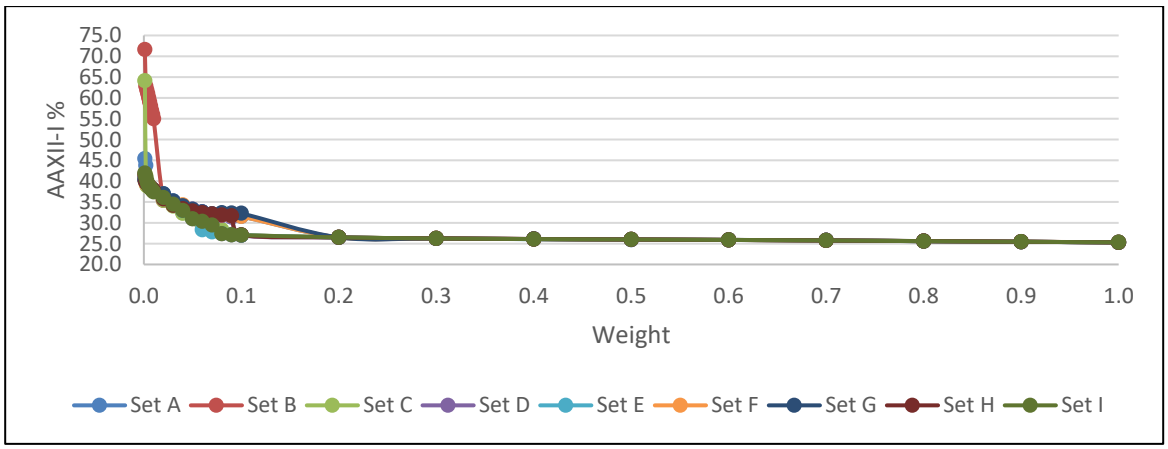

(e)

Figure 18 (continuation) - Results of the Sensitivity Analysis, using the 9 sets of initial estimates: (a) Multiobjective Function (b) Weight range selected for checking the difference in Multiobjective Function values depending on each weight (c) VLE F_{obj} (d) AAXI-II% (e) AAXII-I%. Equilibrium data from DIPPR(DIADEM, 2004) and Abdi(ABEDINZADEGAN ABDI; MEISEN, 1998).

It is possible to verify that with larger weights the calculated values of the parameters are the same, regardless the initial guess used. It is also possible to notice that AAXII-I% values performed better than AAXI-II% values, indicating better Hexadecane modeling in the aqueous phase than the DEA modeling in the organic phase.

In the scale presented in Figure 18 (a) it is not viable to perceive difference in the calculated multiobjective function value considering the different sets of initial guesses. This is due to the small scale shown in this Figure. If a larger scale (Figure 18 (b)) is used for a selected range of weights, it is possible to recognize the different values of the objective function, for each weight considered.

For each case presented in Table 22, two calculated parameters set were selected to be used for a k_{ij} parameter estimation procedure. Thus, 18 k_{ij} were generated. The selection was performed according to two criteria: a) meeting the VLE objective function maximum value criteria (5.10^{-3}) and b) presenting lower AAXI-II% and AAXII-I% values. It is important to note that in the methodology proposed by Santos(SANTOS *et al.*, 2015), only the 10 best sets of parameters would have their k_{ij} estimated (Figure 3). However, during this estimation step, it was observed that there were potential results and the best 18 results were chosen (which does not impact to fulfill the methodology in a complete way).

The binary mixture parameter estimation takes place applying the LLE objective function (Equation 26). Pure DEA parameters (obtained in the sensitivity analysis) and Hexadecane parameters (obtained analytically) are inserted. The only parameter to be estimated is the k_{ij} in this case.

As there was no case that presented lower values of both AAXI-II and AAXII-I, it was decided to consider as best case the one that presented smaller values of the sum of AAXI-II and AAXII-I. According to Table 24, it is possible to verify that the value of k_{ij} that confers smaller values of the sum of AAXI-II (92.1 %) and AAXII-I (23.4 %) is in simulation number eight, coming from Set D.

It follows the graphs of the LLE curve, the mean deviations from the compound's compositions in aqueous phase and organic phase and the behavior of the k_{ij} in relation to the LLE objective function (Figure 19).

Table 24 - k_{ij} parameter estimation for the binary mixture: DEA and Hexadecane. Sets of results obtained in the sensitivity analysis were estimated. Equilibrium data from DIPPR(DIADEM, 2004) and Abdi(ABEDINZADEGAN ABDI; MEISEN, 1998).

N°	Input		Output			
	Parameter Set	w	k_{ij}	F_{obj} (VLE + LLE)	AAXI-II%	AAXII-I%
1	Set A	0.1	-0.006	$9.73E^{-01}$	94.8%	22.9%
2	Set A	0.09	-0.003	$1.04E^{+00}$	96.0%	29.9%
3	Set B	0.1	-0.003	$1.07E^{+00}$	97.2%	30.1%
4	Set B	0.003	-0.012	$1.08E^{+00}$	97.0%	32.0%
5	Set C	0.1	-0.006	$9.73E^{-01}$	94.8%	22.9%
6	Set C	0.02	-0.009	$1.06E^{+00}$	97.0%	29.9%
7	Set D	0.1	-0.006	$9.73E^{-01}$	94.8%	22.9%
8	Set D	0.001	-0.037	$9.27E^{-01}$	92.1%	23.4%
9	Set E	0.1	-0.006	$9.73E^{-01}$	94.8%	22.9%
10	Set E	0.09	-0.006	$9.72E^{-01}$	94.8%	22.8%
11	Set F	0.1	-0.003	$1.07E^{+00}$	97.2%	30.1%
12	Set F	0.001	-0.014	$1.07E^{+00}$	96.9%	31.4%
13	Set G	0.1	-0.006	$1.01E^{+00}$	94.7%	28.5%
14	Set G	0.06	-0.004	$1.04E^{+00}$	96.0%	30.2%
15	Set H	0.1	-0.006	$9.73E^{-01}$	94.8%	22.9%
16	Set H	0.09	-0.003	$1.07E^{+00}$	97.2%	30.1%
17	Set I	0.1	-0.006	$9.73E^{-01}$	94.8%	22.9%
18	Set I	0.07	-0.007	$9.79E^{-01}$	94.6%	24.6%

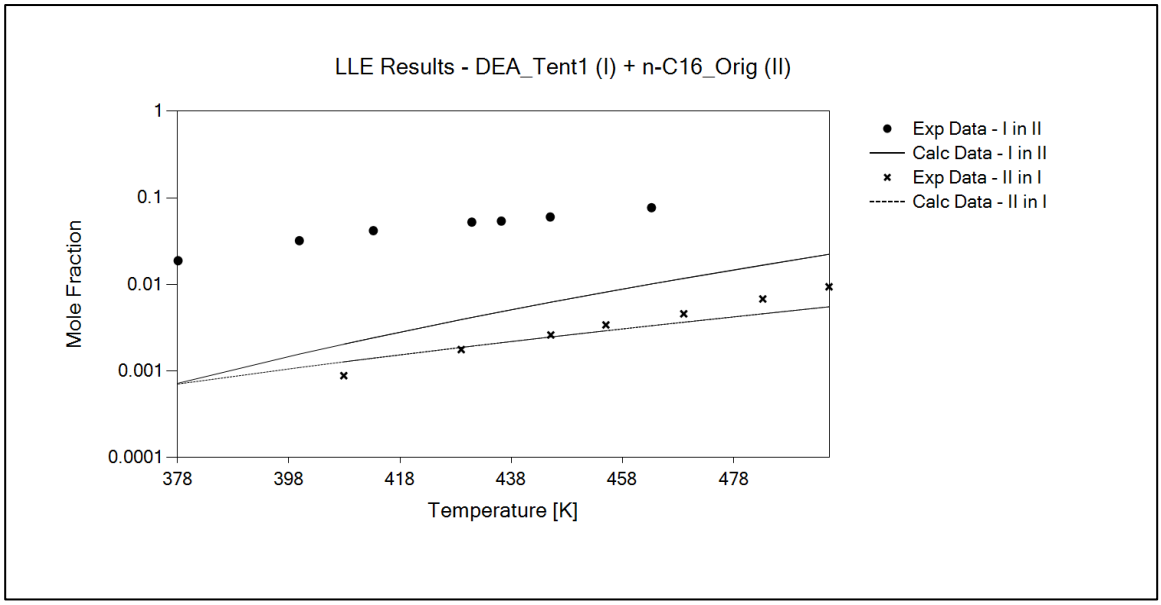

(a)

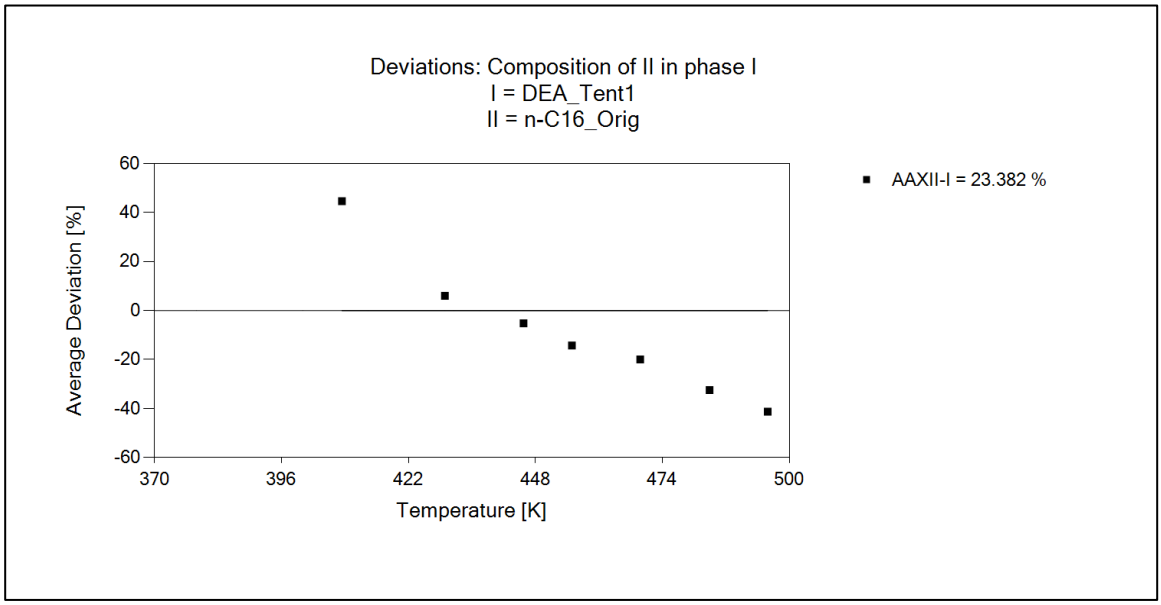

(b)

Figure 19 -DEA-Hexadecane parameter estimation (a) Solute Mole fraction as a function of temperature (aqueous and organic phases) (b) AAXII-I (c) AAXI-II (d) k_{ij} as a function objective function. DEA_Tent1 is the file that pulls the balance data from the Pure DEA. n-C16_Orig is the file that pulls the parameters of Pure Hexadecane. Equilibrium data from DIPPR(DIADEM, 2004) and Abdi(ABEDINZADEGAN ABDI; MEISEN, 1998)

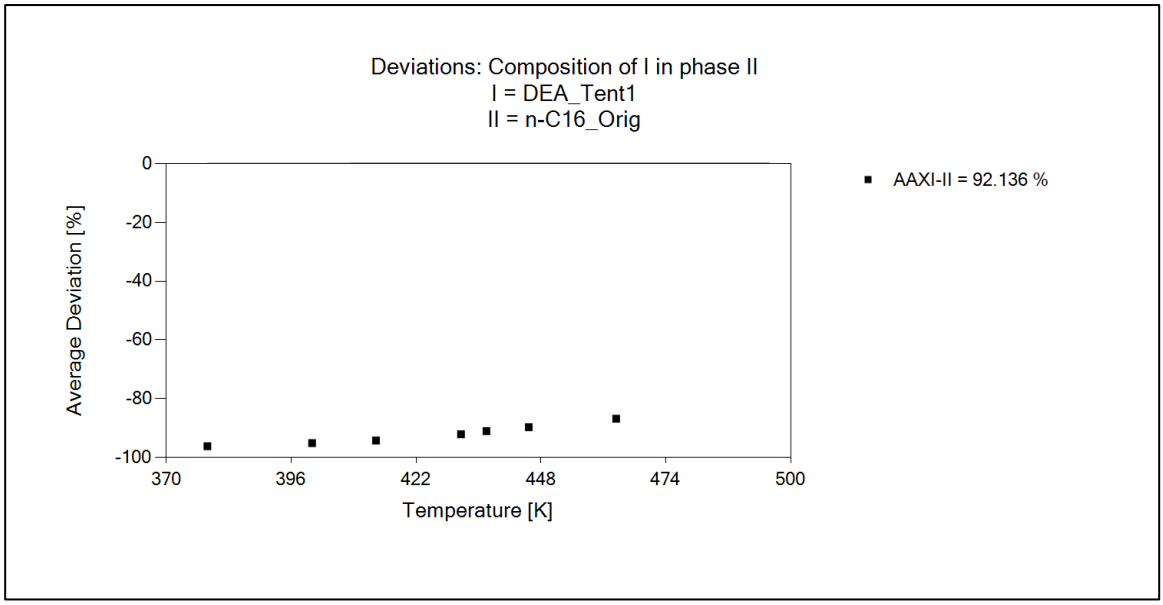

(c)

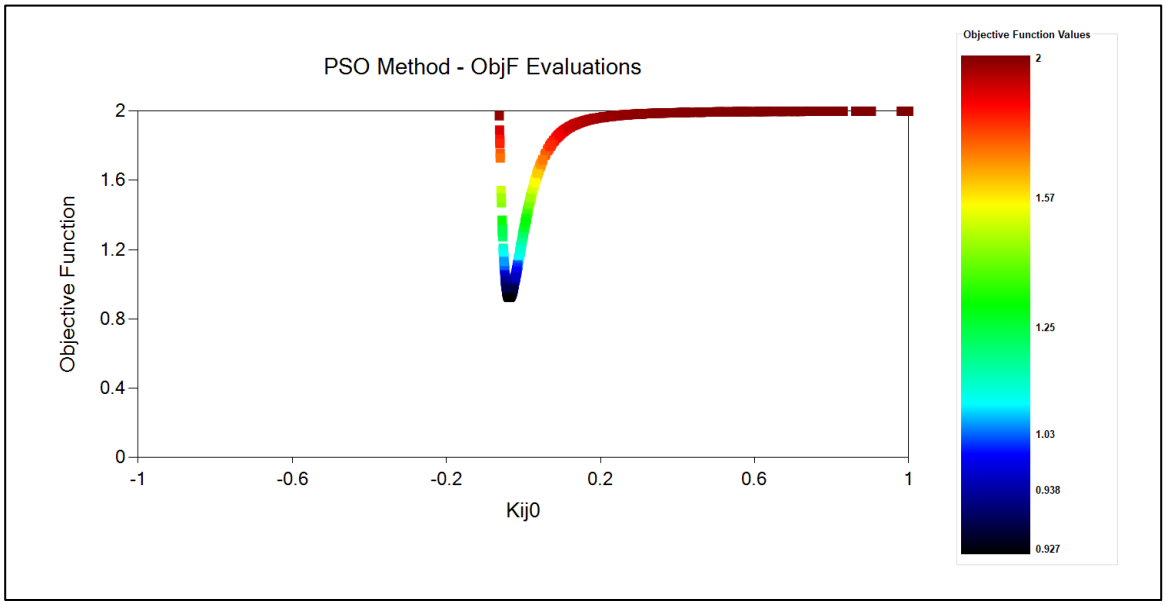

(d)

Figure 19 (continuation)-DEA-Hexadecane parameter estimation (a) Solute Mole fraction as a function of temperature (aqueous and organic phases) (b) AAXII-I (c) AAXI-II (d) k_{ij} as a function objective function. DEA_Tent1 is the file that pulls the balance data from the Pure DEA. n-C16_Orig is the file that pulls the parameters of Pure Hexadecane. Equilibrium data from DIPPR(DIADEM, 2004) and Abdi(ABEDINZADEGAN ABDI; MEISEN, 1998)

Thus, the final parameters of the pure DEA, applying the complete methodology suggested in the literature, are presented in Table 25:

Table 25 - Pure DEA Final parameters. Data obtained through parameter estimation using the complete methodology proposed in the literature (SANTOS *et al.*, 2015).

Compound	a_0 (bar.L^2/mol^2)	b (L/mol)	c_1	ε/R (K)	1000* β
DEA	9.607	0.089	2.522	2442.400	51.245

It is important to note that these parameters are part of the range of parameters that are statistically accepted, based on the experimental errors of pure DEA vapor pressure and liquid density data. This set of parameters generates acceptable VLE objective function ($1.1.10^{-4}$), AAP (0.8%) and AAρ (0.3%) values.

There was interest in comparing the results obtained with the literature (AVLUND; KONTOGEORGIS; MICHELSEN, 2008), however due an issue with bibliographic reference, this validation was not possible. More details on this in Appendix A.

4.3.2 Liquid-Liquid Equilibrium Simulations for mixing DEA and Octadecane

As a measure to validate the pure DEA parameters estimated it was also performed the parameter estimation handling another hydrocarbon in equilibrium with the DEA, the Octadecane. Like the Hexadecane, the Octadecane parameters were obtained through its critical points and acentric factor. The DEA-Octadecane equilibrium data is from Abdi (ABEDINZADEGAN ABDI; MEISEN, 1996).

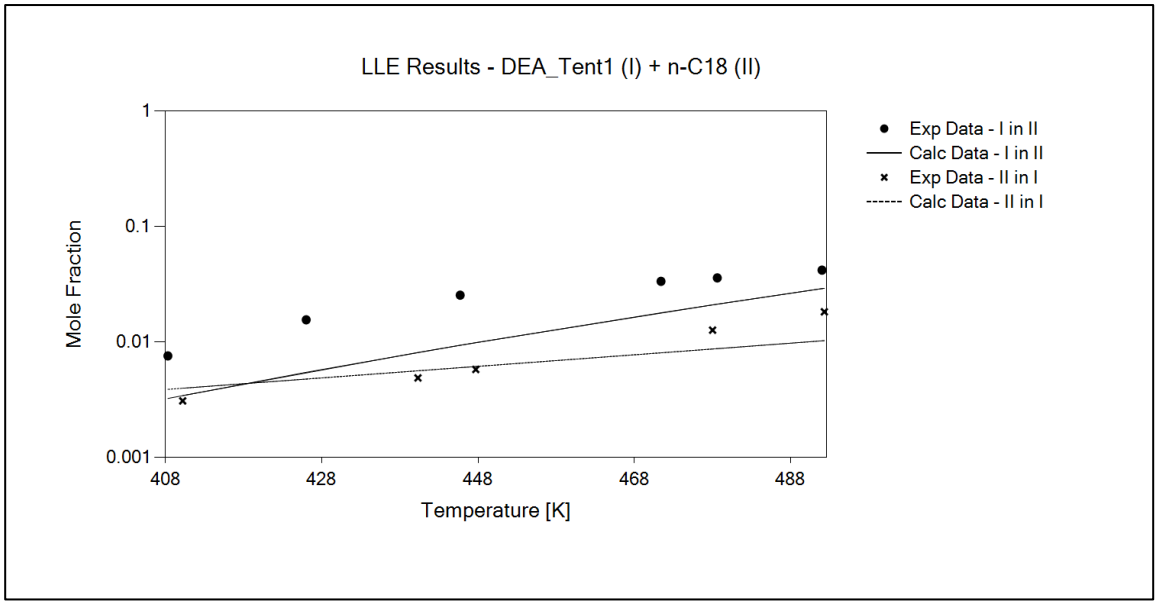

(a)

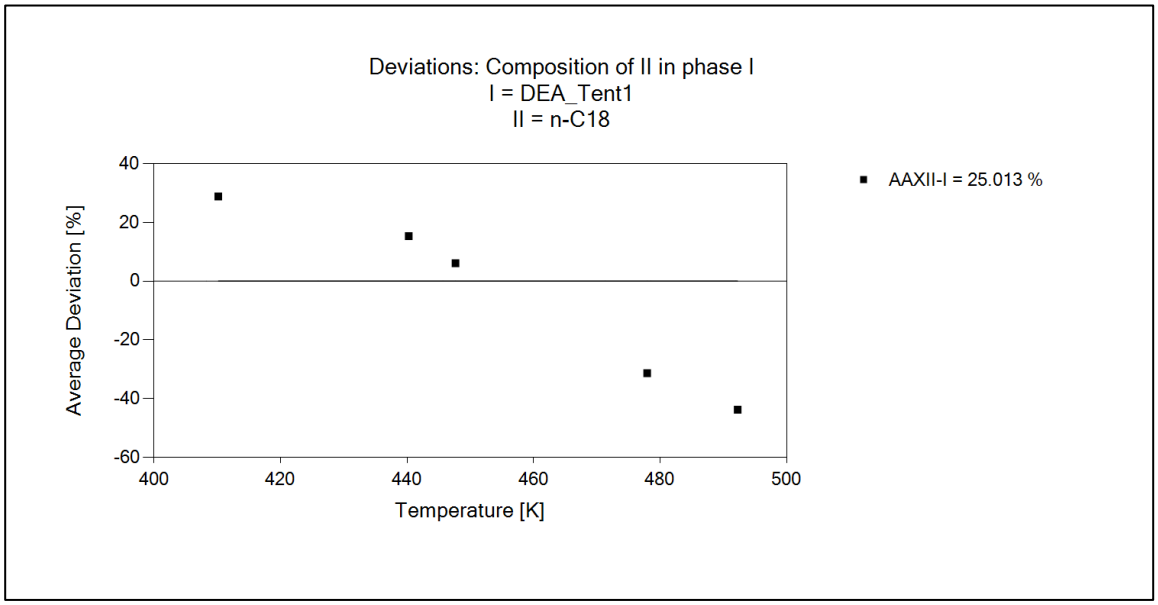

(b)

Figure 20 - DEA-Octadecane parameter estimation (a) Solute Mole fraction as a function of temperature (aqueous and organic phases) (b) AAXII-I (c) AAXI-II (d) k_{ij} as a function objective function. DEA_Tent1 is the file that pulls the balance data from the Pure DEA. n-C18 is the file that pulls the parameters of Pure Octadecane. Equilibrium data from DIPPR (DIADEM, 2004) and Abdi (ABEDINZADEGAN ABDI; MEISEN, 1996).

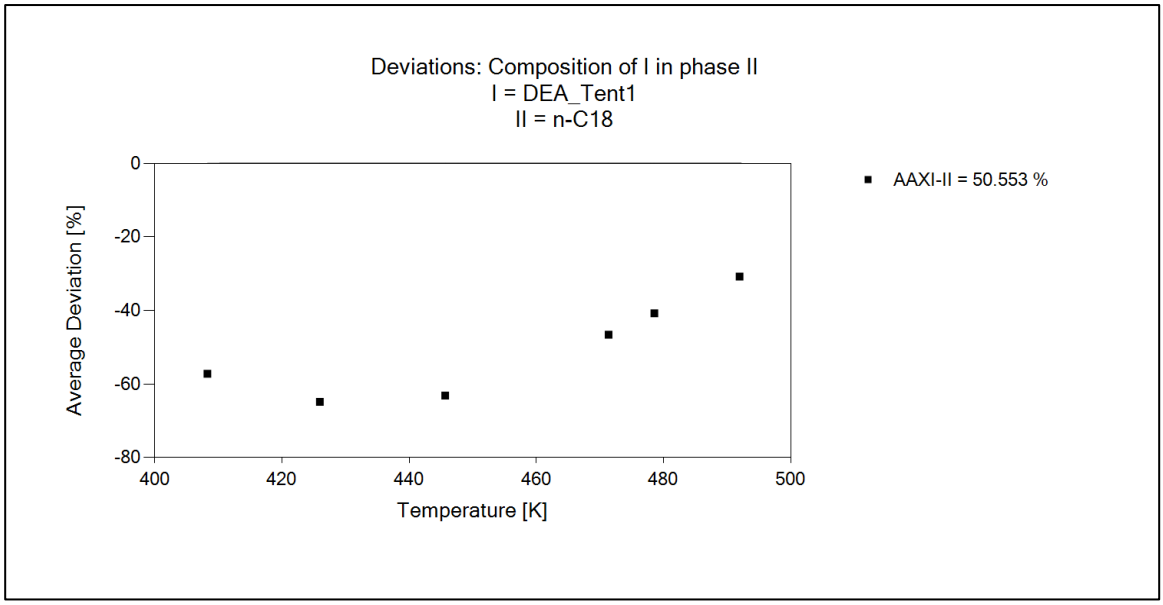

(c)

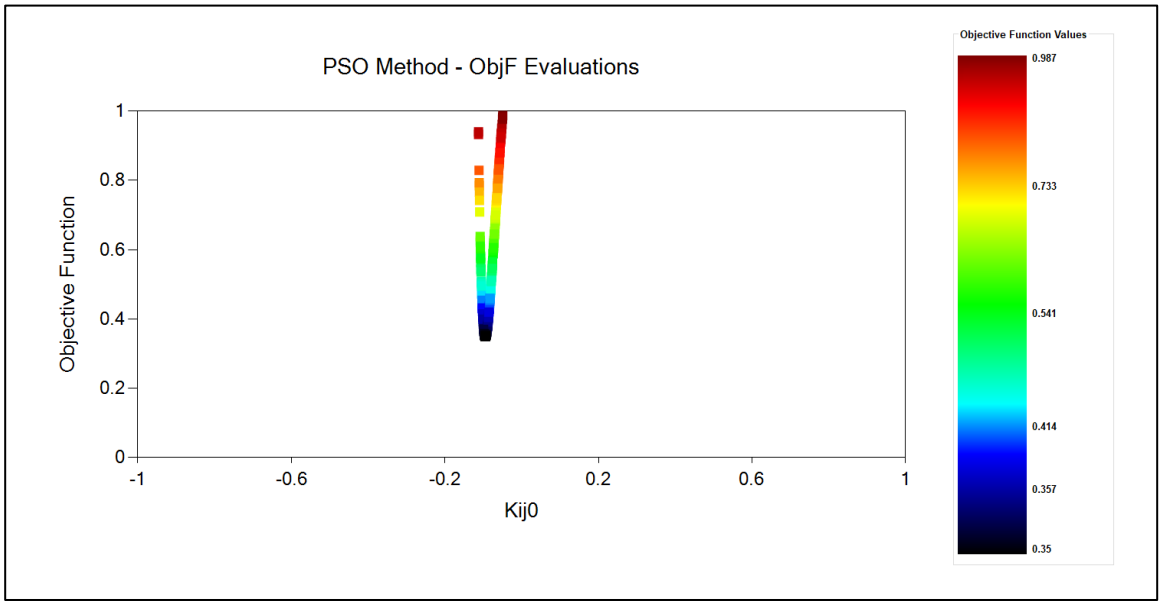

(d)

Figure 20 (continuation) - DEA-Octadecane parameter estimation (a) Solute Mole fraction as a function of temperature (aqueous and organic phases) (b) AAXII-I (c) AAXI-II (d) k_{ij} as a function objective function. DEA_Tent1 is the file that pulls the balance data from the Pure DEA. n-C18 is the file that pulls the parameters of Pure Octadecane. Equilibrium data from DIPPR (DIADEM, 2004) and Abdi (ABEDINZADEGAN ABDI; MEISEN, 1996).

In this case, since the parameters of pure DEA were already estimated, it was proceeded directly to k_{ij} estimation. The results are shown in Figure 20.

According to the results of both parameter estimation using different hydrocarbons, it was considered that the pure DEA estimated parameters were validated for the application of interest in the next step of the work (taking into account the high values of absolute deviations in the composition of the phases). However, it is important to mention that based on these results it is possible to conclude that some work can be performed in the CPA EoS to improve the organic phase modeling.

As a next step, it was necessary to estimate the parameters of the main binaries present in the AGASA industrial unity under study.

4.4 Parameter Estimation of main DEA Binary Systems

Once the pure DEA parameters were defined, the second step was to perform some study in order to calculate k_{ij} for the binary mixture that exist in the evaluated AGASA unity. The goal is to gather available information to conduct an acid gas absorber tower simulation. The main DEA binaries are considered as those whose components have the highest concentration in the process feed and will then produce the greatest difference in the equilibrium calculations.

Unfortunately, experimental data of the desired binaries with DEA are scarce. Most of the experimental data found were ternary aqueous DEA solution with the desired compounds. For example, no data were found on the DEA-Methane binary data, but data from the ternary Water-DEA-Methane were acquired (LAWSON; GARST, 1976). This happened for all hydrocarbons and H_2S. The only set of important experimental data on binary found was that of Water-DEA(ASPEN, 2018).

The DEA-Water k_{ij} parameter estimation was carried out using mixing rule CR-1 and the and the value obtained was 0.595 (Table 26).

Table 26 - Parameter Estimation - DEA – Water Binary System. Pure DEA parameters from Table 19 and Pure Water parameters from DIPPR (DIADEM, 2004).

Mixing Rule	k_{ij}	$\beta^{A_iB_j}$	$\epsilon^{A_iB_j}$	Fobj	AAP
CR-1	0.595	0.060	2222.830	$2.30.E^{-1}$	41.612%

The objective function applied to estimate the Water-DEA binary mixture parameters is the same as in Equation 25.

Experimental data of the pure compounds and important binaries that do not involve DEA were also investigated. Table 27 and Table 28 have the main binaries whose experimental data were searched in the literature (FROST *et al.*, 2012).

Table 27 - Thermodynamic parameters of the pure compounds present in the AGASA unity under evaluation. Pure compounds parameters obtained in literature(FROST *et al.*, 2012).

Compound	*Tc* (K)	*b* (L/mol)	a_0/(R.b)	c_1	ε /R (K)	$\beta.10^3$	scheme
H_2O	647.29	0.015	1017.338	0.674	2003.248	69.2	4C
Methane	190.56	0.029	959.028	0.447	x	x	x
Ethane	305.32	0.043	1544.548	0.585	x	x	x
Propane	369.83	0.058	1896.453	0.631	x	x	x
n-Butane	425.18	0.072	2193.083	0.708	x	x	x
n-Pentane	469.7	0.091	2405.105	0.799	x	x	x
i-Butane	408.14	0.075	2078.622	0.702	x	x	x
Nitrogen	126.2	0.026	634.070	0.499	x	x	x
H_2S	373.53	0.029	1590.102	0.502	654.271	58.32	3B

Table 28 - Thermodynamic parameters of some binaries present in the AGASA unity under evaluation. Binaries Parameters obtained in literature(FROST *et al.*, 2012)

Compound 1	Compound 2	k_{ij}	$\beta^{A_iB_j}$	$\epsilon^{A_iB_j}$	scheme
H_2O	Methane	1.883-0.003*T	x	x	4C
H_2O	Ethane	0.118	x	x	4C
H_2O	Propane	0.114	x	x	4C
H_2O	n-Butane	0.088	x	x	4C
H_2O	n-Pentane	0.062	x	x	4C
H_2O	H_2S	0.191	0.030	108.780	4C/3B
H_2O	CO_2	0.114	0.016	142.000	4C/4C
H_2S	Methane	0.076	x	x	4C
H_2S	Ethane	0.085	x	x	4C
H_2S	Propane	0.092	x	x	4C
H_2S	n-Butane	0.090	x	x	4C
H_2S	i-Butane	0.076	x	x	4C

It can be seen from Table 27 that only H_2O and H_2S compounds have ε and β values, as these are the only compounds shown in this Table which present hydrogen bonds.

4.5 Process Simulations at Petrox

Once the pure DEA parameters and some of its binaries were estimated, these parameters were inserted in the Petrox process simulator (as explained in Section 3.5).

It is important to clarify that at the time of absence of DEA and Water data the arbitrary k_{ij} value of the mixture of 0.153 was inserted in Petrox. The equilibrium data of this binary were obtained in a very advanced stage of this work and for that reason that the simulations presented in the next sections are considering the DEA-Water k_{ij} equals to 0.153. In Section 4.5.4 are presented simulations considering the estimated DEA-Water k_{ij} 0.595 for the best scenario obtained in the first step.

As a final step to reach the targets described in this work objective section (Section 1.2), the absorber tower of an existing industrial gas absorption plant was modeled in Petrox software. Figure 21 extracted from Petrox shows the absorption column to be simulated and its process streams.

DEAP is the “Poor DEA”, CARG is the Process Feed/ “Acid Gas” to be treated, GAST is the “Treated Gas”, DEAR is the “Rich DEA” and ABSV is the Absorbing Column. The simulated process streams are always accompanied by quotation marks, to differentiate from the actual process streams. The “Poor DEA” stream is also called Lean DEA.

The four mentioned process streams are cited again several times. So, it is important to the reader to be clarified that the inlet streams are: “Poor DEA” and “Acid Gas” and the outlet streams are: “Treated Gas” and “Rich DEA”.

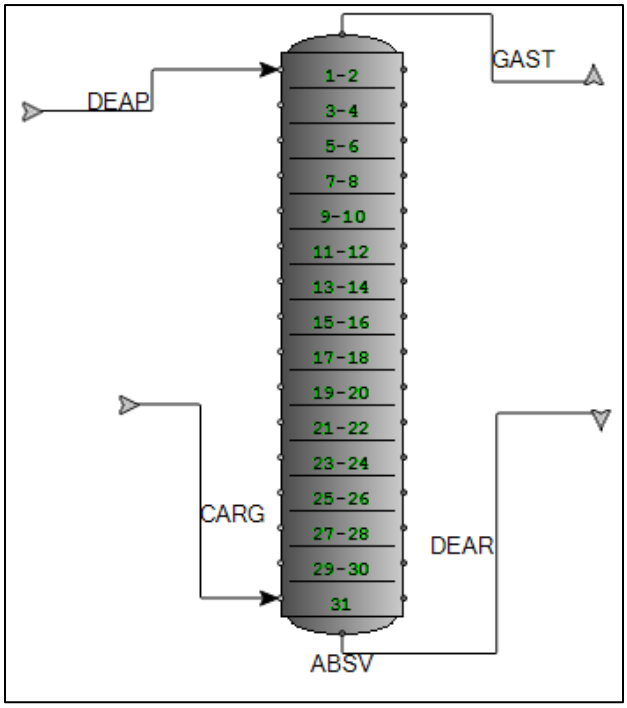

Figure 21 - Simulation of Absorbing Column at Petrox (extracted from Petrox)

In order to conduct a careful analysis of two distinct operating units with specific feeds and operating conditions, they were evaluated for further study. To define the best industrial plant to be examined, the "quality" of the operational information provided by each of these was chosen as a metric. This quality was measured by the plant behavior in the steady state. To this end, the "Moving Window Methodology" (Section 3.4) was adopted.

4.5.1 Moving Window Results

Through the moving window methodology, it was evaluated a set of available data for the two AGASA industrial unity under analysis. The system that presented lower correlation coefficient values for the top and bottom temperatures of the absorption column (chosen metric for the evaluation) was selected as the study object, due to the supposed lower influence of transience in the evaluation period. After this step, once the industrial plant to be chosen was already determined, the confidence intervals of eight significant process variables were calculated.

To facilitate the understanding, it is possible to divide the analyzed data into 3 groups: variables related to the gaseous streams (1); to the liquid streams (2) and to the

absorption column (3). The behavior of these variables can be visualized in Figure 23, Figure 24 and Figure 22. The confidence interval was calculated considering 95 % of confidence, employing INT.CONFIANCA.T Excel's function. The study interval starts at 10:00 pm on April 2013 and ends at 7:40 a.m. on April 14, 2018.

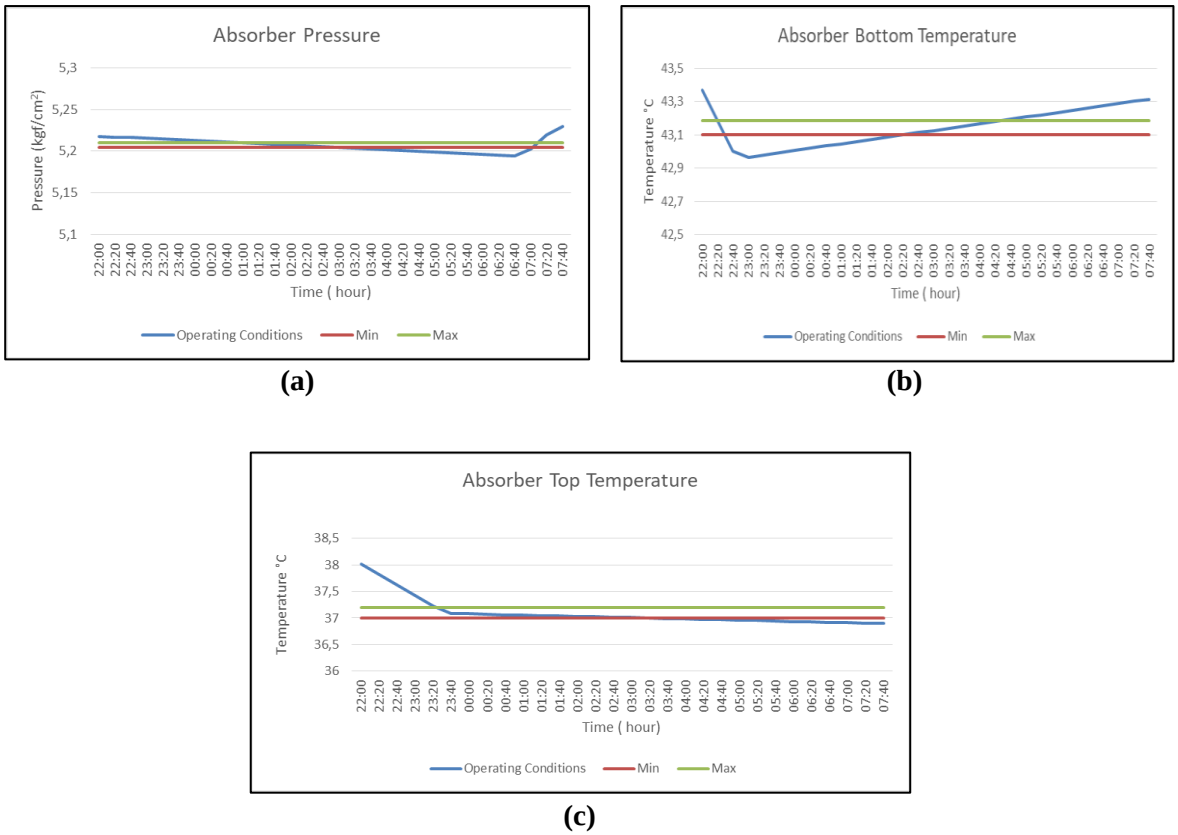

Figure 22 - Process variables related to the absorption column. (a) Absorber Pressure (b) Absorber Bottom Temperature (c) Absorber Top Temperature. Each window with 30 measurements, spaced by 20 minutes. The red and green line respectively indicate the minimum and maximum limits determined by the confidence interval, considering 95% of confidence

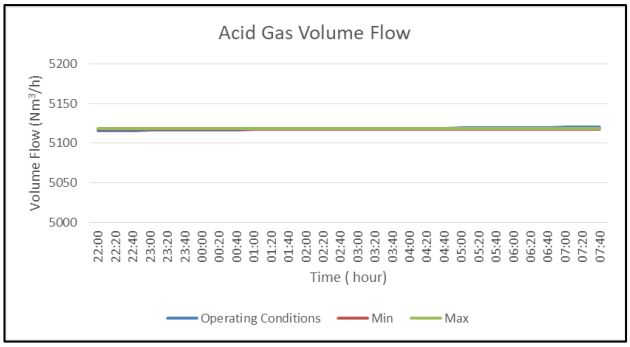

(a)

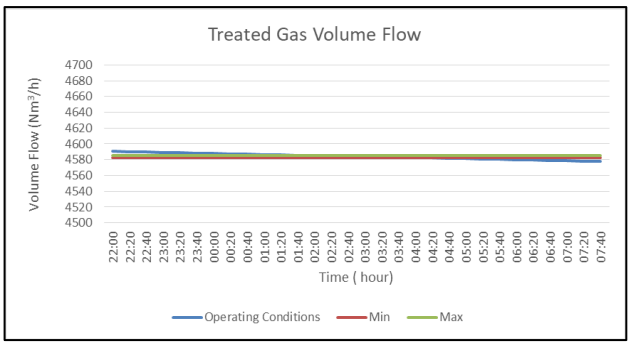

(b)

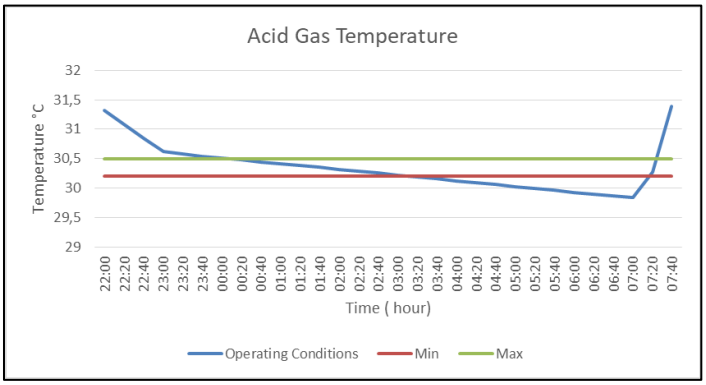

(c)

Figure 23 - Process variables related to the gaseous streams. (a) Acid Gas Volume Flow (b) Treated Gas Volume Flow (c) Acid Gas Temperature. Each window with 30 measurements, spaced by 20 minutes. The red and green line respectively indicate the minimum and maximum limits determined by the confidence interval, considering 95 % of confidence.

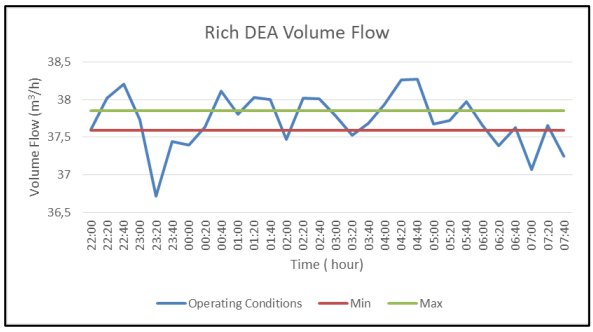

(a)

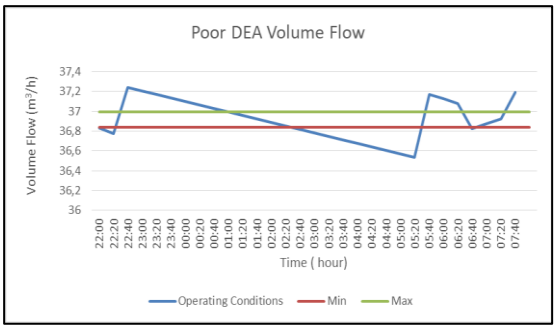

(b)

Figure 24 - Process variables related to the liquid streams from the AGASA unity selected. (a) Rich DEA Volume Flow (b) Poor DEA Volume Flow. Each window with 30 measurements, spaced by 20 minutes. The red and green line respectively indicate the minimum and maximum limits determined by the confidence interval, considering 95 % of confidence

The confidence interval calculated were used for comparison with the results obtained from Petrox simulations. It was sought, as a form of results validation, that the future outcomes generated in the simulation were in agreement with the intervals generated by this statistical study. It should be recalled that the chosen metric to define the steady-state period of the industrial plant were the absorption column top and bottom temperatures behavior, shown in Figure 22.

Details on the specificities in the application of the moving window methodology can be found in Appendix B.

4.5.2 Absorbing Column technical data sheet

The data presented below were obtained from the industrial unit operating manual. The industrial absorption column has a height of 22.95 meters, with a height of 19.95 meters of Pall 1.5" fillings (stainless steel). The tower diameter is 0.8 meters, its design operating pressure is 7.0 kgf/cm^2, with pressure variation between the top and the bottom of the tower of 0.1 kgf/cm^2. Design bottom and top temperatures are 50° C and 60° C respectively.

To estimate the number of the column theoretical stages (KISTER, 1992), since this is an input parameter for the tower simulation, it is used the Equation 41:

$$\boldsymbol{z = N \,.\, HETP} \qquad \textbf{41}$$

z is the height of the filling, N is equal to the number of theoretical stages and $HETP$ a parameter that is a function of the type of packing utilized.

According to the literature (KISTER, 1992), the $HETP$ for this type of filling is 2.17 feet (or 0.661416 m). Considering z = 19.95, N was obtained approximately equal to 31 stages.

4.5.3 Current Operating Conditions Simulation

The metric chosen for the simulation results validation of the plant current operating conditions was based on the results of available chemical analysis and operational data obtained through the plant instrumentation.

The industrial plant to be studied receives the process feed from at least 3 other process units and therefore its feed is not constant. Currently the largest feed contribution comes from a hydrotreatment unit which adopts hydrogen as a rectifier agent for diesel and/or aviation kerosene. And that's why the acid gas treatment unit process feed mostly has hydrogen (more than 80%). Thus, before going to the sulfur recovery unit, the treated gas, rich in hydrogen, will be routed to the hydrogen generating unit. For information, the rectification purpose is to remove light hydrocarbons from the products and thus to adjust their final quality in terms of initial boiling point or flash point. This hydrogen stream is then sent along with other fuel gas streams to the acid gas treating unit.

As simulation input parameters it is necessary to define the composition of the acid gas to be treated and the Poor DEA stream composition. Unfortunately, no Acid Gas composition data was available. However, there was an analysis result of treated gas composition (the only analysis performed in the last 2 years) and from the result of this analysis an estimate of the “Acid Gas” composition was generated.

Table 29 - Chemical Analysis of Treated Gas held on April 13, 2018

Treated Gas Chromatographic Scanning	
Component	**Composition**
Hydrogen	89.96
Methane	3.5
Ethane	1.97
Propane	1.98
N-Butane	1.18
Nitrogen	0.37
I-Butane	0.35
I-Pentane	0.29
Oxygen	0.24
C6+	0.16
H_2S	< 0.01

It is empirically known that the composition of H_2S in the process feed varies between 5% and 11% and therefore, 3 possible process feed compositions were estimated,

with different H_2S molar concentrations (5 %, 8 % and 11 %). It is important to note that for this estimation, it was considered that only H_2S was absorbed by the "Poor DEA" solution (no other compound was entrained by the liquid solution). The analysis results performed on 04/13/18 can be seen in the Table 29.

According to the treated gas analysis, the contribution of H_2S respecting the pre-established concentrations and maintaining the proportions of the species presented in the treated gas analysis (Table 30) was inserted the process feed was inferred:

Table 30 – Possible "Acid Gas" molar compositions according to the inference made through the treated gas analysis, occurred on April 13, 2018. The hydrogen sulphide molar concentration varies from 5 % to 11 %.

Possible Compositions of "Acid Gas" (H_2S in concentrations of 5%, 8% and 11%)			
Component	**Composition (%)**		
Hydrogen	85.462	82.763	80.064
Methane	3.325	3.220	3.115
Ethane	1.872	1.812	1.753
Propane	1.881	1.822	1.762
N-Butane	1.121	1.086	1.050
Nitrogen	0.352	0.340	0.329
I-Butane	0.333	0.322	0.312
I-Pentane	0.276	0.267	0.258
Oxygen	0.228	0.221	0.214
C6+	0.152	0.147	0.142
H_2S	5.0	8.0	11.0

In the simulation, the set of $C6^+$ components were replaced by the N-Hexane component.

An important point of attention is that the acid gas treated today is possibly different from that predicted in the industrial plant design conditions. Mainly in relation to the content of hydrogen and methane (which in the design conditions was 62.6 % and 14.2 %, respectively). The design H_2S content (11.1 %) adheres to the range of H_2S concentration to

be simulated (5 % to 11 %). The detailed assessment of the selected AGASA industrial unity design conditions is presented in Appendix C.

In Table 31 are the results referring to the "Poor DEA" process stream, carried out in 3 different days of April 2018.

Table 31 - Chemical analysis history of "Poor DEA" stream. Data obtained from laboratory tests performed in April 2018

Component	Composition			
	Analysis of April 24	Analysis of April 19	Analysis of April 10	Composition adopted in the simulation
H_2S	0.08%	0.08%	0.04%	0.05%
DEA	20.4%	18.5%	22.1%	20%
H_2O	79.52%	81.42%	77.86%	79.95%

Considering that the data window established in the simulation refers to the interval between April 13 and 14, the "Poor DEA" stream composition adopted is based on the available analysis results (April 10, 19 and 24) and operation report. In the mentioned analysis the H_2S molar concentration ranges from 0.04 % to 0.08 % and the operational report shows that the H_2S content is 0.05 %. As all this information is aligned, it was decided to proceed with a concentration of 0.05 %. Likewise, operational information is that the DEA content in "Poor DEA" stream is set at 20% while analysis results indicate concentration ranging from 18.5 % to 22.1 %. As this information is also aligned, it was decided to proceed the simulation using 20 % DEA concentration. It is acknowledged that the analysis results are in accordance with the operational team reports for "Poor DEA" composition.

One of the objectives and the importance of this work is, indirectly, to estimate the process feed H_2S composition of the simulated industrial unit since, due to corrosive processes, inherent to this plant, it is difficult to maintain a composition analyzer in line. It is assumed, in this research, therefore, that this composition is unknown and three H_2S conceivable molar compositions (5 %, 8 % and 11 %) are evaluated.

From the eight parameters that had their confidence interval calculated (Section 4.5.1), six (1. "Poor DEA" Volume Flow; 2. "Acid Gas" Volume Flow; 3. "Acid Gas" Temperature; 4. Absorption Column Top Pressure; 5. Absorption Column Top Temperature

and; 6. Absorption Column Bottom Temperature) are process simulator input parameters. The ideal situation would be to analyze individually the impact of these variables variation on the simulation results, on the other hand this detailed procedure is quite laborious, especially considering that there are infinite numbers contained in each one of these confidence intervals and the combination of all of these numbers (which would form a specific scenario in process simulation) is not feasible. An expository example of the various possible scenarios is shown in Table 32:

Table 32 - An expository example of the number of scenarios assembled when the process variables are change within the confidence interval. In this case, the "Poor DEA" Volume Flow was varied, keeping fixed the other variables.

Petrox input Process Variables						
	"Poor DEA"		**"Acid Gas"**		**Absorption Column**	
	Volume Flow (m^3/h)	Temperature (°C)	Volume Flow (Nm^3/h)	Temperature (°C)	Bottom Temperature (°C)	Top Pressure (kgf/cm^2)
	Confidence Interval					
Scenario	[36.837; 36.990]	[36.995; 37.196]	[5117.405; 5118.437]	[30.200; 30.496]	[43.103; 43.187]	[5.204; 5.210]
1	36.837	36.995	5117.405	30.200	43.103	5.204
2	36.888	36.995	5117.405	30.200	43.103	5.204
3	36.939	36.995	5117.405	30.200	43.103	5.204
4	36.990	36.995	5117.405	30.200	43.103	5.204

Table 32 presents simply 4 scenarios assembled from the change in "Poor DEA" Volume Flow Rate (all other fixed variables remaining). The number of possible scenarios varying all the process variables is significant.

As aforementioned, performing the conjunction of all intervals is an impractical work and therefore it was decided to evaluate the influence of 4 variables minimum and maximum intervals ("Acid Gas" Temperature and Volume Flow and "Poor DEA" Temperature and Volume Flow). Regard to the fact that it is considered that the Absorption Column top temperature is equal to "Poor DEA" temperature. This consideration is in

accordance with the plant design conditions and with a typical contemplation made by the plant operation team. For the others, an average value of the interval was adopted.

Hereafter, all the simulations performed with the CPA thermodynamic model use the parameters, association schemes and combining rules defined in Sections 4.3 and 4.4.

A process variables sensitivity analysis addressing to verify their influence in the treated gas desired specification was carried out. Through Figure 25 it is possible to verify an example of this sensitivity analysis (considering CPA, SRK and PR EoS), where the analyzed variable is the "Acid Gas" temperature.

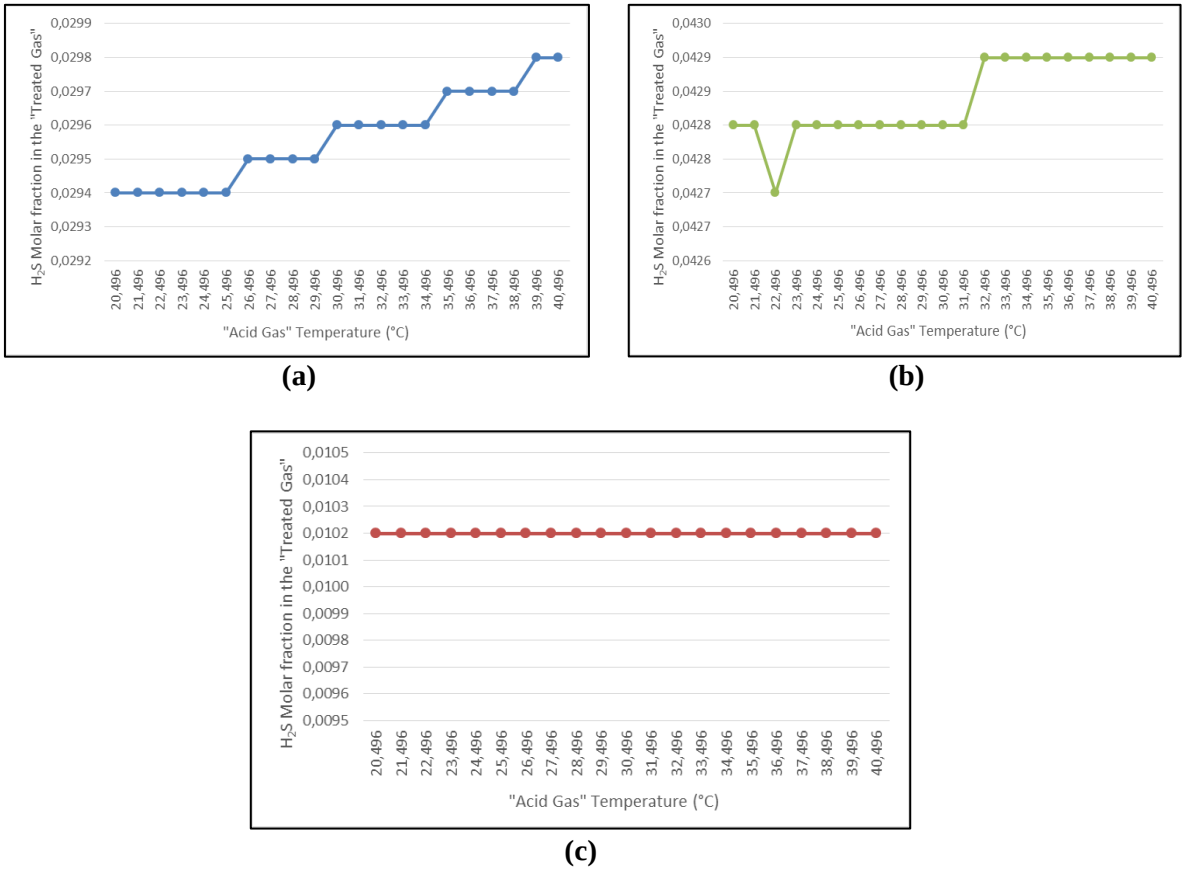

Figure 25 - "Acid Gas" Temperature Sensitivity Analysis, considering "Acid Gas" H_2S molar concentration of 5%, applying CPA, SRK and PR EoS: a) CPA b) SRK c) PR. 21 point were used in each case and the simulation took place at Petrox.

Through Figure 25, it is possible to conclude that regardless of the applied EoS, the "Acid Gas" temperature did not demonstrate as a significant influential variable in the

"Treated Gas" desired specification. The temperature was varied by 20°C but even so the influence on "Treated Gas" H_2S mole fraction was relatively negligible.

A detailed current operating conditions simulation comparison when applying CPA, SRK and PR is found in Appendix D.

It was decided to present in this section only the 13 best simulation results applying CPA EoS (since this thermodynamic model presented the best results among the compared EoS). The best scenario is obtained when it is considered 5 % of H_2S in the process feed (Table 33). The simulations results considering 8 % and 11 % are presented in Appendix E.

Table 33 – CPA - Operating Conditions (5% H_2S in "Acid Gas"). It is represented 13 operational conditions, all within the statistically calculated intervals

	Input				Results
	"Acid Gas"		"Poor DEA"		"Treated Gas"
N°	Volume Flow (Nm^3/h)	Temperature (°C)	Volume Flow (m^3/h)	Temperature (°C)	H_2S in "Treated Gas"
1	5117.405	30.200	36.837	36.995	3.190%
2	5117.405	30.200	36.990	36.995	3.183%
3	5118.437	30.200	36.990	36.995	3.183%
4	5118.437	30.200	36.837	37.196	3.198%
5	5118.437	30.200	36.990	37.196	4.118%
6	5117.405	30.200	36.990	37.196	3.190%
7	5117.405	30.496	36.990	36.995	3.183%
8	5117.405	30.496	36.990	37.196	3.191%
9	5117.405	30.496	36.837	37.196	3.198%
10	5117.405	30.496	36.837	36.995	3.191%
11	5118.437	30.496	36.837	36.995	3.191%
12	5118.437	30.496	36.990	36.995	3.043%
13	5118.437	30.496	36.990	37.196	3.942%

Table 34 presents the process streams molar flow for the best case, where the H_2S content in the "Treated Gas" was 3.043 % (Simulation 12).

Table 34 - Process streams molar flow (kmol/h). "Acid Gas" H_2S concentrations of 5%. The simulations were carried out in Petrox.

	Input			Output
	Process Streams			
Component	**"Acid Gas"**	**"Poor DEA"**	**"Rich DEA"**	**"Treated Gas"**
H_2S	11.418	0.596	5.152	6.862
Hydrogen	195.156	0.000	0.238	194.918
Methane	7.593	0.000	0.081	7.512
Ethane	4.275	0.000	0.145	4.130
Propane	4.295	0.000	0.224	4.071
I-Butane	0.760	0.000	0.077	0.683
N-Butane	2.560	0.000	0.286	2.273
I-Pentane	0.630	0.000	0.132	0.498
H_2O	0.000	953.361	950.390	2.971
DEA	0.000	238.489	238.489	0.000
Oxygen	0.521	0.000	0.002	0.518
Nitrogen	0.804	0.000	0.003	0.801
N-Hexane	0.347	0.000	0.107	0.240

Through Table 34 it is possible to visualize that the model predicts the water migration from "Poor DEA" to the "Treated Gas". In addition, a part of the hydrocarbons, hydrogen, oxygen and nitrogen migrate from the gas phase to the liquid phase. This behavior is possible but not desirable. Table 35 shows the "Treated Gas" composition for this best case (Simulation 12), and its comparison with the chemical analysis performed on April 13, 2018.

With investigative character, the "Treated Gas" H_2S composition was recalculated considering the hypothesis that the two undesirable phenomena had not happened (transfer of water to the gas phase and transfer of gases other than H_2S to the liquid phase). The final molar composition of H_2S in "Treated Gas" would be 1.484% (instead of 3.043% of the best case showed in Table 34). But even so, the final specification of H_2S would not be achieved.

Table 35 - "Treated Gas" Molar Composition (H_2S in concentrations of 5%). Best result for the "Treated Gas" H_2S molar composition (3,043%). Comparison with the chemical analysis performed on April 13, 2018.

Component	Analysis (%)	Simulation Result (%)	Relative Standard Deviation
H_2S	0.01	3.04	30334%
Hydrogen	89.96	86.45	-4%
Methane	3.50	3.33	-5%
Ethane	1.97	1.83	-7%
Propane	1.98	1.81	-9%
I-Butane	0.35	0.30	-13%
N-Butane	1.18	1.01	-15%
I-Pentane	0.29	0.22	-24%
H_2O	0.01	1.32	13076%
DEA	0.00	0.00	-
Oxygen	0.24	0.23	-4%
Nitrogen	0.37	0.36	-4%
N-Hexane	0.16	0.11	-34%

Even if the parameters were varied within the confidence interval, the results were not satisfactory for the reproduction of the treated gas chemical analyzes results (in which the treated gas is specified).

4.5.4 Best Results Simulation with Estimated DEA-Water k_{ij}

As already mentioned, the simulations presented in Section 4.5.3 were calculated using an arbitrary k_{ij} (0.153) for the DEA-Water binary. The simulation to be presented below uses the estimated k_{ij} (0.595) based on VLE data obtained(ASPEN, 2018). Table 36 shows the results considering input data from Petrox according to Simulation 12 from Table 33:

Table 36- CPA - Operating Conditions (5% H_2S in "Acid Gas"). New Simulation using the estimated DEA-Water k_{ij}

	Input				Results
	"Acid Gas"		"Poor DEA"		"Treated Gas"
N°	Volume Flow (Nm^3/h)	Temperature (°C)	Volume Flow (m^3/h)	Temperature (°C)	H_2S in "Treated Gas"
12	5118.437	30.496	36.990	36.995	0.649%

Table 37 presents the process streams molar flow for this case.

Table 37 - Process streams molar flow (kmol/h). "Acid Gas" H_2S concentrations of 5%. The simulations were carried out in Petrox.

	Input			Output
	Process Streams			
Component	"Acid Gas"	"Poor DEA"	"Rich DEA"	"Treated Gas"
H_2S	11.418	0.552	10.555	1.414
Hydrogen	195.156	0.000	0.476	194.680
Methane	7.593	0.000	0.199	7.394
Ethane	4.275	0.000	0.500	3.775
Propane	4.295	0.000	1.162	3.133
I-Butane	0.760	0.000	0.596	0.165
N-Butane	2.560	0.000	2.058	0.502
I-Pentane	0.630	0.000	0.630	0.000
H_2O	0.000	881.841	876.364	5.477
DEA	0.000	220.598	220.598	0.000
Oxygen	0.521	0.000	0.005	0.516
Nitrogen	0.804	0.000	0.008	0.796
N-Hexane	0.347	0.000	0.347	0.000

It is possible to verify that the modification of one binary parameter in the simulation made a lot of difference in the results. While in the best result using arbitrary DEA-Water

k_{ij}, the concentration of H_2S in the treated gas was 3.043%, the (re)simulation of this scenario using an estimated DEA-Water k_{ij} obtained 0.6%; a difference of 80.6%. Thus it is clear that it is important to seek for more experimental data from the main DEA binaries and so enhance the simulation results.

4.5.5 Lessons Learned from Process Simulation

After exhaustive comparisons between the different EoS, it can be concluded that the results presented by CPA EoS were superior to those presented by the SRK and PR, in all spheres studied (parameter estimation and process simulation). The CPA prediction was shown to be better than expected by the other two models. In the industrial plant process simulation development as a whole, CPA was the model that performed (among those who were studied) and probably will best represent the phase equilibrium in DEA absorption and regeneration system.

It is possible to summarize the lessons learned from the Petrox process simulation:

1º) The plant operating conditions are not adherent to the design conditions. Through Table 38 this comparison becomes easier to understand.

Table 38 - Main operating variables comparison considering design and operating conditions from April 14, 2018. The design information was obtained from the industrial plant operating manual. The operational conditions were obtained through chemical analysis and historical data.

Main Operational Variables	Design Conditions	Operating Conditions
Absorbing Column Pressure (kgf/cm^2)	7.1	[5.204; 5.210]
DEA Molar Concentration in "Poor DEA" (%)	4.14	[18.5; 22.1]
H_2S Molar Concentration in "Poor DEA" (%)	0.15	[0.04; 0.08]
H_2S Molar Concentration in "Acid Gas" (%)	11	[5; 11]
"Poor DEA" Temperature (°C)	50	[36.995; 37.196]
"Acid Gas" Temperature (°C)	39.3	[30.200; 30.496]

Design conditions do not greatly favor acid absorption. The DEA content foreseen in the project is notably low (4.14 %) compared to the concentration that is practiced in the DEA units (value around 18.5 % to 22.1 %). In this aspect, it is not recommended to approach the design condition.

The Absorbing Column current pressure hinders the processes of gas absorption. The less the pressure is the more challenging the absorption process will be. The current operating pressure (5.2 kgf /cm^2) is lower than the design pressure (7.1 kgf /cm^2), which requires lower temperatures and more DEA available for gas absorption to take place the required extent.

"Poor DEA" and "Acid Gas" design temperatures (50 °C and 39.3 °C respectively) are higher than the current operating conditions (37 °C and 30.2 °C respectively). As is well known, the gas absorption is favored by lower temperatures and, therefore, the design conditions inhibit this absorption. Therefore, it is not recommended to increase the temperature of these streams with the objective of reaching Treated Gas H_2S specification. Such operational maneuver would further worsen the acid gas absorption by DEA aqueous solution.

2º) The variables that most affect the gas absorption efficiency are the variables related to the poor DEA process stream (current temperature, DEA content and H_2S content). The variables related to the "Acid Gas" process stream were not as sensitive to the absorption efficiency as those of poor DEA process stream.

3º) The simulations indicate that the H_2S composition in the treated gas does not conform to the final specification parameter (which is 300 ppm). Possible reasons for not specifying the final parameter are:

- The available operational data are not reliable.
- Non-knowledge of the process feed causes difficult to simulate this process. The process feed used was an estimate based on the treated gas analysis.
- The thermodynamic model could not predict with accuracy the thermodynamic equilibrium in the Absorption Column, considering the plant data available. One hypothesis is that the absence of some k_{ij} of important binaries with DEA (e.g. DEA-Hydrogen, DEA-Methane, DEA-Ethane) may have influenced the results lower accuracy.

4º) The adjustment of acid gas and the poor DEA flow rates is not considerably significant in the gas absorption results.

Chapter 5

Conclusions and Suggestions

The results indicated that CPA EoS is a useful tool to describe the thermodynamic of the acid gas absorption column. The CPA presented better results than SRK and PR in all aspects addressed in the research: pure MEA and pure DEA parameter estimation and in the process simulation. The latter took place at Petrox and it allowed to verify the absorption column thermodynamic limitations in the Treated Gas H_2S specification.

In Section 1.2, five specific objectives were proposed and finally completed. The parameter estimation step covered two of these objectives: the pure MEA parameter estimation (Section 4.1) and pure DEA parameter (Section 4.2) and its main binaries parameter estimation (Section 4.4), applying a methodology proposed in the literature. The results were satisfactory and allowed the conclusion of the third and fourth objectives: the results application in a process simulator and the equilibrium study in the absorption column of a DEA industrial plant (Section 4.5).

The DEA modeling presented good results for VLE analysis. However, it has been confirmed through the methodology that the LLE with DEA and hydrocarbons (Hexadecane and Octadecane) could not be reproduced. Thus modifications in the thermodynamic model could be suggested to address this issue.

As a suggestion for future work, it is proposed the simulation of the industrial plant as a whole, mainly because the purity requirements of DEA and H_2S in the Treated Gas and Poor DEA generate an energy demand for the Regenerating Tower, which works inherently in tune with the Absorbing Tower. Another suggestion for future work is the application of a thermodynamic model that explicitly takes into account the electrolytic interactions between species and thus to verify the relevance of these interactions in the obtained results.

Chapter 6

Bibliography

ABEDINZADEGAN ABDI, Majid; MEISEN, Axel. Mutual solubility of binary mixtures of octadecane with diethanolamine and bis-hydroxyethyl piperazine. *Fluid Phase Equilibria*, v. 123, n. 1–2, p. 259–270, 1996.

ABEDINZADEGAN ABDI, Majid; MEISEN, Axel. Mutual Solubility of Hexadecane with Diethanolamine and with Bis(hydroxyethyl)piperazine. *Journal of Chemical & Engineering Data*, v. 43, n. 2, p. 138–142, 1998.

ABILDSKOV, J.; KONTOGEORGIS, Georgios M. G.M. A New Challenge of Applied Thermodynamics. *Chemical Engineering Research and Design*, v. 82, n. November, p. 1505–1510, 2004.

ADACHI, Yoshinori; SUGIE, Hidezumi. A new mixing rule-modified conventional mixing rule. *Fluid Phase Equilibria*, v. 28, n. 2, p. 103–118, 1986.

APIO, Andressa; BOTELHO, Viviane R; TRIERWEILER, Jorge O. Parameter Estimation of Models with Limit Cycle based on the Reformulation of the Objective Function. *Computers and Chemical Engineering*, 2017.

ASPEN. *Avaliable at: <https://www.aspentech.com/en/products/engineering/aspen-hysys>. Aspen Company Hysys - [Cited June 2018]*. . [S.l: s.n.]. , 2018

AVLUND, Ane S. *et al.* Application of association models to mixtures containing alkanolamines. *Fluid Phase Equilibria*, v. 306, n. 1, p. 31–37, 2011.

AVLUND, Ane S; KONTOGEORGIS, Georgios M; MICHELSEN, Michael L. Modeling Systems Containing Alkanolamines with the CPA Equation of State Modeling Systems Containing Alkanolamines with the CPA Equation of State. *Chart*, p. 7441–7446, 2008.

BARREAU, A *et al.* Absorption of H 2 S and CO 2 in Alkanolamine Aqueous Solution: Experimental Data and Modelling with the Electrolyte-NRTL Model. *Oil & Gas Science and Technology – Rev. IFP*, v. 61, n. 3, p. 345–361, 2006.

BASTOS, Ana Beztriz Farias D´Oliveira *et al.* Foco Em Redução De Emissões Atmosféricas. 2015.

BELL, Ian; JÄGER, Andreas. Helmholtz energy transformation of common cubic equations of state for use with pure fluids and mixtures. *Journal of Research of the National Institute of Standards and Technology*, v. 121, n. July, p. 238–263, 2016.

BULLIN, Jerry A.; POLASEK, John C.; DONNELLY, Stephen T. Use of MDEA and mixtures of amines for bulk CO2 removal. *Proceedings, Annual Convention - Gas Processors Association*, p. 135–139, 1990.

CHAO, K C; LEET, W A; LAFAYETTE, West. Fluid Phase Equilibria, 11 (1983) 201-204. v. 11, p. 201–204, 1983.

CHAPMAN, Walter G. *et al.* New reference equation of state for associating liquids. *Industrial & Engineering Chemistry Research*, v. 29, n. 8, p. 1709–1721, 1990.

COUTINHO, João A.P.; KONTOGEORGIS, Georgios M.; STENBY, Erling H. Binary interaction parameters for nonpolar systems with cubic equations of state: a theoretical approach 1. CO2/hydrocarbons using SRK equation of state. *Fluid Phase Equilibria*, v. 102, n. 1, p. 31–60, 1994.

DIADEM. *American Institute of Chemical Engineers, Desing Institute for Physical Properties, DIADEM*,. . [S.l: s.n.]. , 2004

EBERHART, R.; KENNEDY, J. A new optimizer using particle swarm theory. *MHS'95. Proceedings of the Sixth International Symposium on Micro Machine and Human Science*, p. 39–43, 1995.

ECHEVERRY, Juan Sebastian Lopez; ACHERMAN, Simon Reif; LOPEZ, Eduard Araujo. Peng-Robinson equation of state: 40 years through cubics. *Fluid Phase Equilibria*, v. 447, p. 39–71, 2017.

FARAMARZI, Leila *et al.* Thermodynamic modeling of the solubility of CO2 in aqueous alkanolamine solutions using the extended UNIQUAC model application to monoethanolamine and methyldiethanolamine. *Energy Procedia*, v. 1, n. 1, p. 861–867, 2009.

FOLAS, Georgios K. *et al.* Recent applications of the cubic-plus-association (CPA) equation of state to industrially important systems. *Fluid Phase Equilibria*, v. 228–229, p. 121–126, 2005.

FREY, Kurt; MODELL, Michael; TESTER, Jefferson W. Density-and-temperature-dependent volume translation for the SRK EOS: 2. Mixtures. *Fluid Phase Equilibria*, v. 343, p. 13–23, 2013.

FROST, Contributors Michael *et al.* The Cubic-Plus-Association EoS. n. September, p. 0–33, 2012.

GLASSCOCK, David A; ROCHELLE, Gary T. Absorption into Aqueous Alkanolamines. v. 39, n. 8, p. 1389–1397, 1993.

GRENNER, Andreas *et al.* On the estimation of water pure compound parameters in association theories. *Molecular Physics*, NULL, v. 105, n. December 2013, p. 1797–1801, 2007.

GROS, H. P.; BOTTINI, S.; BRIGNOLE, E. A. Group contribution equation of state for associating mixtures. *Fluid Phase Equilibria*, NULL, v. 116, n. 1–2 pt 1, p. 537–544, 1996.

HUANG, S. H.; RADOSZ, M. Equation of state for small, large, polydisperse, and associating molecules. *Industrial & engineering chemistry research*, v. 29, n. 11, p. 2284–2294, 1990.

HURON, Marie José; VIDAL, Jean. New mixing rules in simple equations of state for representing vapour-liquid equilibria of strongly non-ideal mixtures. *Fluid Phase Equilibria*, v. 3, n. 4, p. 255–271, 1979.

INDIO DO BRASIL, Nilo; ARAÚJO, Maria Adelina; SOUSA, Elisabeth Cristina Molina De. Processamento de Petróleo e Gás: petróleo e seu derivados, processamento primário, processos de refino,petroquímica, meio ambiente/ Nilo Indio do Brasil, Maria Adelina Santos Araújo, Elisabeth Cristina Molina de Sousa. Rio de Janeiro: LTC, 2012. p. 2012, 2012.

JAVANMARDI, J.; NASRIFAR, Kh.; MOSHFEGHIAN, M. 40 Comparing different methods for prediction of liquefied natural gas densities. *Engineering Journal of University of Qatar*, v. 18, n. c, p. 39–56, 2005.

JI, Wei-Rong; LEMPE, D.A. Density improvement of the SRK equation of state.

Fluid Phase Equilibria, v. 130, n. 1–2, p. 49–63, 1997.

JUNGE, Christian E. Sulfur in the Atmosphere. *Journal of Geophysical Research*, v. 68, n. 1, p. 3975–3976, 1963.

KAARSHOLM, Mads *et al.* Extension of the cubic-plus-association (CPA) equation of state to amines. *Industrial and Engineering Chemistry Research*, v. 44, n. 12, p. 4406–4413, 2005.

KISTER, Henry. *Distillation design*. . [S.l: s.n.]. , 1992

KOHL, Arthur L.; NIELSEN, Richard. *Gas purification*. [S.l: s.n.], 1997.

KONTOGEORGIS, G. M *et al.* An Equation of State for Associating Fluids. *Industrial & Engineering Chemistry Research*, v. 35, n. 11, p. 4310–4318, 1996.

KONTOGEORGIS, Georgios M. Association theories for complex thermodynamics. *Chemical Engineering Research and Design*, v. 91, n. 10, p. 1840–1858, 2013.

KONTOGEORGIS, Georgios M. *et al.* Ten Years with the CPA (Cubic-Plus-Association) equation of state. Part 1. Pure compounds and self-associating systems. *Industrial and Engineering Chemistry Research*, v. 45, n. 14, p. 4855–4868, 2006.

KONTOGEORGIS, Georgios M.; ECONOMOU, Ioannis G. Equations of state: From the ideas of van der Waals to association theories. *Journal of Supercritical Fluids*, v. 55, n. 2, p. 421–437, 2010.

KONTOGEORGIS, Georgios M.; TASSIOS, Dimitrios P. Critical constants and acentric factors for long-chain alkanes suitable for corresponding states applications. A critical review. *Chemical Engineering Journal*, v. 66, n. 1, p. 35–49, 1997.

KONTOGEORGIS, Georgios M. *Chapter 6: Association Models – The CPA Equation of State*. [S.l.]: Elsevier Masson SAS, 2004. v. Volume 19.

KONTOGEORGIS, Georgios M *et al.* Multicomponent phase equilibrium calculations for water–methanol–alkane mixtures. *Fluid Phase Equilibria*, v. 158–160, p. 201–209, 1999.

KONTOGEROGIS, G. M.; FOLAS, G. K. *Thermodynamic models for industrial applications – from classical and advanced mixing rules to association theories*. [S.l: s.n.], 2010.

LAWSON, J. David; GARST, A. W. Hydrocarbon Gas Solubility in Sweetening

Solutions: Methane and Ethane in Aqueous Monoethanolamine and Diethanolamine. *Journal of Chemical and Engineering Data*, v. 21, n. 1, p. 30–32, 1976.

LIN, Y. Development of an equation of state for solutions containing electrolytes. 2007.

LINDVIG, Thomas *et al.* Modeling of multicomponent vapor-liquid equilibria for polymer-solvent systems. *Fluid Phase Equilibria*, v. 220, n. 1, p. 11–20, 2004.

MAIA, Filipa M. *et al.* Equation of state modelling of systems with ionic liquids: Literature review and application with the Cubic Plus Association (CPA) model. *Fluid Phase Equilibria*, v. 332, p. 128–143, 2012.

MANDAL, Bishnupada; BANDYOPADHYAY, Shyamalendu S. Simultaneous absorption of CO2and H2S into aqueous blends of N-methyldiethanolamine and diethanolamine. *Environmental Science and Technology*, v. 40, n. 19, p. 6076–6084, 2006.

MATHIAS, Paul M.; KLOTZ, Herbert C.; PRAUSNITZ, John M. Equation-of-State mixing rules for multicomponent mixtures: the problem of invariance. *Fluid Phase Equilibria*, v. 67, n. C, p. 31–44, 1991.

MEDEIROS, José Luiz De; BARBOSA, Leandro Chagas; ARAÚJO, Ofélia De Queiroz F. Equilibrium approach for CO2 and H2S absorption with aqueous solutions of alkanolamines: Theory and parameter estimation. *Industrial and Engineering Chemistry Research*, v. 52, n. 26, p. 9203–9226, 2013.

MOGENSEN, Bjørn Maribo. *Development of an Electrolyte CPA Equation of state for Applications in the Petroleum and Chemical Industries Equation of State for Applications in the*. [S.l: s.n.], 2014.

MOGENSEN, Bjørn Maribo; KONTOGEORGIS, Georgios M; THOMSEN, Kaj. Modeling of dielectric properties of complex fluids with an equation of state. SUPPLEMENTARY INFORMATION. *The journal of physical chemistry. B*, v. 117, n. 28, p. 3389–97, 2013.

NELDER, J.A.; MEAD, R. A simplex method for function minimization. *The computer journal*, v. 7, n. 4, p. 308–313, 1965.

OLIVEIRA, Mariana B. *et al.* Evaluation of the CO2 behavior in binary mixtures with alkanes, alcohols, acids and esters using the Cubic-Plus-Association Equation of State. *Journal of Supercritical Fluids*, v. 55, n. 3, p. 876–892, 2011.

ORBEY, Hasan; SANDLER, Stanley I. A comparison of various cubic equation of state mixing rules for the simultaneous description of excess enthalpies and vapor-liquid equilibria. *Fluid Phase Equilibria*, v. 121, n. 1–2, p. 67–83, 1996.

PATEL, Navin C.; ABOVSKY, Vitaly; WATANASIRI, Suphat. Mixing rules for van-der-Waals type equation of state based on thermodynamic perturbation theory. *Fluid Phase Equilibria*, v. 152, n. 2, p. 219–233, 1998.

PENG, Ding-Yu; ROBINSON, Donald B. A New Two-Constant Equation of State. *Industrial & Engineering Chemistry Fundamentals*, v. 15, n. 1, p. 59–64, 1976.

POLASEK, John; BULLIN, Jerry A. Process Considerations in Selecting Amine. *GPA Regional Meeting, Sept. 1994.*, p. 1–9, 1994.

SANTOS, Letícia C. Dos *et al.* Modeling water saturation points in natural gas streams containing CO2 and H2S - Comparisons with different equations of state. *Industrial and Engineering Chemistry Research*, v. 54, n. 2, p. 743–757, 2015.

SANTOS, Leticia Cotia Dos *et al.* Modeling MEA with the CPA equation of state: A parameter estimation study adding local search to PSO algorithm. *Fluid Phase Equilibria*, v. 400, p. 76–86, 2015.

SANTOS, Letícia Cotia Dos *et al.* Cubic Plus Association Equation of State for Flow Assurance Projects. *Industrial and Engineering Chemistry Research*, v. 54, n. 26, p. 6812–6824, 2015.

SCHWAAB, Marcio; PINTO, José Carlos. Schwaab, Marcio Análise de dados experimentais, I: fundamentos de estatística e estimação de parâmetros / Márcio Schwaab, José Carlos Pinto. Rio de Janeiro. E-papers, 2007. 462p. : il ; (Escola Piloto em Engenharia Química ; v1). p. 2007, 2007.

SOAVE, Giorgio. Equilibrium constants from a modified Redlich-Kwong equation of state. *Chemical Engineering Science*, v. 27, n. 6, p. 1197–1203, 1972.

TSIVINTZELIS, Ioannis *et al.* Modeling phase equilibria for acid gas mixtures using the CPA equation of state. Part I: Binary mixtures with H2S. *Fluid Phase Equilibria*, v. 306, n. 1, p. 2965–2982, 2011.

TSIVINTZELIS, Ioannis; ALI, Shahid; KONTOGEORGIS, Georgios M. Modeling phase equilibria for acid gas mixtures using the CPA equation of state. Part IV. Applications to mixtures of CO2 with alkanes. *Fluid Phase Equilibria*, v. 397, p. 1–17, 2015.

VALLÉE, Geraldine *et al.* Representation Of CO2 And H2S Absorption By Aqueous Solutions Of Diethanolamine Using An Electrolyte Equation Of State. *Industrial & engineering chemistry research*, v. 38, n. 9, p. 3473–3480, 1999.

VEGA, L.F.; LLOVELL, F. Review and new insights into the application of molecular-based equations of state to water and aqueous solutions. *Fluid Phase Equilibria*, v. 416, p. 150–173, 2016.

WERTHEIM, Michael S. Fluids with highly directional attractive forces.1. Statistical thermodynamics. *Journal of Statistical Physics*, v. 35, n. 1–2, p. 19–34, 1984.

ZARE, A H; MIRZAEI, S. Removal of CO2 and H2S using aqueous alkanolamine solusions. *World Academy of Science, Engineering and Technology*, v. 37, n. 1, p. 194–203, 2009.

ZAVALA, M Solorzano; AROCHE, F Barragan; BAZÚA, E.R. Comparative study of mixing rules for cubic equations of state in the prediction of multicomponent vapor-liquid equilibria. *Fluid Phase Equilibria*, v. 122, n. 1–2, p. 99–116, 1996.

Appendix A

Attempt to Reproduce Literature Data

One of this work proposed goal was the data reproduction from a reliable bibliographic source. For such purpose, the paper by Ane Avlund and co-workers (Modeling Systems Containing Alkanolamines with the CPA Equation of State) was chosen as the most suitable for this reproduction, since the paper study system is comparable to the system found in the AGASA industrial unity under study. In addition, the thermodynamic model adopted in the parameter estimation was CPA, applied in an alkanolamine system. Another positive point is that the data source used by the author was the same employed in this work, the DIPPR. Based on what has already been stated, it was clear the usefulness of the mentioned article data reproduction for the development of this work.

The pure DEA pure data reproduction was a success (which is explained in detail in the later Appendix sections). However, when attempting to reproduce the DEA-Hexadecane equilibrium data, the results obtained were far from the one explicit in the article.

It is important to be aware that a laborious work of pure DEA parameter estimation using only VLE and LLE data was performed (when it was still sought to validate the results with the mentioned literature). In an advanced parameter estimation stage, when comparing the binary parameter k_{ij} estimated with that presented in the Avlund and co-workers paper, it was noticed that there was a problem of reference in the paper and therefore it did not make sense to validate the estimated parameters using that paper as a reference (and because of that it was decided to return to the first estimation step and redo all calculations). However, it is important to leave written all the methodology applied and the results obtained.

The most important results are presented considering the 1. Pure DEA parameter estimation employing only VLE data and; 2. Pure DEA parameter estimation employing VLE

and LLE data, according to the complete methodology proposed by Santos(SANTOS *et al.*, 2015). The logic of presenting the simulations follows the same format already demonstrated in Section 4.2.

A.1 Initial Simulations and Trial and Error Simulations

Similarly, to the parameter estimation methodology presented in Section 4.2, to obtain the most adequate parameter ranges in the search for the global minimum, it was proceeded with the initial simulations (where large data ranges were swept and a large number of particle size) and trial and error simulations (where the intervals became narrower and the number of particles reduced).

Following is Figure A. 1 and Figure A. 2 which exemplifies an initial simulation, where 500 particles and 1000 iterations were applied in the PSO method.

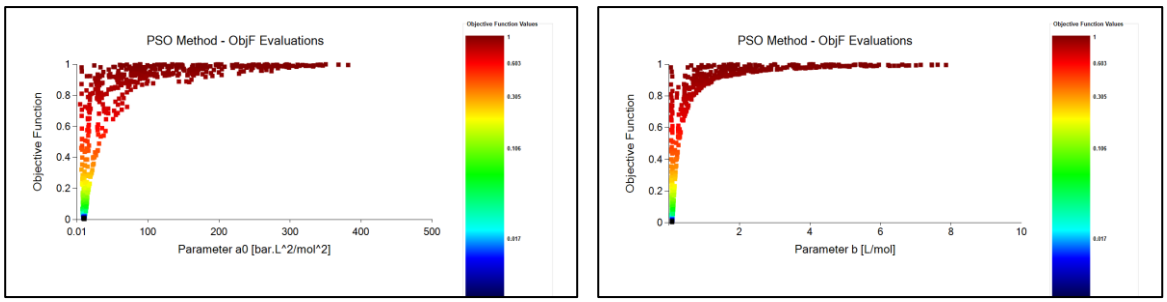

(a) **(b)**

Figure A. 1 - Parametric Analysis of the Initial Simulation (SIM1*). (a) $F_{obj} - a_0$; (b) $F_{obj} - b$; (c) $F_{obj} - c_1$; (d) F_{obj} – eps/R; (e) F_{obj} – beta. Parameters estimated using CPA and optimization method PSO, with maximum number of 1000 iterations and 500 particles. 100 experimental points were used between 0.40 - 0.95 of T_R. Experimental data from DIPPR(DIADEM, 2004).

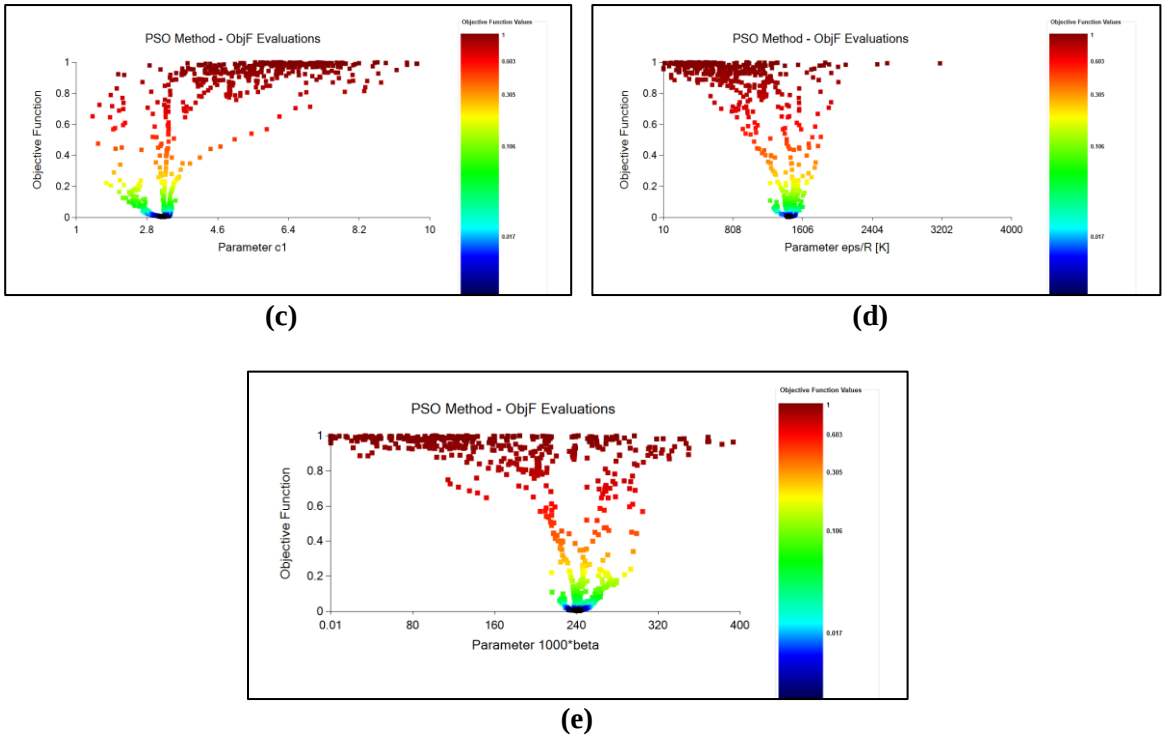

(c) **(d)**

(e)

Figure A. 1 (continuation) - Parametric Analysis of the Initial Simulation (SIM1*). (a) F_{obj} – a_0; (b) F_{obj}– b; (c) F_{obj}– c_1; (d) F_{obj}– eps/R; (e) F_{obj}– beta. Parameters estimated using CPA and optimization method PSO, with maximum number of 1000 iterations and 500 particles. 100 experimental points were used between 0.40 - 0.95 of T_R. Experimental data from DIPPR(DIADEM, 2004).

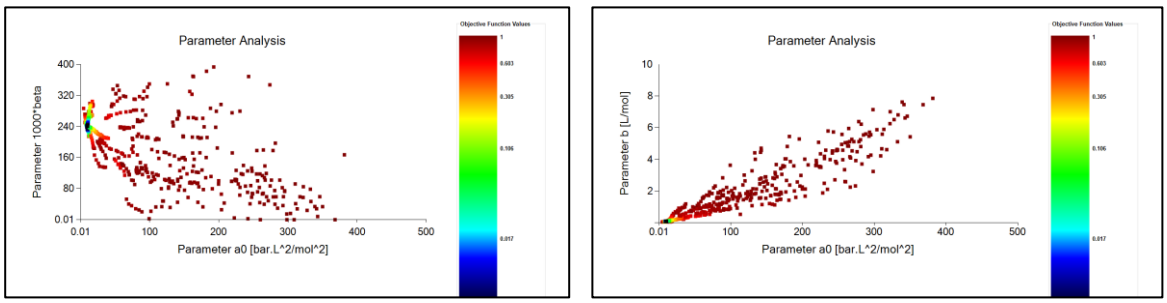

(a) **(b)**

Figure A. 2 - Parametric Analysis of the Initial Simulation (SIM1*). (a) beta – a_0; (b) b – a_0; (c) c_1– a_0; (d) eps/R – a_0; (e) beta – b; (f) c_1– b; (g) eps/R – b; (h) beta – c_1; (i) eps/R – c_1; (j) beta – eps/R. Parameters estimated using CPA and optimization method PSO, with maximum number of 1000 iterations and 500 particles. 100 experimental points were used between 0.40 - 0.95 of T_R. Experimental data from DIPPR(DIADEM, 2004).

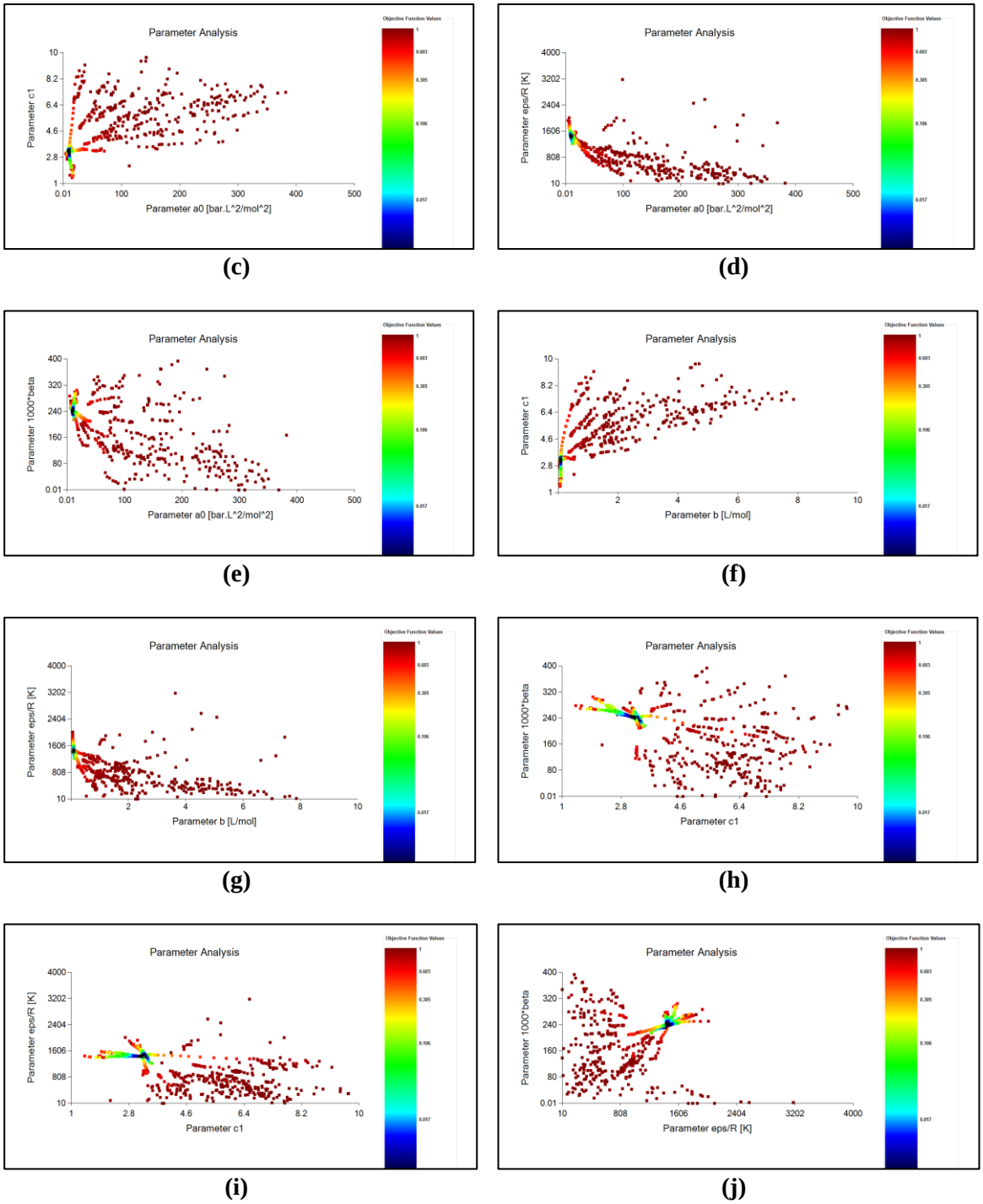

Figure A. 2 (continuation) - Parametric Analysis of the Initial Simulation (SIM1*). (a) beta – a_0; (b) b – a_0; (c) c_1– a_0; (d) eps/R – a_0; (e) beta – b; (f) c_1– b; (g) eps/R – b; (h) beta – c_1; (i) eps/R – c_1; (j) beta – eps/R. Parameters estimated using CPA and optimization method PSO, with maximum number of 1000 iterations and 500 particles. 100 experimental points were used between 0.40 - 0.95 of T_R. Experimental data from DIPPR(DIADEM, 2004).

The idea of using large numbers of particles is to sweep large gaps and thus identify regions where the objective function is minimized. The main comments about the importance of working with a stochastic method such as PSO before employing a deterministic method such as Simplex in parameter estimation have already been mentioned in Section 4.2.

The search intervals presented in Figure A. 1 and Figure A. 2 are in Table A. 1. The best results of this simulation are found in Table A. 2.

Table A. 1 - SIM1* Parameter constraints for pure DEA parameter estimation using CPA EoS considering only VLE data. Equilibrium data from DIPPR(DIADEM, 2004).

Parameters	Lower Bounds	Upper Bounds
a_0 (bar.L^2/mol^2)	0.01	500
b (L/mol)	0,001	10
c_1	1	10
ε/R (K)	10	4000
$\beta.10^3$	0.01	400

Table A. 2 - SIM1* Pure DEA parameter estimation results applying CPA EoS considering only VLE data. Equilibrium data from DIPPR(DIADEM, 2004).

Parameters	Sim1*	
	PSO	Simplex
a_0 (bar.L^2/mol^2)	9.994	31.369
b (L/mol)	0.089	0.093
c_1	3.209	1.475
ε/R (K)	1438.588	35.653
1000* β	241.154	384.368
F_{obj}	7.039.E^{-03}	1.072.E^{-03}
AAP%	9.212%	3.731%

The simulation Sim1 * represents the initial simulation when trying to reproduce the literature data (AVLUND; KONTOGEORGIS; MICHELSEN, 2008). This is not the same simulation Sim1 presented in Section 4.2.

After several simulations, a more precise interval for the parameters was fed in the final simulations.

A.2 Final Simulations

The final simulations aimed to obtain the final set of parameters for pure DEA, considering only VLE data. For this, a large number of particles (from 300 to 1000) and iterations (from 300 to 500) of the PSO associated with a narrow range of parameters were used. In addition, the maximum iterations of the simplex method were also increased (from 1000 to 5000 iterations).

The intervals obtained in trial and error simulations served as the basis for the determination of the intervals set in final simulations (intervals which are more restrictive), Table A. 3.

Table A. 3 – SIM2* Parameter constraints for pure DEA parameter estimation applying CPA EoS considering only VLE data. Equilibrium data from DIPPR(DIADEM, 2004).

Parameters	Sim2*	
	Lower Bounds	Upper Bounds
a_0 (bar.L^2/mol^2)	3.5	8.5
b (L/mol)	0.05	0.1
c_1	1.5	4.5
ε/R (K)	2300	3600
$\beta.10^3$	15	80

The results are in Table A. 4:

Table A. 4 - Results of final simulations SIM2* considering Pure DEA parameter estimation applying CPA EoS considering only VLE data. Equilibrium data from DIPPR(DIADEM, 2004).

Parameters	Sim2*	
	PSO	Simplex
a_0 (bar.L^2/mol^2)	7.125	7.359
b (L/mol)	0.086	0.087
c_1	2.644	2.619
ε/R (K)	2830.875	2799.256
1000* β	36.403	37.342
F_{obj}	7.505.E^{-05}	6.591.E^{-05}
AAP%	0.476%	0.419%

The simulation Sim2 * represents the final simulation when trying to reproduce the literature data. This is not the same simulation Sim2 presented in 4.2.

Following is Figure A. 3 and Figure A. 4, which exemplifies a final simulation, where 1000 particles and 1000 iterations were used in the PSO method.

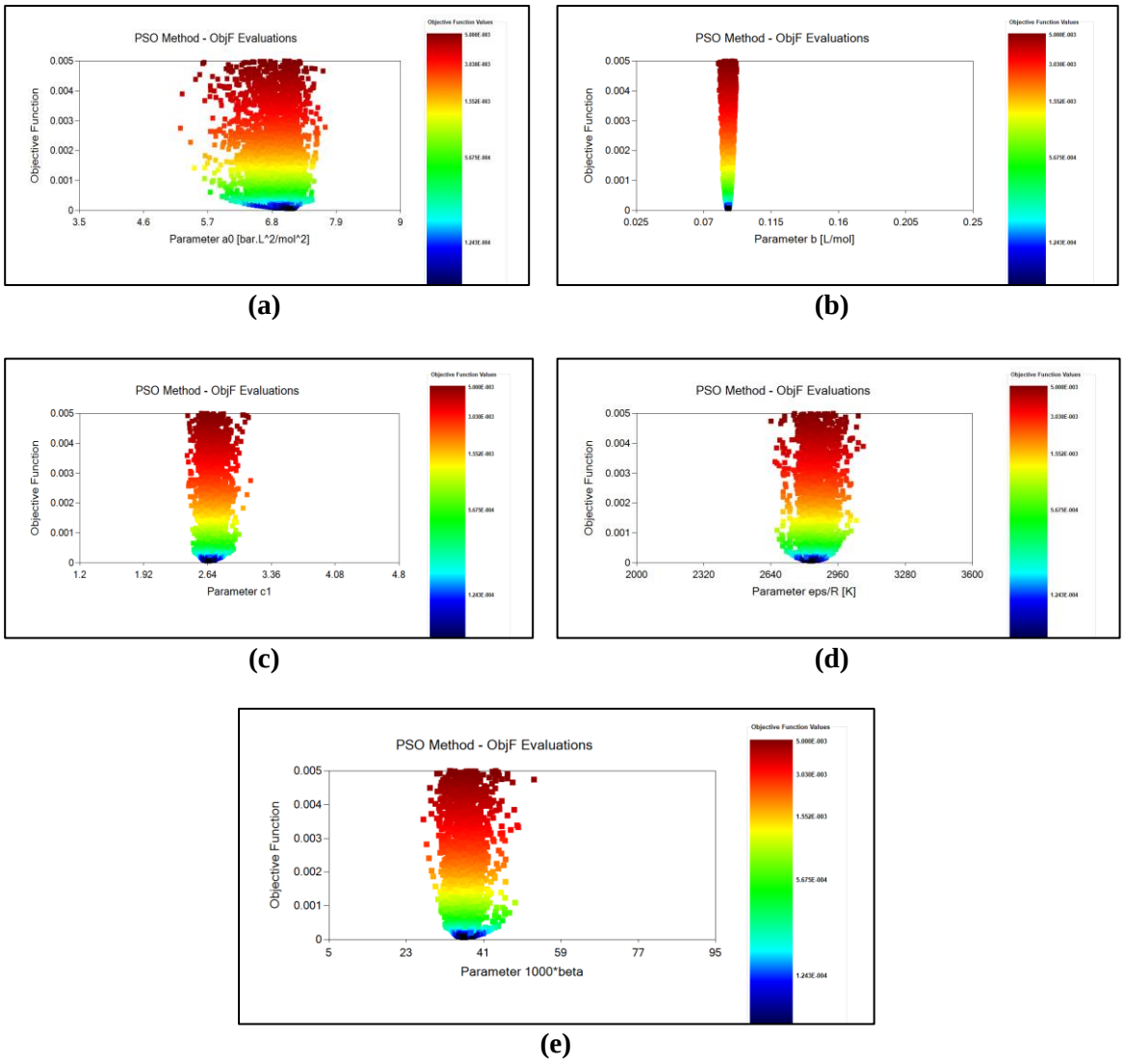

Figure A. 3 - Parametric Analysis of the Final Simulation (SIM2*). (a) F_{obj}– a_0; (b) F_{obj}– b; (c) F_{obj}– c_1; (d) F_{obj}– eps/R; (e) F_{obj}– beta. Parameters estimated using CPA and optimization method PSO, with maximum number of 1000 iterations and 1000 particles. 100 experimental points were used between 0.40 - 0.95 T_R. Experimental data from DIPPR(DIADEM, 2004).

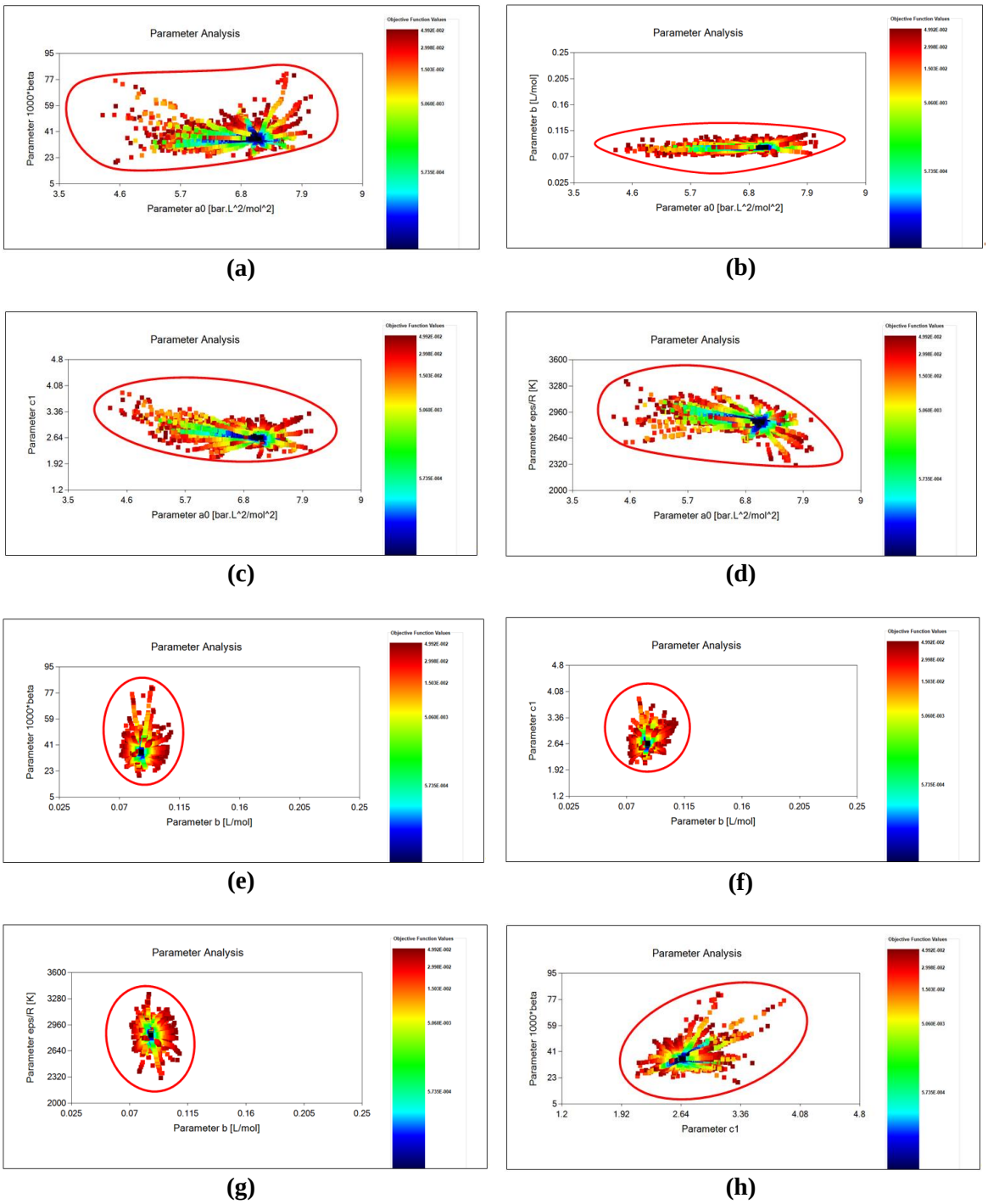

Figure A. 4 - Parametric Analysis of the Final Simulation (SIM2*). (a) beta – a_0; (b) b – a_0; (c) c_1– a_0; (d) eps/R – a_0; (e) beta – b; (f) c_1– b; (g) eps/R – b; (h) beta – c_1; (i) eps/R – c_1; (j) beta – eps/R. Parameters estimated using CPA and optimization method PSO, with maximum number of 1000 iterations and 1000 particles. 100 experimental points were used between 0.40 - 0.95 T_R. Experimental data from DIPPR(DIADEM, 2004).

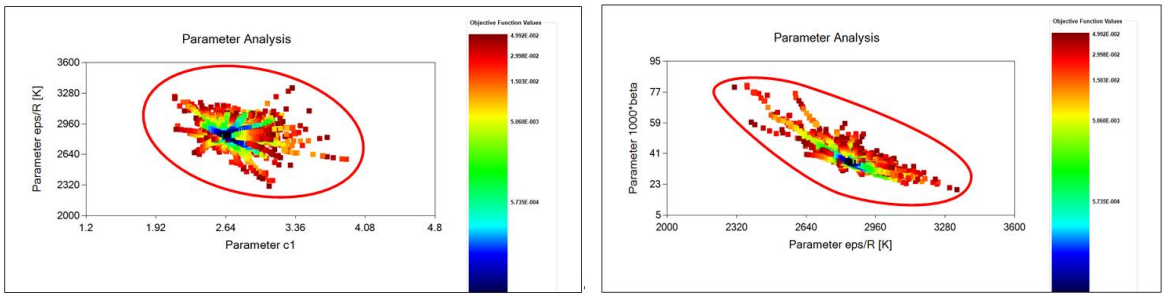

(i) **(j)**

Figure A. 4 (continuation) - Parametric Analysis of the Final Simulation (SIM2*). (a) beta – a_0; (b) b – a_0; (c) c_1– a_0; (d) eps/R – a_0; (e) beta – b; (f) c_1– b; (g) eps/R – b; (h) beta – c_1; (i) eps/R – c_1; (j) beta – eps/R. Parameters estimated using CPA and optimization method PSO, with maximum number of 1000 iterations and 1000 particles. 100 experimental points were used between 0.40 - 0.95 T_R. Experimental data from DIPPR(DIADEM, 2004).

Based on the ellipses identified in Figure A. 4, the pure DEA parameters ranges to be used in the next simulations (which considers the LLE data) were obtained. These ranges are shown in Table A. 5.

Table A. 5 - Final parameter intervals generated from pure DEA parameter estimation applying CPA considering only VLE data, obtained by SIM2*. The parameter interval was generated based on the pure DEA experimental data estimated error.

Parameters	Lower Bounds	Upper Bounds
a_0 (bar.L^2/mol^2)	5.23	7.71
b (L/mol)	0.080	0.092
c_1	2.41	3.12
ε/R (K)	2640	3080
β.10^3	26.99	52.73

A.3 Comparison of the estimated parameters with the Literature

The obtained results were then verified with the parameters obtained in the literature (AVLUND; KONTOGEORGIS; MICHELSEN, 2008). This comparison is in Table A. 6:

Table A. 6 - Comparison of pure DEA estimated parameters with Literature(AVLUND; KONTOGEORGIS; MICHELSEN, 2008). Equilibrium data from DIPPR(DIADEM, 2004).

	a_0 $\left(\frac{bar \cdot L^2}{mol^2}\right)$	b $\left(\frac{L}{mol}\right)$	c_1	ε/R (K)	1000* β	F_{obj}	AAP%	AAρ%	T_R range
Avlund	20.942	0.094	1.574	1943.481	33.2	-	1.56	1.60	0.55-0.9
Sim2*	7.5251	0.087	2.570	2800.526	36.69	6.36.E^{-5}	0.44	0.46	0.41-0.95

It is possible to verify that the results obtained were slightly better (lower values of AAP% and AAρ%) than those presented by Avlund and co-workers. In addition, it was possible to obtain better results for a wider temperature range than in the Avlund study. The beginning of the range used in this research is the DEA triple point, which corresponds to 41% of the critical temperature; while Avlund and co-workers worked with a narrower range, starting at 55% of T_R.

By inserting Avlund final parameters values in the ThermOptimizer, adopting the same EoS (CPA), mixing rule (CR-1) and association scheme (4C) it was possible to reproduce with certain precision the results (Table A. 7).

Table A. 7 - Calculation of pressure and liquid density deviations applying Avlund and co-workers data(AVLUND; KONTOGEORGIS; MICHELSEN, 2008) in Pure DEA parameter estimation.

	a_0 $\left(\frac{bar \cdot L^2}{mol^2}\right)$	b $\left(\frac{L}{mol}\right)$	c_1	ε/R (K)	1000* β	F_{obj}	AAP%	AAρ%	T_R range
Reprod Avlund	20.942	0.094	1.574	1943.481	33.2	6.43.E^{-5}	1.49	1.57	0.55-0.9

The parameters obtained by Avlund and co-workers in the T_R range (0.41 – 0.95) considered in SIM2* were also applied (Table A. 8):

Table A. 8 - Calculation of pressure and liquid density deviations applying Avlund and co-workers data(AVLUND; KONTOGEORGIS; MICHELSEN, 2008) in Pure DEA parameter estimation, with narrower temperature range (0.41-0.95).

	a_0 $\left(\frac{bar \cdot L^2}{mol^2}\right)$	b $\left(\frac{L}{mol}\right)$	c_1	ε/R (K)	1000* β	F_{obj}	AAP%	AAρ%	T_R range
Reprod Avlund	20.942	0.094	1.574	1943.481	33.2	-	469.87	251.23	0.41-0.95

The results indicate that the parameters obtained by Avlund and co-workers do not meet a higher T_R range (0.41-0.95) than those of this research (0.55-0.9).

A.4 Liquid-Liquid Equilibrium Simulation

As already explained in Section 4.3, in order to comply with all the steps indicated in the parameter estimation methodology used, the parameter estimation was performed considering a binary mixture of DEA and Hexadecane.

The pure hexadecane data were obtained through their critical conditions.

A.4.1. Reproduction of Literature Results considering the DEA-Hexadecane Binary System

In order to enable the possibility of comparing the future results when considering the LLE data, it was first pursued for the reproduction of Avlund's LLE results. Due to a problem in the reproduction of this data, which led to an investigation into the origin of the bibliographic reference indicated in the literature (AVLUND; KONTOGEORGIS; MICHELSEN, 2008), this step was reassessed. It follows the detailed information about this step that generated several back and forth in the parameter estimation.

The results obtained by Avlund and co-workers for the DEA LLE with Hexadecane are presented in graph form (Figure A. 5):

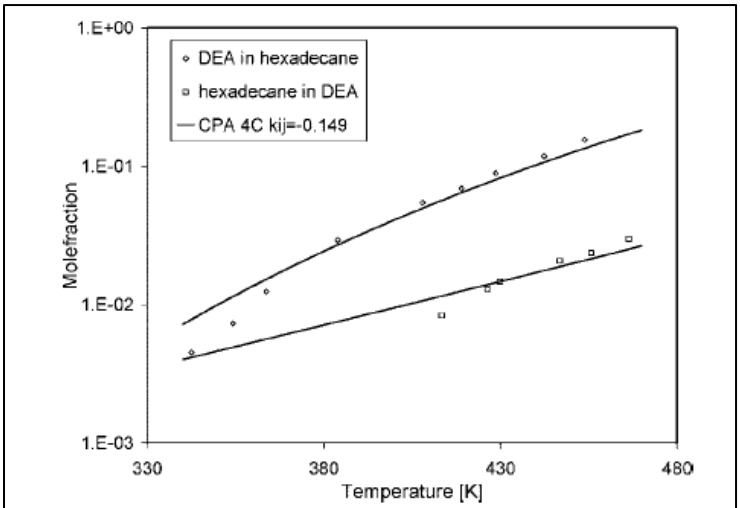

Figure 5. DEA−hexadecane LLE with an optimal interaction parameter (experimental data taken from ref. 16).

Figure A. 5 - Temperature versus phase composition (binary mixture DEA-Hexadecane) (Extracted from Avlund). The dots represent the experimental data and the solid line represents the model results.

The experimental data obtained from the Avlund and co-workers reference is presented in Table A. 9:

Table A. 9 - Experimental data obtained from Majid Abedinzadegan Abdi - Mutual Solubility of Hexadecane with Diethanolamine and with Bis (hydroxyethyl) piperazine

DEA in organic phase	Hexadecane in polar phase	Temperature (K)
0.018762943	-	378.55
0.031965485	-	400.35
0.041692784	-	413.65
0.052335417	-	431.35
0.053758608	-	436.65
0.060034562	-	445.45
0.076824016	-	463.65
-	0.009386475	495.55
-	0.006784987	483.65
-	0.004574108	469.45
-	0.003402663	455.45
-	0.002607878	445.55
-	0.001767921	429.45
-	0.00088306	408.35

In an attempt to reproduce the Avlund and co-workers data, using the reference indicated in its article, the final parameters obtained are as follows (Table A. 10).

Table A. 10 - Attempt to reproduce Avlund's results considering Pure DEA parameter estimation.

Reference	k_{ij}	F_{obj}	AAXI-II%	AAXII-I%
This Work	-0.0940	$9.57.E^{-2}$	21.83	12.83
Avlund (2008)	-0.149	Not informed	Not informed	Not informed

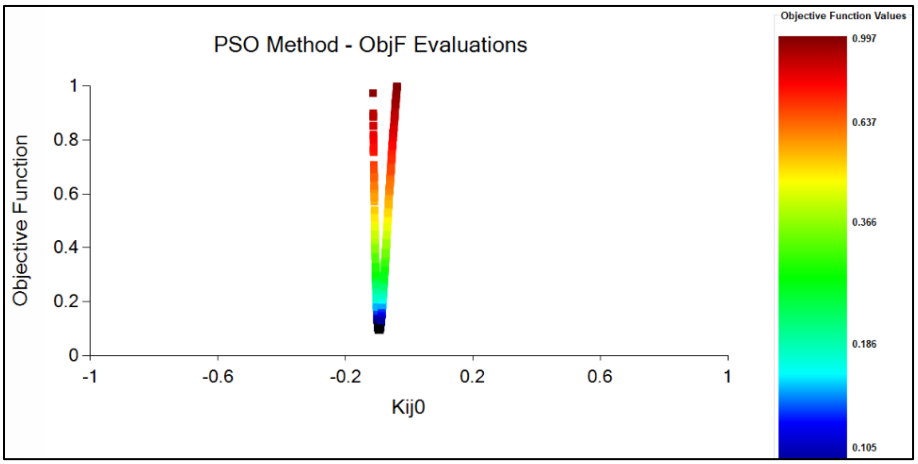

Figure A. 6 - k_{ij} Estimation (Reproduction of Results). Equilibrium data from DIPPR (DIADEM, 2004) and Abdi (ABEDINZADEGAN ABDI; MEISEN, 1998).

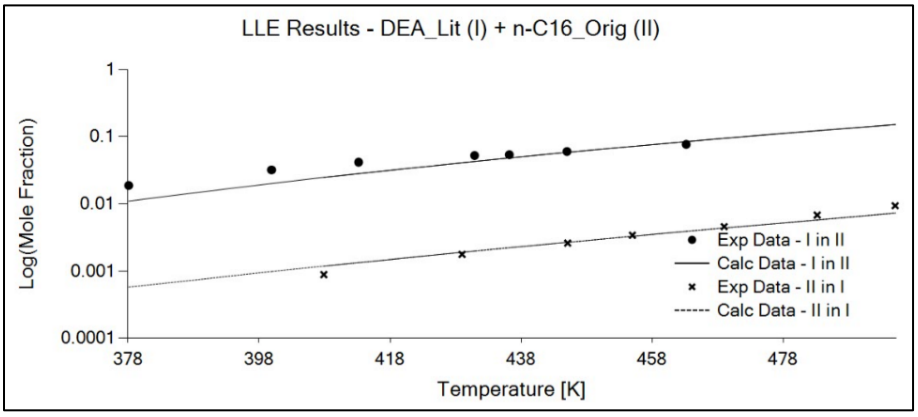

Figure A. 7 - LLE Results (Reproduction of Results). DEA_Lit is the file that pulls the balance data from the Pure DEA. n-C16_Orig is the file that pulls the parameters of Pure Hexadecane. Equilibrium data from DIPPR (DIADEM, 2004) and Abdi (ABEDINZADEGAN ABDI; MEISEN, 1998).

The final value of k_{ij} (-0.0940) is 36.92% lower than that obtained by Avlund and co-workers (0.146). In conclusion, using the experimental data of the cited reference, it was not possible to reproduce the paper data.

As the experimental points for the binary mixture were not available, only the bibliographic reference from where they were obtained, it was decided to operate with "PegaPonto" software, which estimated the experimental data through analysis of Figure A. 6 (Table A. 11):

Table A. 11 - DEA - Hexadecane LLE Experimental data obtained through the "PegaPonto" Software.

DEA in organic phase	Hexadecane in polar phase	Temperature (K)
0.0044657	-	342.56
0.0072436	-	354.36
0.0121100	-	363.59
0.0291000	-	384.10
0.0540810	-	407.95
0.0678440	-	418.97
0.0890580	-	428.72
0.1186900	-	442.31
0.1534600	-	453.85
-	0.0082992	413.33
-	0.0128650	426.41
-	0.0147400	430.00
-	0.0205550	446.92
-	0.0235500	455.64
-	0.0299930	466.41

Considering the experimental data obtained by "Pega Ponto", it was possible to reproduce the Avlund data, obtaining k_{ij}= -0.146. This value is 2 % lower than that found by Avlund and co-workers (Table A. 12).

Table A. 12 - Reproduction of Avlund's results. LLE equilibrium data obtained through the "Pega Ponto" Software). Equilibrium data from DIPPR (DIADEM, 2004) and Abdi (ABEDINZADEGAN ABDI; MEISEN, 1998)

Reference	k_{ij}	F_{obj}	AAXI-II%	AAXII-I%
This Work	-0.146	$1.314.E^{-1}$	23.65	17.82
Avlund (2008)	-0.149	Not informed	Not informed	Not informed

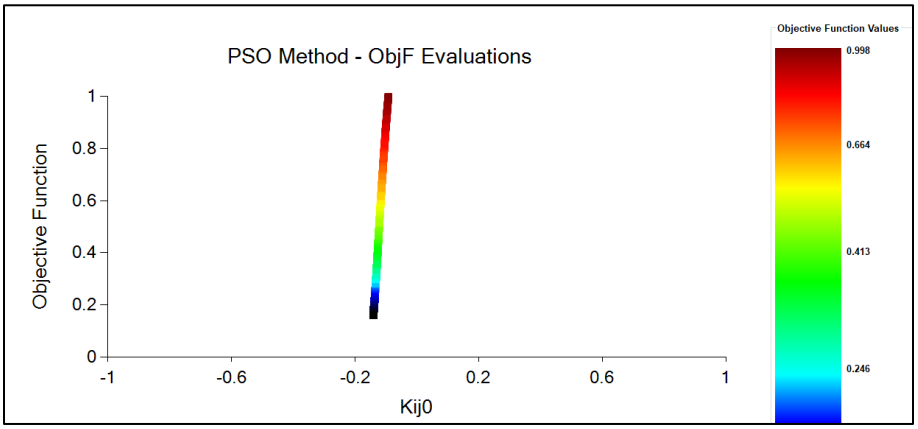

Figure A. 8 - k_{ij} estimation (LLE equilibrium data obtained through the "PegaPonto" Software). Equilibrium data from DIPPR (DIADEM, 2004) and Abdi (ABEDINZADEGAN ABDI; MEISEN, 1998)

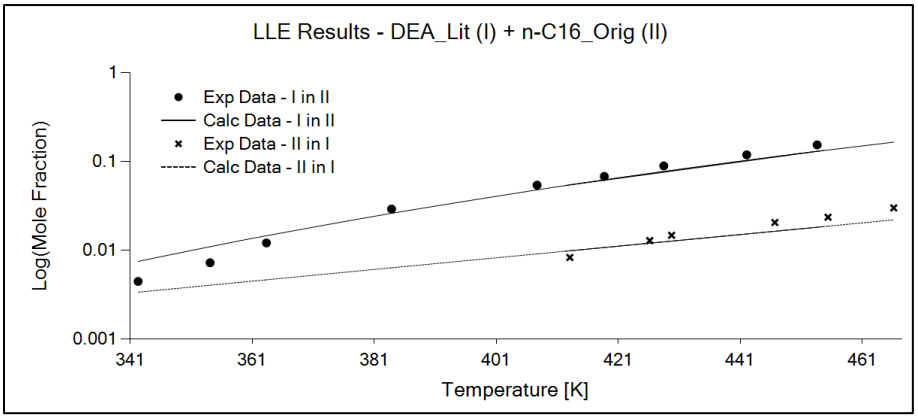

Figure A. 9 - LLE Results (LLE equilibrium data obtained through the "PegaPonto" Software). DEA_Lit is the file that pulls the balance data from the Pure DEA. n-C16_Orig is the file that pulls the parameters of Pure Hexadecane. Equilibrium data from DIPPR (DIADEM, 2004) and Abdi (ABEDINZADEGAN ABDI; MEISEN, 1998).

Thus, it was concluded that it was possible to reproduce the k_{ij} obtained by Avlund and co-workers only using the experimental data obtained by "PegaPonto". It was not possible to reproduce them using the bibliographic reference indicated in the article.

The lack of success in reproducing Avlund's article data and the non-correspondence of the experimental data presented by Avlund and co-workers in their paper and their cited bibliographical reference generated doubts about the real origin of the experimental data. In contact with Professor Georgis Kontogeorgis (co-author of the Avlund's paper), when the situation was explained, it was found with his help that there was a mistake made in the article reference and that the figure shown in the article was of another binary mixture (DEA and BHEP system instead of DEA and Hexadecane).

Thus, new simulations were carried out, now considering the reference of experimental data of the DEA and Hexadecane binary system and no longer with the interest of reproducing the Avlund and co-workers data.

Once the work would return to an earlier stage, it was also decided to modify the T_R range. The original range was 0.41 to 0.95. However, since for the DEA industrial application such temperature ranges are not used, it was decided to narrow the strip in order to better model the interval. The chosen T_R range was 0.55 to 0.9, which is a more suitable range for DEA industrial application.

Appendix B

The Moving Window Methodology

In this section explains in detail the step-by-step moving window methodology applied. It was noticed the demand to apply this methodology for two major reasons: 1. Determine which process unit would be chosen as the study object; 2. Define the confidence intervals for the process variables evaluated.

B.1 Moving Window Methodology Application

In this methodology, a defined data set has its correlation coefficient calculated by considering data from this set and its subsequent (the two distanced from a certain time interval). Optimal values of correlation coefficient are less than 0.5. Values above 0.5 indicate influence of transience on the data obtained (SCHWAAB; PINTO, 2007).

The operational data were obtained in the process units' PIs. PI (plant information) is a software that allows a remote analysis of the different operational variables measured by field instruments, which communicate with the software. The PI allows to obtain data with different time intervals. Data were obtained at intervals of 5, 10, 15, 20, 30, 45 and 60 minutes.

It was then defined the absorber tower bottom and top temperatures variables to be monitored and studied.

Once the data is collected, it is critical to determine the moving window size. Different sizes of windows in the search for the correlation coefficient lowest values were used. Windows of 60, 50, 40, 30 and 20 points were evaluated.

Data were obtained from 01/01/2018 to 06/30/2018.

B.2 Moving Window Results

From the two operational units evaluated in this work, one did not present any interval in which the correlation coefficients of both the top and bottom temperature of the absorber tower were lower than 0.75 (although it presented isolated intervals where only the top temperature or the bottom temperature had a correlation coefficient less than 0.5, but never both). In the other, intervals were obtained in which both correlation coefficients were smaller than 0.1. For this comparison the 5 minutes time interval was considered. Thus, it was decided to investigate the second industrial plant, located in the state of Rio de Janeiro.

After this step, it was searched for laboratory analysis data of the chosen industrial plant process streams. Due to sample lines clogging problems in the plant, sporadic analyzes are performed and only the treated gas composition was available for the year 2018 (analysis of April 13) and Poor DEA composition data (Data of 10, 19 and 24 April). Note that there is no available analysis of the industrial unit process feed. Thus, the window chosen from 01/01/2018 to 06/30/2018 might not necessarily represent the information of the process feed. Thus, the moving window step was revisited and it was decided that the study interval would be 24 hours before and after April 13. Thus, the new data range was restructured from April 12 (0:00) until April 14 (24:00). The moving window best results are shown in Table B. 1.

The data in Table B. 1 are still adequate for the study, since the correlation coefficients (0.574 and 0.450) are close to 0.5.

Note that to be considered in steady state it was defined that both top and bottom temperature correlation coefficients shall be with values below (or near) of 0.5.

Table B. 1 - Best results of the moving window methodology applied in the AGASA unity under evaluation. The best data set refers to 30 points window with data spaced every 20 minutes. The information was obtained in the PI.

30-POINTS WINDOW (20-MINUTE INTERVALS)		
DATE	**BOTTOM TEMPERATURE (°C)**	**TOP TEMPERATURE (°C)**
13-Apr-18 22:00:00	43.368	38.014
13-Apr-18 22:20:00	43.185	37.816
13-Apr-18 22:40:00	43.002	37.618
13-Apr-18 23:00:00	42.966	37.420
13-Apr-18 23:20:00	42.980	37.222
13-Apr-18 23:40:00	42.993	37.086
14-Apr-18 00:00:00	43.006	37.078
14-Apr-18 00:20:00	43.020	37.070
14-Apr-18 00:40:00	43.033	37.062
14-Apr-18 01:00:00	43.047	37.054
14-Apr-18 01:20:00	43.060	37.047
14-Apr-18 01:40:00	43.073	37.039
14-Apr-18 02:00:00	43.087	37.031
14-Apr-18 02:20:00	43.100	37.023
14-Apr-18 02:40:00	43.114	37.015
14-Apr-18 03:00:00	43.127	37.007
14-Apr-18 03:20:00	43.140	36.999
14-Apr-18 03:40:00	43.154	36.991
14-Apr-18 04:00:00	43.167	36.983
14-Apr-18 04:20:00	43.181	36.975
14-Apr-18 04:40:00	43.194	36.967
14-Apr-18 05:00:00	43.207	36.959
14-Apr-18 05:20:00	43.221	36.951
14-Apr-18 05:40:00	43.234	36.943
14-Apr-18 06:00:00	43.248	36.935
14-Apr-18 06:20:00	43.261	36.927
14-Apr-18 06:40:00	43.274	36.919
14-Apr-18 07:00:00	43.288	36.911
14-Apr-18 07:20:00	43.301	36.903
14-Apr-18 07:40:00	43.315	36.895
14-Apr-18 08:00:00	44.610	38.676
MEAN VALUE	43.145	37.095
STANDARD DEVIATION	0.112	0.270
VARIANCE	0.013	0.073
CORRELATION COEFFICIENT	0.574	0.450
CONFIDENCE INTERVAL 95%	[43.103;43.187]	[37.196;36.995]

B.3 Moving Window Chosen Sets Statistical Treatment

Once the data set to be studied was determined, other operational data were obtained through PI: Acid Gas Temperature, Acid Gas Volume Flow, Treated Gas Volume Flow, Poor DEA Volume Flow, Rich DEA Volume Flow, Absorption Column Top Pressure, Top Temperature and Bottom Temperature.

The mean, standard deviation, variance and 95 % confidence interval of the obtained data were then calculated. The results are in Table B. 2, Table B. 3 and Table B. 4.

Table B. 2 - Operational data obtained after applying the moving data window methodology- Related information of Poor DEA and Rich DEA Streams. The information was obtained from PI.

Statistical Treatment	RICH DEA VOLUME FLOW (m^3/h)	POOR DEA VOLUME FLOW (m^3/h)	POOR DEA TEMPERATURE (°C)
MEAN	37.722	36.914	37.095
STANDARD DEVIATION	0.355	0.205	0.270
VARIANCE	0.130	0.043	0.044
CORRELATION COEFFICIENT	0.377	0.685	0.450
INTERVAL OF CONFIDENCE 95%	[37.589; 37.854]	[36.837; 36.990]	[36.995; 37.196]

It was considered that the temperature and supply of the Poor DEA stream is equal to the Absorption Column top temperature. There is no temperature measurement of this process stream.

The confidence interval calculation allows to delimit a region in which the parameters satisfy the desired confidence level.

Table B. 3 - Operational data obtained after applying the moving data window methodology- Related information of Acid Gas (Process Feed) and Treated Gas Streams. The information was obtained from PI.

Statistical Treatment	TREATED GAS VOLUME FLOW (Nm3/h)	ACID GAS VOLUME FLOW (Nm3/h)	ACID GAS TEMPERATURE (°C)
MEAN	4584.127	5117.921	30.348
STANDARD DEVIATION	3.943	1.382	0.397
VARIANCE	14.546	1.786	0.129
CORRELATION COEFFICIENT	1.000	1.000	0.796
INTERVAL OF CONFIDENCE 95%	[4582.654; 4585.599]	[5117.405; 5118.437]	[30.200; 30.496]

Table B. 4 - Operational data obtained after applying the moving data window methodology- Related information of Absorption Column. The information was obtained from PI.

Statistical Treatment	ABSORBER TOP PRESSURE (kgf/cm^2 man)	ABSORBER TOP TEMPERATURE (°C)	ABSORBER BOTTOM TEMPERATURE (°C)
MEAN	5.207	37.095	43.145
STANDARD DEVIATION	0.008	0.270	0.112
VARIANCE	0.000	0.044	0.011
CORRELATION COEFFICIENT	0.900	0.450	0.574
INTERVAL OF CONFIDENCE 95%	[5.204; 5.210]	[36.995;37.196]	[43.103; 43.187]

The operational data quality presented depends greatly on the field instrument integrity and calibration. Each instrument has its preventive inspection plan, however its realization is erratic (according to operational report), since instrumentalists availability in the refinery is scarce. In addition, many instruments require investment for their repair, a fact that creates a financial constraint.

Appendix C

Plant Design Conditions Evaluation

In this section is presented the evaluation of the selected AGASA industrial unity design conditions.

C.1 Industrial Plant Design Conditions

The process simulation first goal is to examine the absorbing column design conditions, focusing on verifying the H_2S final specification viability in the treated gas and to learn more about the variable sensitivity. For example, are the results more sensitive to the process feed temperature modification or are they more sensitive to the H_2S concentration in Poor DEA stream? These kinds of questions have been solved with these simulations.

As one of this research objectives, the simulations are conduct using three different models (SRK, PR and CPA) for comparison.

Table C. 1, Table C. 2 and Table C. 3 show the industrial plant design conditions:

Table C. 1 Process variables of the streams that compose the acid gas Absorption Column operation, for use in process simulation at Petrox. Data obtained from the Plant Operation Manual.

Stream	Molar Flow (kmol/h)	Temperature (°C)	Pressure (kgf/cm^2)
"Acid Gas"	190	39.3	7.10
"Treated Gas"	171	50.1	7.10
"Poor DEA"	1353	50	7.10
"Rich DEA"	1372	60.2	7.04

Table C. 2 - Molar flow of streams that constitute the acid gas Absorption Column operation, for use in process simulation at Petrox. Data obtained from the Plant Operation Manual.

	Stream (kgmol/h)			
Component	**"Acid Gas"**	**"Treated Gas"**	**"Poor DEA"**	**"Rich DEA"**
H_2S	21	0	2	23
H_2	119	119	0	0
Methane	27	27	0	0
Ethane	8	8	0	0
Propane	6	6	0	0
I-Butane	3	3	0	0
N-Butane	4	4	0	0
N-Pentane	1	1	0	0
H_2O	1	2	1295	1294
DEA	0	0	56	56
Total	190	170	1353	1373

Table C. 3 - Molar compositions of main streams that constitute the acid gas Absorption Column operation, for use in process simulation at Petrox. Data obtained from the Plant Operation Manual.

	Stream (%)			
Component	**"Acid Gas"**	**"Treated Gas"**	**"Poor DEA"**	**"Rich DEA"**
H_2S	11.053%	0.000%	0.148%	1.675%
H_2	62.632%	70.000%	0.000%	0.000%
Methane	14.211%	15.882%	0.000%	0.000%
Ethane	4.211%	4.706%	0.000%	0.000%
Propane	3.158%	3.529%	0.000%	0.000%
I-Butane	1.579%	1.765%	0.000%	0.000%
N-Butane	2.105%	2.353%	0.000%	0.000%
N-Pentane	0.526%	0.588%	0.000%	0.000%
H_2O	0.526%	1.176%	95.713%	94.246%
DEA	0.000%	0.000%	4.139%	4.079%

However, according to the plant's operating team, it never operated according to the design conditions (the reason for this fact is unclear). It is also known that the plant's current operating conditions are relatively distant from the design conditions, in order to specify H_2S in the treated gas. As mentioned in Section 4.5.3, the AGASA industrial unity receives loads of at least 3 other industrial plants and thus its process feed is noticeably variable. A detailed comparison of these differences is found in Section 4.5.4.

C.2 Design Conditions Simulation

In the first simulations at Petrox, the plant design conditions were simulated. The purpose of these simulations is to verify the sensitivity of the operational variables in the obtained results. Thus, this evaluation could answer questions such as "In the context of H_2S in the treated gas, what are the most relevant variables?". These responses facilitate plant simulations in accordance with current operating conditions and the actual conclusions of this work.

The design parameters process simulation resulted in H_2S content in the “Treated Gas” of 10.37 %. The absorption efficiency was lower (5.72 %) than the efficiency required (99.72 %) to specify the “Treated Gas” in a maximum of 300 ppm H_2S.

The design conditions were also simulated using the three thermodynamic models mentioned in Section 2.2 (CPA, SRK and PR) for comparison. By using the SRK and PR models it was not possible to obtain convergence in the simulation using the values presented in

Table C. 1 and Table C. 2. In this way, it was necessary to apply modifications to the simulation input data, in order to obtain a condition in which the three models could be compared. It follows Table C. 4, with the parameters that had to be modified for the simulation convergence. Table C. 5 indicates a gas absorber simulation applying 3 different thermodynamic models:

Table C. 4 - Variables adjusted for Thermodynamic Models comparison (SRK, PR and CPA).

Simulation	Acid Gas Molar Flow (kgmol/h)	H_2S Concentration in Acid Gas
Required Simulation Input Data Modifications	110	9%
Design Conditions	190	11%

Table C. 5 - Molar composition of H_2S in the "Treated Gas" for each concentration of H_2S in the Acid Gas. The simulation took place in Petrox.

Thermodynamic Model	Molar composition of H_2S in the "Treated Gas"
CPA	9.97%
SRK	11.76%
PR	10.12%

It is possible to verify that the CPA model showed the best results regarding the efficiency of absorption of H_2S by DEA. However, the results are still far short of those reported in the industrial unit's operation manual. A possible hypothesis is that the plant can be far from the design conditions since the results indicate treated gas specification divergent from the purpose. This matter may suggest a plant design error.

A variables sensitivity analysis was performed to verify the impact of the selected process variables on the final specification parameter.

In the follow simulations presented all design parameters remain constant except for those presented in the Table C. 6 to Table C. 14. Since the results presented in Table C. 5 indicate that CPA yields better results, this model was selected for the next steps.

Table C. 6 - Variation in the "Acid Gas" Molar Flow (Design Conditions). The simulation took place in Petrox.

"Acid Gas" Molar Flow (kgmol/h)	Molar H_2S in the "Treated Gas"
110	9.99 %
190 (Project)	10.37 %
300	10.56 %

The decrease in the molar flow rate of the process feed facilitates the removal of H_2S by the "Poor DEA". It is worth noting that the concentrations of H_2S in the "Acid Gas" were maintained according to the design condition (11.053 %) Table C. 3.

Table C. 7 - Variation in the "Poor DEA" Molar Flow (Design Conditions). The simulation took place in Petrox

Molar "Poor DEA" Flow (kgmol/h)	Molar H_2S in the "Treated Gas"
811.8	10.58 %
1353 (Project)	10.37 %
1894.2	10.16 %

The increase in the "Poor DEA" flow rate facilitates the removal of H_2S from the "Acid Gas". The concentrations of H_2S in the "Poor DEA" were maintained according to the design condition (0.148 %) Table C. 3.

Table C. 8 - Variation in Concentration of H_2S in "Poor DEA" (Design Conditions). The simulation took place in Petrox.

Concentration of H_2S in the "Acid Gas"	Molar H_2S in the "Treated Gas"	H_2S Removal Efficiency
6%	6.16 %	-2.67%
11 % (Project)	10.37 %	5.72%
16%	14.21 %	11.19%

The increase in H_2S content in the "Acid Gas" facilitates the absorption of H_2S by "Poor DEA" (Table C. 8).

Table C. 9 - Variation in the Concentration of H_2S in the "Poor DEA" (Design Conditions). The simulation took place in Petrox.

Concentration of H_2S in the "Poor DEA"	Molar H_2S in the "Treated Gas"
0.04 %	9.66 %
0.15 % (Project)	10.37 %
0.30 %	11.30 %

The decrease of H_2S concentration in the "Poor DEA" favors the absorption process of H_2S in the "Acid Gas" (Table C. 9).

Table C. 10 - Variation in the Concentration of DEA in the "Poor DEA" (Design Conditions). The simulation took place in Petrox.

Concentration of DEA in the "Poor DEA"	Molar H_2S in the "Treated Gas"
2.07 %	10.88 %
4.14 % (Project)	10.37 %
6.21 %	9.80 %

The increase of DEA content in the "Poor DEA" stream facilitates the acid gas absorption process (Table C. 10).

Table C. 11 - Variation in the Column Top Pressure (Design Conditions). The simulation took place in Petrox.

Column Top Pressure (kgf/cm^2)	Molar H_2S in the "Treated Gas"
5	10.67 %
7.1 (Project)	10.37 %
10	9.88 %

The simulation is according to theory, which clarifies that greater pressures facilitate the gas absorption. The solubility of the gas in the liquid is a function of the nature of both components, the temperature, the gas partial pressure in the gas phase and the liquid composition. Solubility decreases with temperature and increases with total pressure (KOHL; NIELSEN, 1997).

Table C. 12 - Variation in the "Poor DEA" Temperature (Design Conditions). The simulation took place in Petrox.

"Poor DEA" Temperature	Molar H_2S in the "Treated Gas"
40	10.21 %
50 (Project)	10.37 %
60	9.45 %

As mentioned above, the decreasing the “Poor DEA” stream temperature facilitates gaseous absorption.

Table C. 13 - Variation in the “Acid Gas” Temperature (Design Conditions). The simulation took place in Petrox.

“Acid Gas” Temperature	Molar H_2S in the “Treated Gas”
35	10.36 %
39.3 (Project)	10.37 %
45	10.38 %

According to Table C. 13, it is possible to conclude that decreasing the “Acid Gas” stream temperature the gas absorption is facilitated.

Table C. 14 - Variation in the Number of Theoretical Stages (Design Conditions). The simulation took place in Petrox.

Number of Theoretical Stages	Molar H_2S in the “Treated Gas”
15	10.37 %
31 (Estimated)	10.37 %
50	10.37 %

The variation in the number of theoretical stages in the absorption column did not show any influence on the results of the specification parameter.

Since the column design conditions simulation did not show good results in the H_2S specification in the “Acid Gas”, it was proceeded to modify some parameters simultaneously in order to specify that stream. Only the design parameters that have changed in order to obtain results that reflect the environmental specifications for “Acid Gas” are listed in the Table C. 15.

Table C. 15 - Comparison of Simulations between the required simulation input data modifications scenario and design conditions.

Design Variables	Design Conditions	Modified Scenario Best Simulation
"Acid Gas" Temperature	39.3	25
Column Top Pressure	7.1	10
"Poor DEA" Temperature	50	30
DEA Conc. In "Poor DEA"	0.15%	0.0015%
H_2S Conc. In "Poor DEA"	4.14%	20%
Molar H_2S in the "Treated Gas" (ppm)	103703	93

It is possible to notice that several variables had to be manipulated concerning the acid gas specification. In general, the main design conditions that hinder the H_2S specification are the "Poor DEA" temperature, DEA content in "Poor DEA" and the H_2S content in "Poor DEA".

Appendix D

Operating Conditions Simulation Comparison applying CPA, SRK and PR EoS

In this section a comparison of the current operating conditions is presented applying CPA, SRK and PR. Its objective is to verify which model best predicts the behavior of the final specification of the treated gas in relation to process variables fluctuations.

D.1 Required Modifications for EoS Comparison

For the simulations referring to the plant operational conditions, the conditions were first simulated using three thermodynamic models (CPA, SRK and PR). However, when the SRK and PR thermodynamic models were applied, the process simulator numerical method did not obtain any solution (did not converge). In this way, it was necessary to modify the simulation input data, so that the same conditions could be simulated for the three thermodynamic models and thus a comparison could be made. There was a concern to modify the simulation input data to a region as close as possible to the operating conditions. Table D. 1 shows the necessary modifications in each case.

Table D. 1 - Simulation input data for analysis of the operating conditions after required simulation input data modifications for thermodynamic models (CPA, SRK and PR) comparison.

Concentration of H_2S in "Acid Gas"	Temperature of "Poor DEA" (°C)	DEA in "Poor DEA"	H_2S in "Poor DEA"
5%	36.60	27.27%	0.455%
8%	33.40	20%	0.5%
11%	34.25	23.81%	0.476%
Oper. Cond.	36.837 - 36.990	20%	0.5%

The variables that most affected the convergence or not of the method were, according to Table D. 1, the "Poor DEA" temperature and the DEA and H_2S content in "Poor DEA". The variables not shown are those that are equal to the operating conditions.

D.2 Comparison Results

The results for each simulated scenario of "Acid Gas" H_2S molar concentration are shown in Table D. 2:

Table D. 2 - Results of the thermodynamic model comparison for each molar composition of H_2S in the "Acid Gas". The composition of H_2S in the "Treated Gas" for each H_2S composition in the process feed (5%, 8% and 11%) is shown. The simulations took place with Petrox.

	H_2S Molar composition in "Treated Gas"		
Thermodynamic Model	**5%**	**8%**	**11%**
CPA	2.956%	0.048%	0.065%
SRK	4.284%	0.070%	0.085%
PR	1.017%	0.014%	0.021%

It is extremely important to know that the PR model provided a lower mole fraction of H_2S in the "Treated Gas" not because of better acid absorption but as a result of the aqueous phase migration to the gaseous phase to a great extent (large amount of water being carried by the gas phase), an unwanted condition. For a better understanding about this

explanation, it follows the streams total composition for each simulation. The compositions comparison for each case is shown in Table D. 3, Table D. 4 and Table D. 5.

Table D. 3 - Mole Fractions of Process Streams in the Absorbing Tower (EoS CPA). The required simulation input data modifications scenario took place at Petrox.

5% of H_2S in the "Acid Gas" - CPA				
Component	**Input Data**		**Output Data**	
	"Acid Gas"	"Poor DEA"	"Rich DEA"	"Treated Gas"
H_2S	5.000	0.046	0.551	2.956
Hydrogen	85.460	0.000	0.023	86.684
Methane	3.325	0.000	0.009	3.338
Ethane	1.872	0.000	0.019	1.823
Propane	1.881	0.000	0.034	1.769
I-Butane	0.333	0.000	0.011	0.291
N-Butane	1.121	0.000	0.046	0.945
I-Pentane	0.276	0.000	0.021	0.192
H_2O	0.000	72.682	72.093	1.347
DEA	0.000	27.273	27.172	0.000
Oxygen	0.228	0.000	0.000	0.230
Nitrogen	0.352	0.000	0.000	0.356
N-Hexane	0.152	0.000	0.020	0.069

Table D. 4 - Mole Fractions of Process Streams in the Absorbing Tower (EoS SRK). The required simulation input data modifications scenario took place at Petrox.

5% of H_2S in the "Acid Gas" - SRK				
Component	**Input Data**		**Output Data**	
	"Acid Gas"	"Poor DEA"	"Rich DEA"	"Treated Gas"
H_2S	5.000	0.046	0.220	4.284
Hydrogen	85.460	0.000	0.005	85.490
Methane	3.325	0.000	0.002	3.319
Ethane	1.872	0.000	0.011	1.830
Propane	1.881	0.000	0.022	1.791

Table D. 4 (continuation) - Mole Fractions of Process Streams in the Absorbing Tower (EoS SRK). The required simulation input data modifications scenario took place at Petrox.

5% of H_2S in the "Acid Gas" - SRK				
Component	**Input Data**		**Output Data**	
	"Acid Gas"	"Poor DEA"	"Rich DEA"	"Treated Gas"
I-Butane	0.333	0.000	0.004	0.315
N-Butane	1.121	0.000	0.026	1.016
I-Pentane	0.276	0.000	0.008	0.245
H_2O	0.000	72.682	72.426	1.010
DEA	0.000	27.273	27.269	0.000
Oxygen	0.228	0.000	0.000	0.227
Nitrogen	0.352	0.000	0.000	0.352
N-Hexane	0.152	0.000	0.008	0.121

Table D. 5 – Process Streams Mole Fractions in the Absorbing Tower (EoS PR). The required simulation input data modifications scenario took place at Petrox.

5% of H_2S in the "Acid Gas" - PR				
Component	**Input Data**		**Output Data**	
	"Acid Gas"	"Poor DEA"	"Rich DEA"	"Treated Gas"
H_2S	5.000	0.046	0.647	1.017
Hydrogen	85.460	0.000	0.019	16.859
Methane	3.325	0.000	0.009	0.656
Ethane	1.872	0.000	0.071	0.369
Propane	1.881	0.000	0.196	0.369
I-Butane	0.333	0.000	0.051	0.065
N-Butane	1.121	0.000	0.301	0.218
I-Pentane	0.276	0.000	0.110	0.053
H_2O	0.000	72.682	0.004	59.054
DEA	0.000	27.273	98.437	21.197
Oxygen	0.228	0.000	0.001	0.045
Nitrogen	0.352	0.000	0.000	0.069
N-Hexane	0.152	0.000	0.155	0.029

Attention that the input data is the same in the model comparison presented in Table D. 2 - Results of the thermodynamic model comparison for each molar composition of H_2S in the "Acid Gas". The composition of H_2S in the "Treated Gas" for each H_2S composition in the process feed (5%, 8% and 11%) is shown. The simulations took place with Petrox.. From Table D. 5, it is possible to identify that the PR model predicted the transfer of water from the liquid phase ("Poor DEA" stream) to the gas phase, which generated a high concentration of water in the "Treated Gas" (59,054 %), which caused a lower concentration of H_2S in the "Treated Gas" similarly to what has been mentioned previously.

Considering the Gas Absorption Efficiency (Equation D. 1):

$$\textbf{Gas Absorption Efficiency} = \frac{Molar\ Flow\ of\ H2S\ in\ Acid\ Gas - Molar\ Flow\ of\ H2S\ in\ Treated\ Gas}{Molar\ Flow\ of\ H2S\ in\ Acid\ Gas} \qquad \textbf{D. 1}$$

It is possible to construct a comparative table (Table D. 6) considering the gas absorption efficiency for each thermodynamic model. It is possible to notice that the PR model presented the worst absorption among all the models. It was the only thermodynamic model that instead of predicting gas absorption by the DEA, it predicted the migration of H_2S from the "Poor DEA" to the gaseous stream.

Table D. 6 - Comparison between gas absorption efficiencies for each case simulated (H_2S concentration) in the "Acid Gas".

Comparison between gas absorption efficiencies for each case of H_2S concentration in the "Acid Gas"			
EoS	**5%**	**8%**	**11%**
CPA	42%	41%	44%
SRK	14%	13%	18%
PR	-3%	-2%	-1%

This PR model behavior was repeated in all other cases regardless the H_2S content in the "Acid Gas" (this same behavior occurred at concentrations of 8 % and 11 %).

From these initial simulations, sensitivity analyzes were performed. In the ordinate axis, in all the graphs, is presented the "Treated Gas" H_2S mole fraction, which is the main gas specification variable.

In the Figure D. 1 are presented the graphs related to the sensitivity analysis for 5 % of “Acid Gas” H_2S molar concentration:

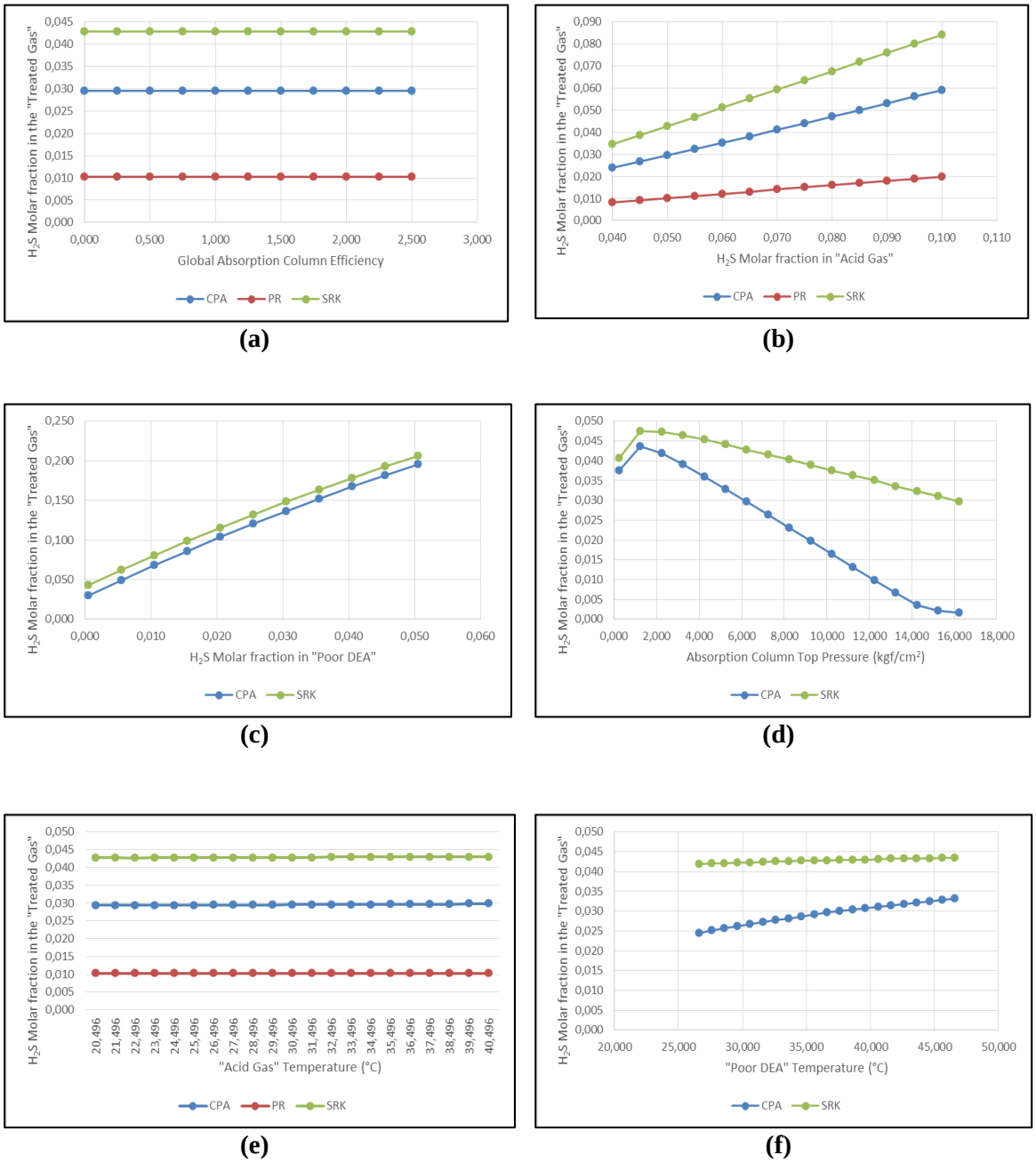

Figure D. 1 - Sensitivity analysis considering "Acid Gas" H_2S molar concentration of 5%, applying CPA, SRK and PR EoS. a) Global Absorption Column Efficiency b) “Acid Gas” H_2S Mole Fraction c) “Poor DEA” H_2S Mole Fraction d) Absorption Column Top Pressure e) “Acid Gas” Temperature f) “Poor DEA” Temperature g) “Acid Gas” Molar Flow h) “Poor DEA” Molar Flow i) Absorption Column First Stage Thermal Load j) Absorption Column

Last Stage Thermal Load. Blue line represents the CPA EoS, red line represents the PR EoS and green line represents the SRK EoS. 21 points were used in each case. The simulations took place in Petrox.

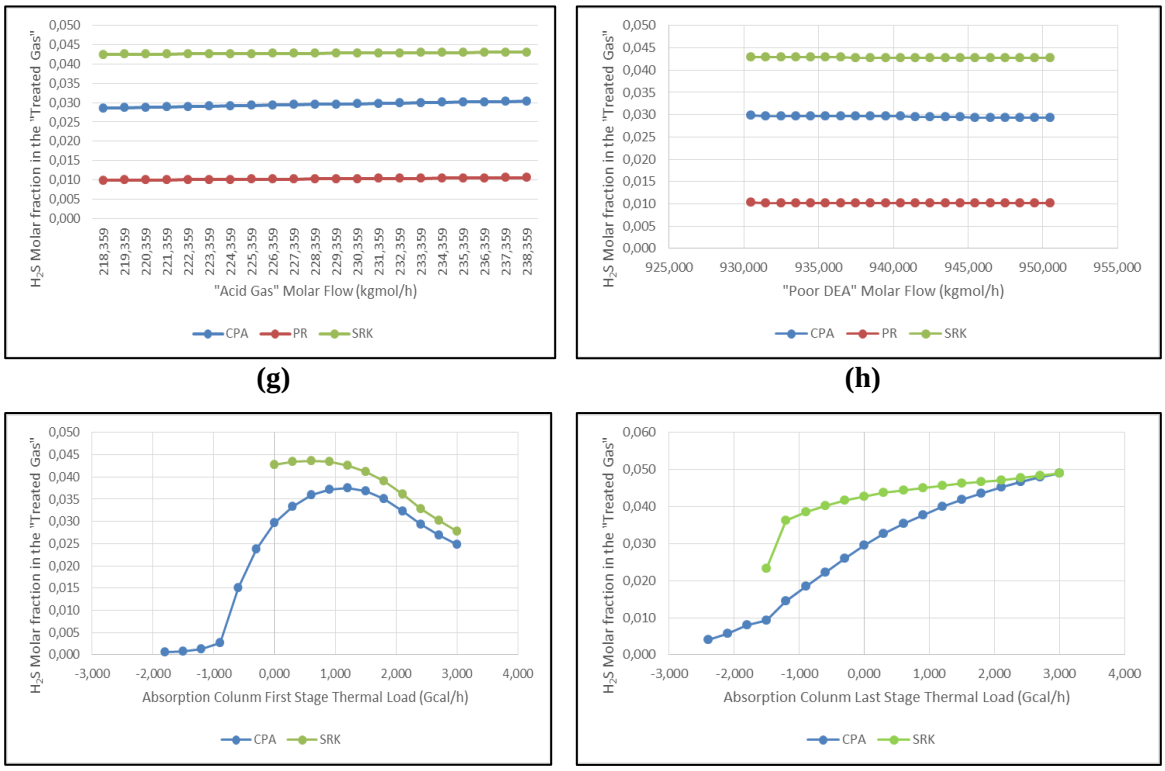

Figure D. 1(continuation) - Sensitivity analysis considering "Acid Gas" H_2S molar concentration of 5%, applying CPA, SRK and PR EoS. a) Global Absorption Column Efficiency b) "Acid Gas" H_2S Mole Fraction c) "Poor DEA" H_2S Mole Fraction d) Absorption Column Top Pressure e) "Acid Gas" Temperature f) "Poor DEA" Temperature g) "Acid Gas" Molar Flow h) "Poor DEA" Molar Flow i) Absorption Column First Stage Thermal Load j) Absorption Column Last Stage Thermal Load. Blue line represents the CPA EoS, red line represents the PR EoS and green line represents the SRK EoS. 21 points were used in each case. The simulations took place in Petrox.

It can be seen from Figure D. 1 (b), (c) and (d) that the variables "Acid Gas" H_2S Mole Fraction, "Poor DEA" H_2S Mole Fraction and Absorbing Column Top Pressure are those that most influence the "Treated Gas" specification. The understanding of the influence of "Acid Gas" H_2S Mole Fraction is more obvious, since the lower the Process Feed H_2S content, the less it will be required of the gaseous absorption. Thus, naturally lower treated gas H_2S concentration is expected. The "Poor DEA" H_2S Mole Fraction is important for the extent of gas absorption because the lower the H_2S content in this stream, the greater the driving force for mass transfer (this happens as a result of a H_2S concentration differential

between the phases increase). On the Absorption Column Top Pressure, higher pressures facilitate the gas absorption and thus, when increasing the pressure of the Absorption Column a decrease in Treated Gas H_2S concentration is foreseen.

From the process variables inquiry, the ones that apparently have the least influence on the H_2S specification in the "Treated Gas" are the 1. Global Absorption Column Efficiency (a mathematical parameter that influences the process simulator calculations); 2. "Acid Gas" Temperature; 3. "Acid Gas" molar flow and; 4. the "Poor DEA" molar flow.

A possible explanation for the low influence of the "Acid Gas" temperature and molar flow is due to the fact the temperature that will dictate the extent of gas absorption are the Absorption Column top and bottom temperatures (which are a product of the energy balance between the streams and the release / absorption of energy occurring in the domain). The temperature and the flow of the "Acid Gas" are just terms of this energy balance composed of several variables. The "Acid Gas" flow becomes critical when it reaches considerably high values and that can cause the drag of the liquid stream by the top of the Absorption Column.

For Figure D. 1 (c), (d), (f) and (i) results were only presented applying the CPA and SRK models since there was no simulation convergence when the thermodynamic model PR was applied.

Looking at Figure D. 1 (h) it is possible to conclude that the "Poor DEA" molar flow does not have an important impact on the H_2S content in the gas treatment. Nevertheless, from Figure D. 2, where each thermodynamic model is represented separately, it is possible to verify that there is a dependence but this is limited.

Just as for the "Acid Gas" temperature and molar flow, the low influence of the "Poor DEA" molar flow can be associated to the fact that it is one term within a more complex energy balance.

Figure D. 2 is related to the sensitivity analysis for 8 % of "Acid Gas" H_2S molar concentration.

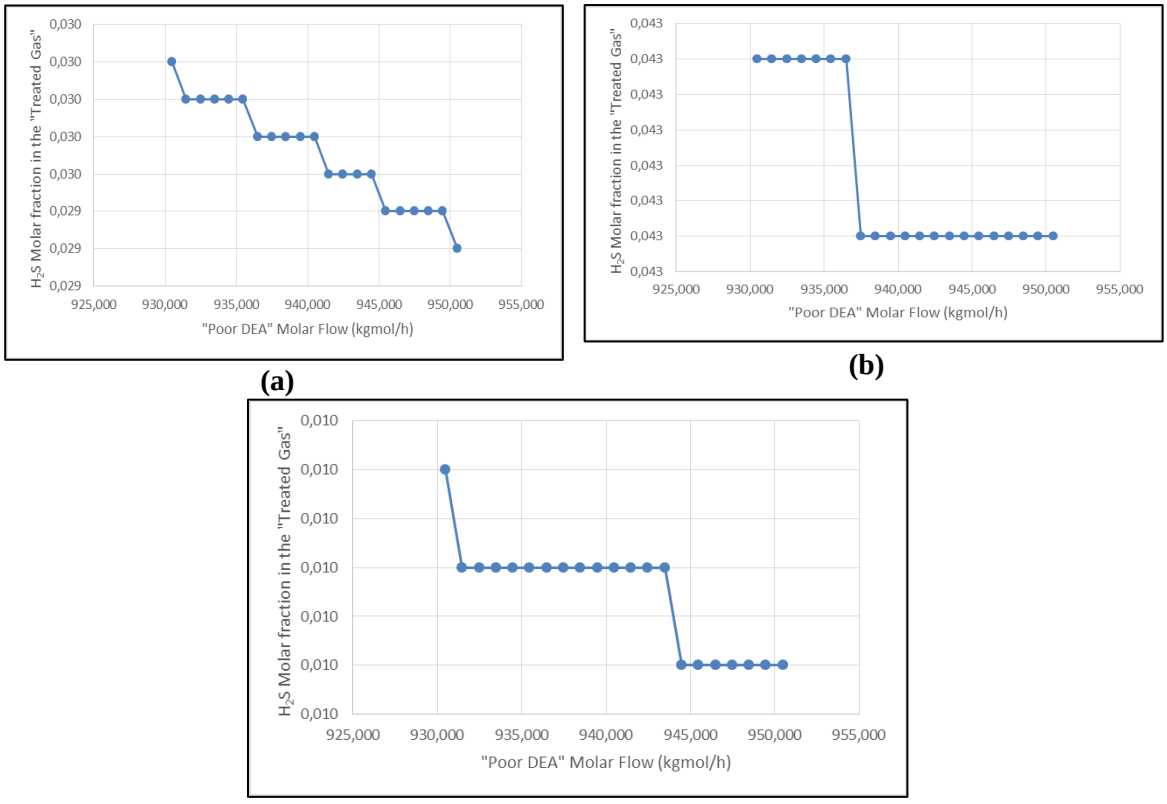

Figure D. 2 - "Poor DEA" flow influence analysis on H_2S composition in the "Treated Gas", using three different EoS, CPA, SRK and PR. a) CPA b) SRK c) PR. 21 points were used in each case. The simulations took place in Petrox.

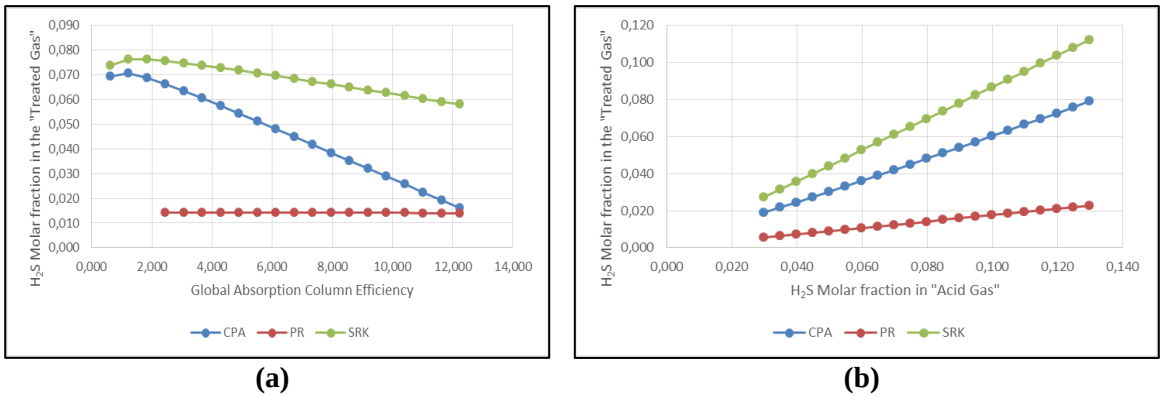

Figure D. 3 - Sensitivity analysis considering "Acid Gas" H_2S molar concentration of 8%, applying CPA, SRK and PR EoS. a) Global Absorption Column Efficiency b) Mole Fraction of H_2S in "Acid Gas" c) Mole Fraction of H_2S in "Poor DEA" d) Absorption Column Top Pressure e) "Acid Gas" Temperature f) "Poor DEA" Temperature g) "Acid Gas" Molar Flow h) "Poor DEA" Molar Flow i) Absorption Column First Stage Thermal Load j Absorption Column Last Stage Thermal Load. Blue line represents the CPA EoS, red line represents the PR EoS and green line represents the SRK EoS. 21 points were used in each case. The simulations took place in Petrox.

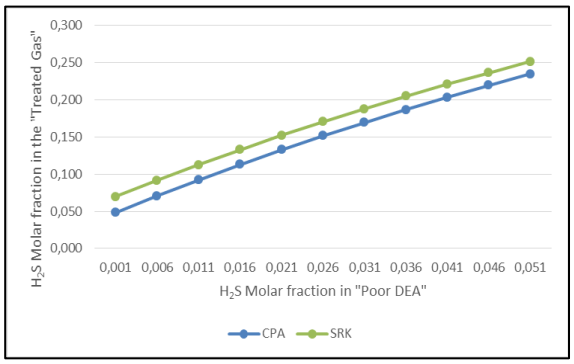

(c)

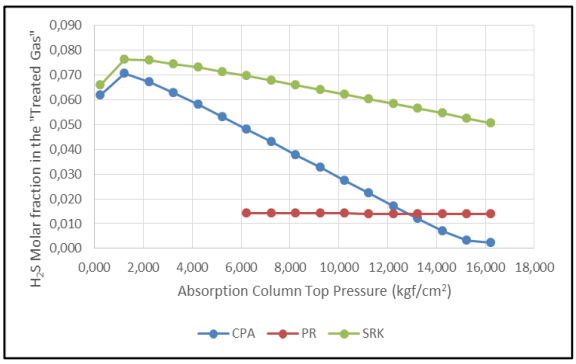

(d)

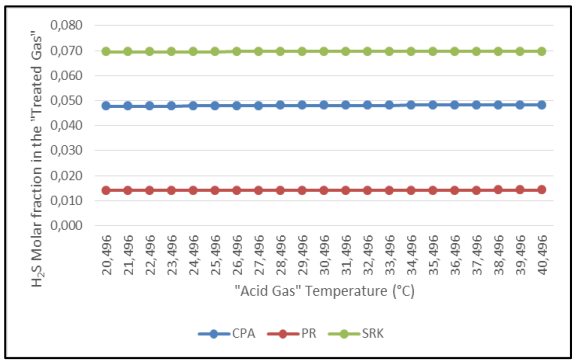

(e)

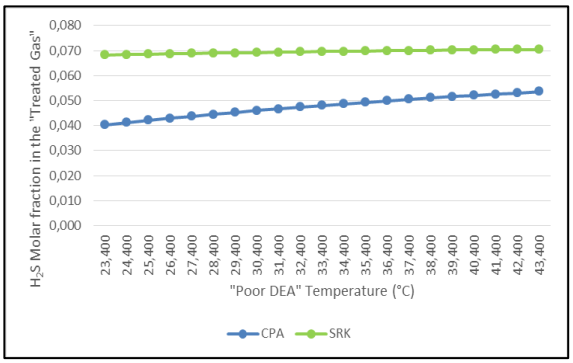

(f)

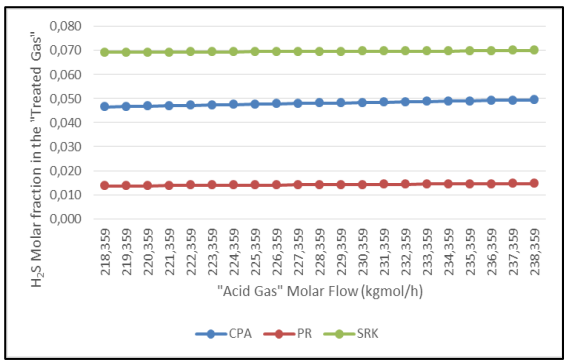

(g)

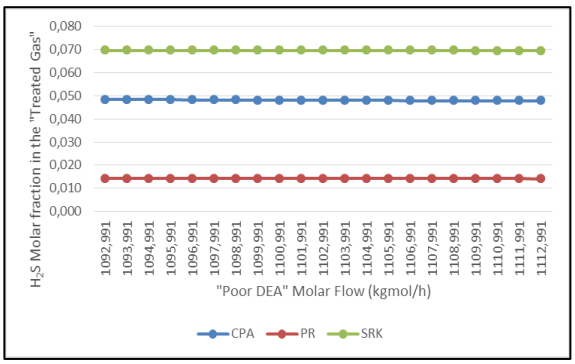

(h)

Figure D. 3 (continuation) - Sensitivity analysis considering "Acid Gas" H_2S molar concentration of 8%, applying CPA, SRK and PR EoS. a) Global Absorption Column Efficiency b) Mole Fraction of H_2S in "Acid Gas" c) Mole Fraction of H_2S in "Poor DEA" d) Absorption Column Top Pressure e) "Acid Gas" Temperature f) "Poor DEA" Temperature g) "Acid Gas" Molar Flow h) "Poor DEA" Molar Flow i) Absorption Column First Stage Thermal Load j Absorption Column Last Stage Thermal Load. Blue line represents the CPA EoS, red line represents the PR EoS and green line represents the SRK EoS. 21 points were used in each case. The simulations took place in Petrox.

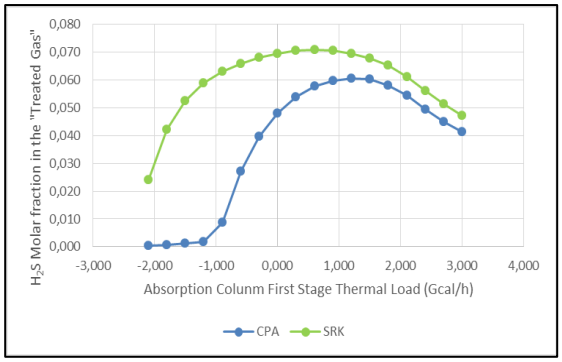

(i)

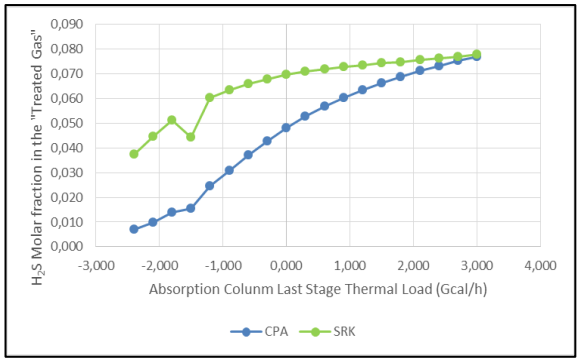

(j)

Figure D. 3 (continuation) - Sensitivity analysis considering "Acid Gas" H_2S molar concentration of 8%, applying CPA, SRK and PR EoS. a) Global Absorption Column Efficiency b) Mole Fraction of H_2S in "Acid Gas" c) Mole Fraction of H_2S in "Poor DEA" d) Absorption Column Top Pressure e) "Acid Gas" Temperature f) "Poor DEA" Temperature g) "Acid Gas" Molar Flow h) "Poor DEA" Molar Flow i) Absorption Colunm First Stage Thermal Load j Absorption Colunm Last Stage Thermal Load. Blue line represents the CPA EoS, red line represents the PR EoS and green line represents the SRK EoS. 21 points were used in each case. The simulations took place in Petrox.

The variables behavior when applied SRK EoS was similar to CPA's, with the exception of Global Absorption Column Efficiency, which significantly affected the H_2S content in the "Treated Gas". However, the simulated values are hypothetical, since the column theoretical global efficiency should not exceed 1.

Figure D. 4 is related to the sensitivity analysis for 11 % of "Acid Gas" H_2S molar concentration.

As explained above, the sensitivity analysis presented aims to verify the main process variables performance when applying different EoS. The variables behavior was delineated to be fairly coherent and concordant among the EoS.

Working with CPA EoS, the operational conditions (without the input data modifications) were simulated, considering the minimum and maximum limits of each variable (calculated in the statistical treatment already presented in the Section 4.5.1.

It is significant keep in mind that simulations when applying the SRK and PR models did not converge when the full operating ranges were employed (and that is why modifications were made to the simulation input data).

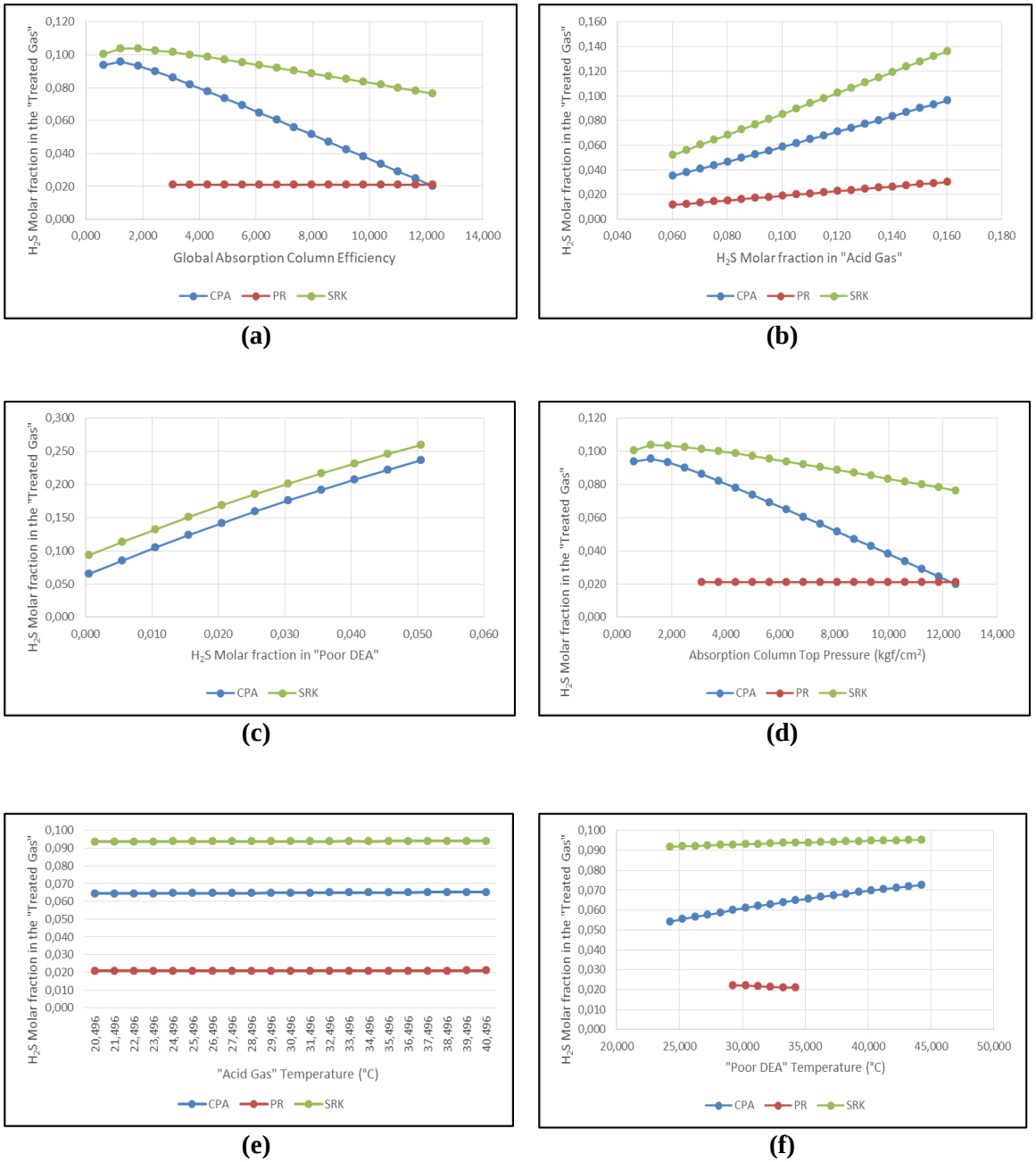

Figure D. 4 - Sensitivity analysis considering "Acid Gas" H_2S molar concentration of 11%, applying CPA, SRK and PR EoS. a) Global Absorption Column Efficiency b) Mole Fraction of H_2S in "Acid Gas" c) Mole Fraction of H_2S in "Poor DEA" d) Absorption Column Top Pressure e) "Acid Gas" Temperature f) "Poor DEA" Temperature g) "Acid Gas" Molar Flow h) "Poor DEA" Molar Flow i) Absorption Column First Stage Thermal Load j) Absorption Column First Stage Thermal Load. Blue line represents the CPA EoS, red line represents the PR EoS and green line represents the SRK EoS. 21 points were used in each case. The simulations took place in Petrox.

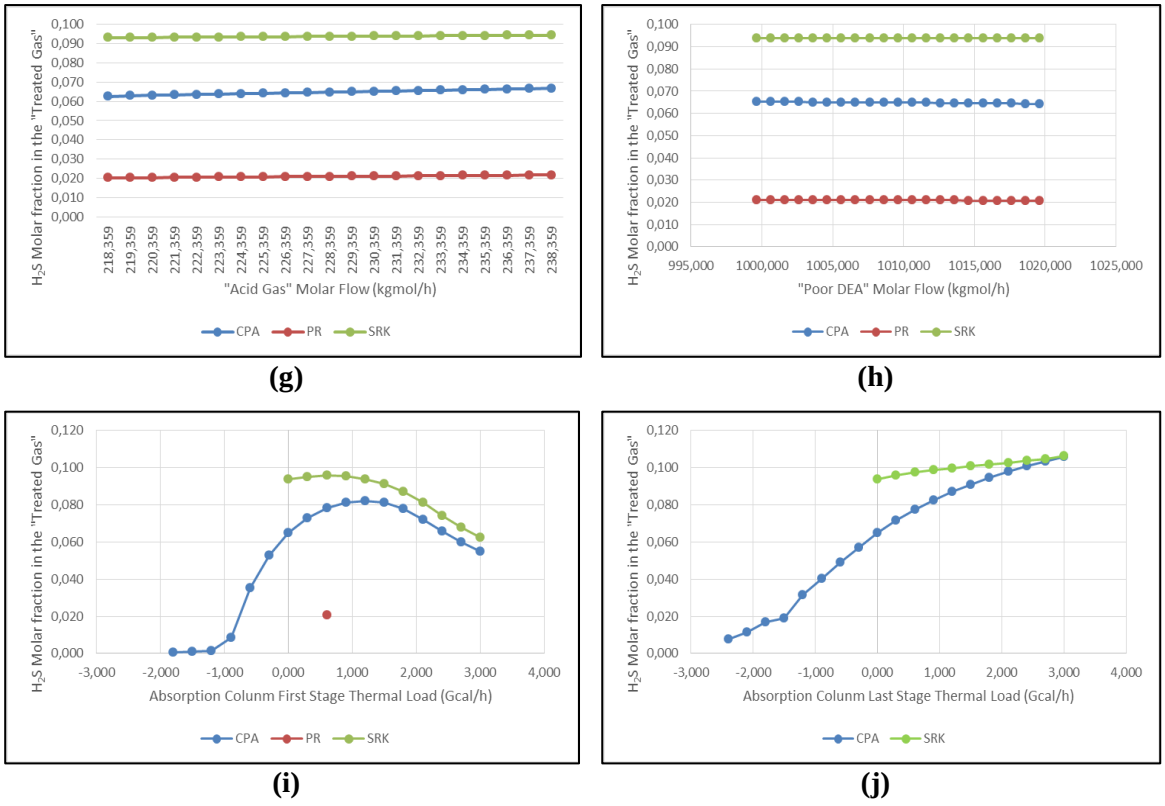

Figure D. 4 (continuation) - Sensitivity analysis considering "Acid Gas" H_2S molar concentration of 11%, applying CPA, SRK and PR EoS. a) Global Absorption Column Efficiency b) Mole Fraction of H_2S in "Acid Gas" c) Mole Fraction of H_2S in "Poor DEA" d) Absorption Column Top Pressure e) "Acid Gas" Temperature f) "Poor DEA" Temperature g) "Acid Gas" Molar Flow h) "Poor DEA" Molar Flow i) Absorption Column First Stage Thermal Load j) Absorption Column First Stage Thermal Load. Blue line represents the CPA EoS, red line represents the PR EoS and green line represents the SRK EoS. 21 points were used in each case. The simulations took place in Petrox.

Appendix E

Current Operation Conditions Simulation (8% and 11% of H_2S in the Process Feed)

In this section is presented the process simulations considering the "Acid Gas" H_2S content of 8 % and 11 %. The results of these simulations indicated "Treated Gas" H_2S composition larger than when considering 5 % of H_2S. However, it is relevant to present these simulations, since there is no certainty to the percentage of H_2S in the process feed. Thus, it is important to study the entire composition possible range (from 5 % to 11 %).

E.1 8% and 11% Results

Similarly, as in Section 4.5.3, it is presented the Petrox simulation results applying the CPA, considering however 8 % and 11 % of H_2S molar concentration in the "Acid Gas".

Table E. 1 shows the results considering 8 % H_2S molar concentration in the "Acid Gas".

Table E. 1 - CPA - Operating Conditions (8% H_2S in "Acid Gas"). It is represented 13 operational conditions, all within the statistically calculated intervals.

	Input				Results
	"Acid Gas"		"Poor DEA"		"Treated Gas"
N°	Volume Flow (Nm^3/h)	Temperature (°C)	Volume Flow (m^3/h)	Temperature (°C)	H_2S in "Treated Gas"
1	5117.405	30.200	36.837	36.995	5.046%
2	5117.405	30.200	36.990	36.995	5.033%
3	5118.437	30.200	36.990	36.995	5.034%
4	5118.437	30.200	36.837	37.196	5.058%
5	5118.437	30.200	36.990	37.196	5.046%
6	5117.405	30.200	36.990	37.196	5.045%
7	5117.405	30.496	36.990	36.995	5.035%
8	5117.405	30.496	36.990	37.196	5.046%
9	5117.405	30.496	36.837	37.196	5.058%
10	5117.405	30.496	36.837	36.995	5.046%
11	5118.437	30.496	36.837	36.995	5.047%
12	5118.437	30.496	36.990	36.995	5.035%
13	5118.437	30.496	36.990	37.196	5.047%

Table E. 2 presents the process streams molar flow for the best case, where the H_2S content in the "Treated Gas" was 5.033 % (Simulation 2).

Through Table E. 2 it is possible to visualize that the model predicts the water migration from "Poor DEA" to the "Treated Gas" and the migration of undesirable gases from "Acid Gas" to the "Rich DEA". Table E. 3 shows the "Treated Gas" composition for the best case (Simulation 2), and its comparison with the chemical analysis performed on April 13, 2018.

Table E. 2 - Process streams molar flow (kmol/h). "Acid Gas" H_2S concentrations of 8%. The simulations were carried out in Petrox.

	Input			Output
	Process Streams			
Component	**"Acid Gas"**	**"Poor DEA"**	**"Rich DEA"**	**"Treated Gas"**
H_2S	18.265	0.552	7.587	11.230
Hydrogen	188.959	0.000	0.216	188.741
Methane	7.352	0.000	0.073	7.279
Ethane	4.137	0.000	0.130	4.008
Propane	4.160	0.000	0.202	3.958
I-Butane	0.735	0.000	0.069	0.666
N-Butane	2.480	0.000	0.257	2.222
I-Pentane	0.610	0.000	0.119	0.491
H_2O	0.000	881.841	878.854	2.988
DEA	0.000	220.598	220.598	0.000
Oxygen	0.505	0.000	0.002	0.503
Nitrogen	0.776	0.000	0.003	0.773
N-Hexane	0.336	0.000	0.096	0.239

Table E. 3 - "Treated Gas" Molar Composition (H_2S in concentrations of 8%). Best result for the "Treated Gas" H_2S molar composition (5.033%). Comparison with the chemical analysis performed on April 13, 2018.

Component	Analysis (%)	Simulation Result (%)	Relative Standard Deviation
H_2S	0.01	5.033	50230%
Hydrogen	89.96	84.600	-6%
Methane	3.50	3.263	-7%
Ethane	1.97	1.796	-9%
Propane	1.98	1.774	-10%
I-Butane	0.35	0.299	-15%
N-Butane	1.18	0.996	-16%
I-Pentane	0.29	0.220	-24%
H_2O	0.01	1.339	13290%
DEA	0.00	0.000	-
Oxygen	0.24	0.225	-6%
Nitrogen	0.37	0.347	-6%
N-Hexane	0.16	0.107	-33%

The "Treated Gas" H_2S composition was recalculated, in the hypothetical situation that the undesirable phenomena had not occurred and the result of its final composition was of 2.429 % (instead of 5.033 % of the best case in Table E. 1). But even so, the desirable specification of H_2S (300 ppm) would not be achieved.

Table E. 4 shows the results considering 11 % H_2S molar concentration in the "Acid Gas".

Table E. 4 - CPA - Operating Conditions (11% H_2S in "Acid Gas"). It is represented 13 operational conditions, all within the statistically calculated intervals.

	Input				Results
	"Acid Gas"		"Poor DEA"		"Treated Gas"
N°	Volume Flow (Nm^3/h)	Temperature (°C)	Volume Flow (m^3/h)	Temperature (°C)	H_2S in "Treated Gas"
1	5117.405	30.200	36.837	36.995	6.976%
2	5117.405	30.200	36.990	36.995	6.960%
3	5118.437	30.200	36.990	36.995	6.961%
4	5118.437	30.200	36.837	37.196	6.992%
5	5118.437	30.200	36.990	37.196	6.976%
6	5117.405	30.200	36.990	37.196	6.975%
7	5117.405	30.496	36.990	36.995	6.961%
8	5117.405	30.496	36.990	37.196	6.977%
9	5117.405	30.496	36.837	37.196	6.993%
10	5117.405	30.496	36.837	36.995	6.977%
11	5118.437	30.496	36.837	36.995	6.978%
12	5118.437	30.496	36.990	36.995	6.962%
13	5118.437	30.496	36.990	37.196	6.977%

Table E. 5 presents the process streams molar flow for the best case, where the H_2S content in the "Treated Gas" was 6.961 % (Simulation 3).

Table E. 5 - Process streams molar flow (kmol/h). "Acid Gas" H_2S concentrations of 11%. The simulations were carried out in Petrox.

	Input		Output	
	Process Streams			
Component	**"Acid Gas"**	**"Poor DEA"**	**"Rich DEA"**	**"Treated Gas"**
H_2S	25.167	0.552	10.376	15.344
Hydrogen	183.176	0.000	0.211	182.962
Methane	7.127	0.000	0.071	7.056
Ethane	4.011	0.000	0.126	3.885
Propane	3.706	0.000	0.180	3.526
I-Butane	0.714	0.000	0.067	0.647
N-Butane	2.402	0.000	0.250	2.153
I-Pentane	0.490	0.000	0.096	0.394
H_2O	0.000	881.841	878.846	2.996
DEA	0.000	220.598	220.598	0.000
Oxygen	0.490	0.000	0.002	0.488
Nitrogen	0.753	0.000	0.003	0.750
N-Hexane	0.325	0.000	0.094	0.231

Through Table E. 5 the same unsatisfactory phenomena of previous cases can be identified. Table E. 6 shows the "Treated Gas" composition for the best case (Simulation 3), and its comparison with the chemical analysis performed on April 13, 2018.

It was recalculated the "Treated Gas" H_2S molar composition, considering exclusively H_2S mass transfer from the "Acid Gas" to DEA stream and the result was of 3.319 % (instead of 6.961% of the best case in Table E. 4).

It can be concluded that, if the process feed H_2S concentration is 8 % to 11 %, the desirable H_2S molar concentration in the Treated Gas would not be achieved. Suggestions for accomplishing the gas specification (300 ppm) were presented in Section 4.5.4.

Table E. 6 - "Treated Gas" Molar Composition (H_2S in concentrations of 11%). Best result for the "Treated Gas" H_2S molar composition (6.961%). Comparison with the chemical analysis performed on April 13, 2018.

Component	Analysis (%)	Simulation Result (%)	Relative Standard Deviation
H_2S	0.01	6.96	69499%
Hydrogen	89.96	83.00	-8%
Methane	3.50	3.20	-9%
Ethane	1.97	1.76	-11%
Propane	1.98	1.60	-19%
I-Butane	0.35	0.29	-16%
N-Butane	1.18	0.98	-17%
I-Pentane	0.29	0.18	-38%
H_2O	0.01	1.36	13492%
DEA	0.00	0.00	-
Oxygen	0.24	0.22	-8%
Nitrogen	0.37	0.34	-8%
N-Hexane	0.16	0.11	-34%